

**Cellular mechanisms involved in stress-induced coma and CNS
spreading depression in the locust.**

by

Corinne Ivy Rodgers

A thesis submitted to the Department of Biology
in conformity with the requirements for
the degree of Doctor of Philosophy

Queen's University
Kingston, Ontario, Canada
(August, 2010)

Copyright © Corinne Ivy Rodgers, 2010

Abstract

Spreading depression (SD) is an interesting and important phenomenon due to its role in mammalian pathologies such as migraine, seizures, and stroke. Until recently investigations of the mechanisms involved in SD have mostly utilized mammalian cortical tissue, however in my thesis I demonstrated that SD-like events occur in the CNS of an invertebrate model, *Locusta migratoria*. Locusts enter comas in response to stress during which neural and muscular systems shut down until the stress is removed, and this is believed to be an adaptive strategy to survive extreme environmental conditions.

Using the ventilatory central pattern generator (vCPG) as a model circuit I was able to show that stress-induced arrest of vCPG function is associated with SD-like events in the locust metathoracic ganglion (MTG) that closely resemble cortical SD (CSD) in many respects, including mechanism of induction, extracellular potassium ion ($[K^+]_o$) changes, and propagation in areas equivalent to mammalian grey matter. SD-like events in the locust were characterized as abrupt $[K^+]_o$ increases associated with electrical activity silence in the locust CNS that propagate to other areas within the MTG. In this thesis I described the generation of comas by several cellular stressors (hyperthermia, metabolic stressors, Na^+/K^+ -ATPase inhibition, and KCl) and the associated SD-like events in the locust, provide a description of the similarities to CSD, and show how they can be manipulated both by stress preconditioning and pharmacologically. I showed that hyperthermic vCPG arrest can be preconditioned by prior heat shock (HS) treatment and induced-thermotolerance was associated with an increased rate of $[K^+]_o$ clearance associated with vCPG recovery that was not linked to changes in ATP levels or total

Na⁺/K⁺-ATPase activity. I also provided evidence for the involvement of the stress-sensor AMP-activated protein kinase (AMPK) in stress-induced comas in the locust. AMPK activation was linked to a switch in motor pattern behavior following recovery from anoxia-induced vCPG arrest and exacerbated repetitive SD-like events induced by ouabain (Na⁺/K⁺-ATPase inhibitor). I suggested that locust SD-like events are adaptive by conserving energy and preventing cellular damage, and I provided a model for the mechanism of SD onset and recovery in the locust nervous system.

Co-Authorship

This thesis consists of four manuscripts on which I am first author.

Chapter 1 (Introduction): Environmental stress-induced comas in locust.

Authors: Rodgers CI*, Armstrong GAB* and Robertson RM.

* Equal first authors.

Journal of Insect Physiology (2010) 56:980-990.

Sections of the Introduction and General Discussion were taken and modified from the above review article on which Armstrong and I are equal first authors. The article will be published in a special issue of the Journal of Insect Physiology on locust research.

Chapter 2: Stress preconditioning of spreading depression in the locust CNS.

Authors: Rodgers CI, Armstrong GAB, Shoemaker KL, LaBrie JD, Moyes CD and Robertson RM.

PLoS ONE (2007) 2:e1366.

I was primarily responsible for the design of all experiments and I collected and analyzed the majority of the data. LaBrie provided some data on ouabain-induced SD-like events. Armstrong provided the data on SD-like events evoked by local injections of KCl and propagation of SD-like events. Armstrong, Shoemaker and LaBrie assisted with the collection of data for ATP and Na⁺/K⁺-ATPase activity assays (with supervision and help from Moyes). I wrote the manuscript with editorial input from Robertson.

Chapter 3: K⁺ homeostasis and central pattern generation in the metathoracic ganglion of the locust.

Authors: Rodgers CI, LaBrie JD and Robertson RM.

Journal of Insect Physiology (2009) 55:599-607.

LaBrie was an undergraduate student under my supervision who collected more than half of the data in this manuscript. I re-worked LaBrie's Honours thesis text, re-analyzed LaBrie's data, and designed the figures in this manuscript. I also collected and analyzed the data shown in Figure 3 and designed the diagram shown in Figure 4 with input from Robertson. LaBrie and I wrote the manuscript with editorial input from Robertson.

Chapter 4:

Authors: Rodgers CI, Yu Y and Robertson RM.

In preparation for The Journal of Neuroscience.

I designed all the experiments, collected and analyzed the majority of data and wrote the manuscript with editorial input from Robertson. Yu collected two datasets that are included in Figures 4.1 and 4.3.

Acknowledgements

First and foremost I would like to acknowledge my supervisor, Mel Robertson. Mel, you recognized my ability to do research and accepted me into your lab as a graduate student six years ago when the odds were against me, and for this I am forever grateful. Thank you for always being fair and flexible, for challenging me, and for helping me reach my potential. Mel I am very grateful to have been a part of the wonderful lab environment that you have created. I would also like to thank all Robertson lab members, past and present, for your help and motivation over the years. I would like to especially thank Gary Armstrong, Tomas Money, and Kelly Shoemaker who have been there for me both personally and professionally during difficult times and who I believe will be lifelong friends.

I would like to thank Chris Moyes and David Andrew for serving as my committee members and for guiding me through each chapter of both my MSc and PhD theses. I would also like to acknowledge Michael O'Donnell, Yuxiang Wang, William Bendena, Sharon Regan and Ken Rose for your important influences during my graduate research at Queen's. I would like to thank my mother, Leslie Rodgers, for persevering with me through the long years of my education, for both emotional and financial support, and for always patiently listening and offering advice. Last, but certainly not least, I would like to thank my husband, Kristopher Garlick, to whom this thesis is dedicated. Kris, you have been nothing but patient, encouraging, and accommodating during my graduate studies and I don't believe I could have reached the end of my PhD without you. Thank you for being my rock over the past six years and for your constant love and support.

Table of Contents

Abstract.....	ii
Co-Authorship.....	iv
Acknowledgements.....	vi
Table of Contents.....	vii
List of Figures.....	ix
List of Abbreviations.....	xi
Chapter 1 - General Introduction: Environmental stress-induced comas in locust....	1
1.1 Introduction.....	2
1.2 Effects of anoxia on neural function and post-anoxic recovery.....	3
1.3 Environmental stress-induced comas in locust.....	8
1.4 Characteristics of spreading depression (SD).....	11
1.5 Preconditioning of neural circuits in locust.....	14
1.6 Energy status.....	17
1.7 Thesis overview.....	19
1.8 References.....	21
Chapter 2: Stress preconditioning of spreading depression in the locust CNS.	35
2.1 Abstract.....	36
2.2 Introduction.....	37
2.3 Results.....	40
2.4 Discussion.....	66
2.5 Materials and Methods.....	72
2.6 References.....	82

Chapter 3: K⁺ homeostasis and central pattern generation in the metathoracic ganglion of the locust.	88
3.1 Abstract	89
3.2 Introduction	90
3.3 Materials and Methods	94
3.4 Results	100
3.5 Discussion	113
3.6 References	122
Chapter 4: Central pattern generation is modulated by AMP-activated protein kinase (AMPK) in response to energy compromise.	127
4.1 Abstract	128
4.2 Introduction	129
4.3 Materials and Methods	132
4.4 Results	137
4.5 Discussion	165
4.6 References	171
5.1 General Discussion	175
5.2 Summary	195
5.3 References	197

List of Figures

Figure 2.1 Stress-induced motor pattern failure is associated with surges of $[K^+]_o$	40
Figure 2.2 Characteristics of $[K^+]_o$ surges	42
Figure 2.S1 Gradual increases in the volume of K^+ injected triggered a tissue response.....	45
Figure 2.3 The hyperthermic $[K^+]_o$ event is not representative of complete collapse of the K^+ gradient.....	47
Figure 2.4 The hyperthermic $[K^+]_o$ event is delayed by TTX and diminished by TEA	49
Figure 2.5 Failure and recovery of the CPG are not dependent on MTG ATP levels.....	52
Figure 2.6 HS and ouabain affect $[K^+]_o$	56
Figure 2.7 HS delays the $[K^+]_o$ event and speeds recovery by increasing the rate of $[K^+]_o$ clearance	58
Figure 2.S2 The degree of the $[K^+]_o$ disturbance was the same in CON and HS locusts ..	61
Figure 3.1 Ouabain-induced inhibition of the Na^+/K^+ -ATPase elicits repetitive $[K^+]_o$ events in a concentration-dependent manner	100
Figure 3.2 Characteristics of $[K^+]_o$ surrounding the vCPG during continuous bath application of 10^{-4} M and 10^{-3} M ouabain	105
Figure 3.3 TEA delayed the onset of ouabain-induced SD and reduced the amplitude of $[K^+]_o$ events.....	109
Figure 3.4 A model for the mechanism of $[K^+]_o$ increase and subsequent recovery in response to cellular stressors in the MTG.....	113
Figure 4.1 Duration and period of expiratory bursts post-recovery from anoxia-induced vCPG arrest progressively increased over time	137
Figure 4.2 Concentration-dependent effects of NaN_3 treatment.....	139

Figure 4.3 NaN ₃ -induced arrest does not appear to cause permanent neuronal damage..	142
Figure 4.4 AMPK inhibition had no effect when induced in non-stressed preparations.....	147
Figure 4.5 AMPK inhibition using compound-C reversed the effects of a high dose of AICAR on the ventilatory motor pattern	149
Figure 4.6 AMPK inhibition using compound-C “reversed” the effects of NaN ₃ and AICAR on the ventilatory motor pattern	151
Figure 4.7 Ouabain-induced repetitive SD-like events in the locust MTG	155
Figure 4.8 AMPK inhibition suppresses ouabain-induced spreading depression.....	157
Figure 4.9 Additional effects of AMPK inhibition on ouabain-induced repetitive SD-like events in the locust MTG.....	161

List of Abbreviations

2DG	2-deoxy-D-glucose
AD	anoxic depolarization
AICAR	5-aminoimidazole-4-carboxamide-1-riboside, or AICA-riboside
AMPK	AMP-activated protein kinase
cGMP	cyclic guanosine monophosphate
CNS	central nervous system
CSD	cortical spreading depression
E_k	equilibrium potential for potassium
EMG	electromyographic
HS	heat shock
HSP	heat shock protein
HSP70	heat shock protein with an average molecular weight of 70 kDa
HSR	heat shock response
$[K^+]_o$	extracellular potassium concentration
LTP	Long Term Potentiation
MTG	metathoracic ganglion
mTOR	mammalian Target of Rapamycin
NaN_3	sodium azide
NMDA	N-methyl-D-aspartate
NO	nitric oxide
NOS	nitric oxide synthase

nNOS	neuronal nitric oxide synthase
ONOO	peroxynitrite
PID	peri-infarct depolarization
PKG	protein kinase G
SD	spreading depression
TEA	tetraethylammonium chloride
TREK	TWIK-related K ⁺ channel
TTX	tetrodotoxin
vCPG	ventilatory central pattern generator
V _m	resting membrane potential
ZMP	AICA-ribotide

Chapter 1 - General Introduction

Environmental stress-induced comas in locust.

1.1 Introduction

In the natural environment of many animals oxygen deprivation or extremes in ambient temperature are examples of unfavourable conditions that can impair the operation of the nervous system and threaten survival long before these conditions directly cause cellular damage. Survival depends on employing coping strategies that preserve the neural circuitry underlying important behaviours. Under conditions of anoxia or high temperature stress many insects enter a reversible coma which is protective. A temporary shutdown of neural and muscular systems can be considered protective by preventing the irreversible consequences of complete energy loss. Until recently the neural underpinnings of coma were little understood. However over the course of my PhD thesis I have helped to describe the phenomena underlying environmental stress-induced coma in locusts. Our lab has found that such coma is associated with dramatic surges of extracellular K^+ concentration ($[K^+]_o$) and temporary electrical silence in the central nervous system (CNS). Remarkably the phenomenon bears all the hallmarks of spreading depression (SD) in vertebrate CNS grey matter. Given the important role of vertebrate SD in a variety of significant neural dysfunctions the ability to address mechanisms in a system that is as eminently accessible and understood as the locust thoracic nervous system is of considerable potential value. The process can be studied in preparations that have intact neuronal architecture allowing the simultaneous investigation of cellular and subcellular neuronal responses with physiological and behavioural responses without anaesthetic.

In this thesis I describe the generation of comas by environmental stressors in locust and make the case that they are equivalent to the mechanisms of cortical SD (CSD). In addition I show that the onset and severity of locust SD can be modulated both by pre-treatments and pharmacologically, suggesting that CSD may be similarly modifiable. Finally I speculate about the future use of this model and suggest experimental steps to substantiate it.

1.2 Effects of anoxia on neural function and post-anoxic recovery

Insects are a highly successful class of invertebrates and this is due in part to their capacity to very efficiently utilize oxygen and ATP for intense activities such as flight. Insect flight muscles have the highest metabolic rates of all muscles and bring about wing-beat frequencies of several hundred Hertz (sec^{-1}) (Wegener, 1993). Land-living insects, like mammals, have evolved aerobic and physiologically active lifestyles due to ample oxygen in the atmosphere (Wegener, 1993). Natural environmental stressors such as low oxygen, therefore, can profoundly affect neural properties and thus have dramatic consequences for insects. In their normal habitat, locusts are subjected to high temperature extremes of up to 60°C at the surface of the substrate (Wehner et al. 1992) and rely on behavioural responses such as postural adjustments (Waloff, 1963) and moving to the shade-cast side of a leaf or branch to survive. In addition to scorching temperatures, flash floods and monsoons are also common occurrences in the habitat of locusts and leave little time for behavioural responses. Development from near-aquatic eggs to first instar hoppers and population transformations from solitary hoppers to gregarious locusts requires high rainfall and thus anoxia by water immersion is a natural

hazard for locusts (Rainey, 1951; Pedgley, 1979; Stige et al. 2007). Young hoppers that cannot escape by flying can experience long periods of submersion under water. Salt-marsh inhabiting spiders (*Arctosa fulvolineata* and *Pardosa purbeckenis*) held under water for up to 36 hours recovered completely after removal, whereas a forest species (*Pardosa lugubris*) had a much reduced tolerance to submersion (Pétillon et al. 2009). Thus arthropods are able to develop tolerance to flooding conditions in their natural habitat by entering a coma state (Pétillon et al. 2009). Mammals are highly vulnerable to lack of oxygen and the ischemia is a common and serious and clinical problem (Krnjević, 2008). Despite their highly aerobic metabolism insects are much more tolerant of oxygen lack than mammals. The ability to tolerate anoxia may be due to differences in the complexity of tissues, especially crucial neural tissues, in insects compared to mammals.

Neither terrestrial insects nor mammals are adapted to survive prolonged periods of anoxia, but mammals are much more vulnerable to anoxia than insects. Insects can fully recover from many hours of anoxia and mammals are irreversibly damaged after only a few minutes of anoxia. This shows that the high metabolic rate of insects is not necessarily connected with a low tolerance of anoxia. The superior ability of insects to tolerate low oxygen may reflect the ease with which oxygen can reach tissues. The insect respiratory system is very efficient due to an elaborate network of tracheae that carry oxygen directly to tissues and even cells (Wegener, 1993). Insect brains and flight muscles have a highly aerobic metabolism and tracheae conveniently supply oxygen to the nervous system and flight muscles independently, avoiding competition (Wegener, 1993). Insect ganglia are solid masses of neural tissue that are isolated and protected by

tissue sheaths forming a “blood-brain barrier”, but are not innervated by capillaries. In contrast, health of the mammalian CNS is directly related to vascular supply of oxygen and nutrients to cells. Even in fully oxygenated tissue high energy demand can be detrimental to tissue that is not in close proximity to capillaries (Takano et al. 2007). In mammals, the response to anoxia involves directing blood flow to preserve CNS and brain function at the expense of other vital organs (Krnjević, 2008). Vascular occlusion quickly results in oxygen/glucose deprivation (OGD), cerebral ischemia, and cell death. Neuronal death due to ischemia reflects both necrosis and apoptosis that have some shared mechanisms but are distinguishable by morphological changes such as cell swelling and loss of cytoplasmic membrane integrity (Snider et al. 1999; Love, 2003). Thus, the necessity of a circulatory system and vascular delivery of oxygen and nutrients to the nervous system in mammals may result in greater vulnerability to low oxygen conditions compared to insects.

Metabolic rate depression via molecular and biochemical mechanisms enables long-term survival in the absence of oxygen in several anoxia-tolerant vertebrates and invertebrates (Storey and Storey, 2004). Metabolic depression reduces heat production and the cellular energy state is stabilized at a much lower level than during normoxia in both anoxia-tolerant vertebrates and invertebrates (Bickler and Buck, 2007). Much research has focused on the freshwater turtle *Trachemys scripta*, a true facultative anaerobe able to survive months in the total absence of oxygen (Milton and Prentice, 2007). Mechanisms permitting neuronal survival in vertebrates adapted to tolerate prolonged full anoxia include decreased K^+ efflux, K_{ATP} channel opening, decreased extracellular glutamate

and dopamine levels, upregulation of heat shock proteins (Hsps), and modulation of MAP kinase pathways (Milton and Prentice, 2007). Similar mechanisms in anoxic insects have not been reported however insects adapted to hypoxic habitats survive by inhibiting key aerobic pathways and switching to anaerobic metabolic pathways (Hoback and Stanley, 2001). Insect larvae seem to be more anoxia-tolerant than adults and can survive prolonged periods of anoxia by drawing on haemoglobin oxygen stores and mechanisms such as alcoholic fermentation and changes in hemolymph solutes (Hoback and Stanley, 2001). Unlike such anoxia-tolerant vertebrates and invertebrates, the functions of all terrestrial insect and mammalian organs are suspended during anoxia exposure. Similarly in terrestrial insects and mammals CNS function is rapidly lost during exposure to anoxia. Both suffer a rapid loss of brain function and body posture, followed by whole-body muscular convulsions (Wegener, 1993). Induction of anoxia in locusts by exposure to pure nitrogen gas, for example, results in elevated escape movements followed by hyperventilation and loss of body coordination within one minute (Wegener, 1993). The locust then falls on its side and the legs twitch, stretch, and tremble, leading to total immobility after one to two minutes of anoxia (Wegener, 1993). Anoxic conditions eventually result in cessation of hemolymph circulation, nerve cell activity, and metabolic flux and a decreased metabolic rate. Decreased metabolic activity during anoxia in locusts is reflected by an abrupt loss in heat production (Wegener, 1993). During anoxia-induced loss of neuronal function ATP decreases to very low levels in insect tissues (the rate of decrease differs in different insect species) and ATP breakdown results in increased ADP, AMP, and IMP (Wegener, 1993; Hoback and Stanley, 2001). The main end-products of anaerobic metabolism in insects are lactate and alanine

(Hoback and Stanley, 2001), although inhibition of glycolysis during anoxia results in only minute increases in these metabolites in the insect brain (Wegener, 1993).

Differences between insects and mammals lie in the capacity to recover from anoxia. Mammals cannot last more than a few minutes in anoxia, whereas insects can be kept in pure nitrogen for many hours and yet recover fully and spontaneously when air is readmitted (Wegener, 1993). Anoxic insect tissues resemble ischemic vertebrate tissues in that there is a lack of hemolymph circulation. Thus, both have to rely on carbohydrate substrates that are readily available in tissues of close proximity in response to anoxia (Wegener, 1993). In contrast to insects, glycolytic flux dramatically increases in the ischemic mammalian brain and the build-up of lactate and acidosis in mammalian tissues may complicate recovery from anoxia (Wegener, 1993). Post-anoxic recovery in mammals is directly related to the capacity to stabilize cellular energy status and the ATP loss that occurs in anoxic insects would result in cell death (Wegener, 1993). When insects are returned to air after 60 minutes of anoxia, ATP is rapidly resynthesized and the energy state of the brain is almost normal after only 5 minutes of recovery (Wegener, 1993). ATP by-products are retained in the tissues of anoxic insects and hence ATP can readily be resynthesized when oxygen is readmitted. This is due to the presence of adenylates, especially AMP, in insect tissues despite dramatic ATP loss in insect organs during prolonged anoxia (Wegener, 1993). Rapid loss of adenylates in capillarized mammalian tissues could be due to wash out of ATP byproducts during reperfusion thus preventing metabolism and anaerobic catabolism of AMP (Wegener, 1993). Postanoxic recovery in insects is largely dependent on respiration through tracheae that allow easy

access of oxygen to tissues independent of circulation (Wegener, 1993). In vertebrates, postanoxic recovery depends on reperfusion which can be insufficient when there is lack of circulation (Wegener, 1993).

Thus, insects provide interesting experimental animals for investigating the physiological mechanisms of stress tolerance, especially the properties that enable tissue survival during anoxia. In my thesis I investigated the cellular events during stress-induced comas in the African migratory locust (*Locusta migratoria*) and the nature of neural circuit recovery following severe stresses such as anoxia.

1.3 Environmental stress-induced comas in locust

In response to anoxic conditions locusts experience a silencing of activity in the nervous and muscular systems that we interpret as a stress-induced coma. After return to normoxia, locusts completely recover from up to at least 6 hours of anoxia-induced coma (Wu et al. 2002; Armstrong et al. 2009). Given the reversibility of locust comas it is likely that locusts enter this state as a protective strategy to cope with environmental stressors. Ambient temperature is a major stress for insects inhabiting highly variable thermal environments and environmental temperature fluctuation can strongly influence neuronal circuit function and the behaviour of animals. Our locust research has largely focused on the effects of high temperature stress on a locust model of CNS function, the operation of the ventilatory central pattern generator (vCPG) (Newman et al. 2003; Robertson, 2004b; Armstrong and Robertson, 2006; Rodgers et al. 2006).

The vCPG is a robust neuronal circuit that controls ventilation, a crucial motor activity to locusts. Ventilation is a continuous rhythm that expands and contracts the abdomen of the locust and is responsible for circulation of respiratory gases through the tracheal system as well as heat dissipation with increased ventilatory frequency (Albrecht, 1953; Prange, 1990, 1996). The vCPG is located in the metathoracic ganglion (MTG) and the rhythm is generated within the first three fused abdominal neuromeres (Hustert, 1975; Burrows, 1996; Bustami and Hustert, 2000). Using a semi-intact preparation (Newman et al. 2003) we are able to obtain extracellular recordings from both nerves and muscles, as well as intracellular recordings from ventilatory neurons within the ganglion. Locusts ventilate discontinuously while at rest and at room temperature and ventilate continuously when exposed to stressful conditions which allows easy determination of vCPG arrest and recovery. In our experimental protocols standard locust saline at room temperature is bath-applied over the MTG in semi-intact preparations for 10 to 20 minutes prior to experimental treatments. At this stage, the frequency of the ventilatory motor pattern is around 1Hz (Newman et al. 2003). An increase in ventilatory frequency occurs during increased activity, heat stress, and octopamine neuromodulation (Newman et al. 2003; Rodgers et al. 2006; Armstrong and Robertson, 2006). Ventilation is thermosensitive and a ramped increase in the saline temperature increases the frequency of ventilatory bursts and decreases the duration of ventilatory bursts. At higher temperatures arrhythmias occur prior to vCPG arrest and electrical silence at ~40°C. A subsequent return to room temperature permits recovery of pattern generation within 2 to 3 minutes (Newman et al. 2003; Armstrong and Robertson, 2006). Given the importance of ionic gradients in neuronal signaling it is not surprising that hyperthermia-induced

failure of ventilation and the associated neural activity silence is associated with an extracellular K^+ concentration ($[K^+]_o$) disturbance within the MTG.

To measure changes in $[K^+]_o$ associated with vCPG arrest a K^+ -sensitive microelectrode can be inserted through the sheath of the MTG into the extracellular space surrounding the vCPG and referenced to an adjacent voltage electrode. There are likely ionic gradients across the MTG sheath, or blood-brain-barrier, in the locust as in cockroaches (Treherne and Schofield, 1981) however we only place electrodes within the extracellular space of the MTG. To monitor vCPG output from a ventilatory muscle an electromyographic (EMG) electrode can be placed on ventilatory muscle 176 in the abdomen of the locust. To determine the extent of neuronal depolarization associated with vCPG arrest, sharp intracellular microelectrodes are used to record neuronal activity in the MTG concurrently with recordings of the ventilatory motor pattern and $[K^+]_o$. Measurements of $[K^+]_o$ made in the MTG revealed a tight correlation between heat-induced arrest of ventilatory motor pattern generation and a surge in $[K^+]_o$ surrounding the vCPG. The rapid rise in $[K^+]_o$ at the moment of heat-induced CNS failure increased from a baseline level of 10 mM to a plateau of around 50 mM (Robertson, 2004b). When the heater was switched off and the superfusing saline was allowed to return to room temperature, $[K^+]_o$ returned to pre-surge levels and ventilatory motor pattern generation recovered. This ionic disturbance in the locust MTG is very similar to disturbances associated with spreading depression (SD) in mammalian cortex (Somjen, 2001, 2002). In this thesis I examined $[K^+]_o$ changes during stress-induced comas in response to

multiple different stressors in the locust MTG to characterize these events and determine their similarity to SD-like events that occur in mammalian cortical tissue.

1.4 Characteristics of spreading depression (SD)

SD can be defined as a major redistribution of ions and nearly complete depolarization of neurons that propagates across cortical gray matter (Somjen, 2001). SD was first discovered in 1944 by Aristides Leão (Leão, 1944), and therefore is often referred to as Leão's SD. SD has been widely studied in mammals ranging from mouse to human (Leão, 1944; Van Harreveld et al. 1956a; Van Harreveld and Khattab, 1967; Aitken et al. 1991; Gorji et al. 2001), and the characteristic depression of electrical activity and associated $[K^+]_o$ changes have also been observed in insects (Hoyle, 1952; Chapman, 1958; Rounds, 1967). When SD occurs in cortex it is referred to as cortical SD (CSD) and constitutes the neurological basis of migraine with aura (Hadjikhani et al. 2001), and is also associated with other pathologies including stroke and seizures.

During SD, spike inactivation and silencing of electrical activity reflects a massive redistribution of ions across neuronal membranes (Somjen, 2001). SD provokes large increases in $[K^+]_o$ (Vyskočil et al. 1972; Müller and Somjen, 2000) and decreases in the extracellular concentrations of chloride ($[Cl^-]_o$), sodium ($[Na^+]_o$), and calcium $[Ca^{2+}]_o$ (Müller and Somjen, 2000; Jiang et al. 1992; Basarasky et al. 1998). This disordered regulation of ionic homeostasis results in neuronal hyperexcitation followed by suppression of electrical activity. Neuronal hyperexcitation and spontaneous bursting of action potentials known as 'prodromal spikes' at the onset of the SD wave front is due to

increased $[K^+]_o$, which depolarizes neurons (Huxley and Stämpfli, 1951; Snow et al. 1983; Czéh et al. 1993; Müller and Somjen, 2000). A substantial neuronal depolarization and strong DC field potential shift are important characteristics of SD (Müller and Somjen, 2000). The membrane potential of CA1 pyramidal neurons depolarized completely, to zero or close to zero, during SD (Snow et al. 1983; Czéh et al. 1993). This depolarization and the associated synaptic activity cessation propagate across cortical gray matter at a rate of 2-5mm/min and propagation is resistant to areas of the CNS that contain white matter such as the spinal cord (Grafstein, 1956; Van Harreveld et al. 1956b; Hull and Van Harreveld, 1964; Nicholson et al. 1978; Czéh and Somjen, 1990).

SD can be induced by means that affect ionic homeostasis such as contusions, chemicals, and high frequency stimulation (Leão, 1944; Leão and Morrison, 1945; Balestrino, 1999; Müller and Ballanyi, 2003). SD can be evoked by anoxia, ouabain, simulated ischemia, and increased $[K^+]_o$ at normal temperature as well as hyperthermia (Wu and Fisher, 2000). Targeting of the Na/K pump using ouabain has been widely used to induce SD (Haglund and Schwartzkroin, 1990; Balestrino et al. 1999; Menna et al. 2000; Xiong and Stringer, 2000; Leis et al. 2005). SD has generally been considered benign when coursing through normoxic tissue, however a recent paper provided evidence that SD is linked to hypoxia and neuronal swelling even when oxygen supply is sufficient (Takano et al. 2007). Oxygen/glucose deprivation (OGD) results in anoxic depolarization (AD), a situation during ischemia or stroke when the depolarization occurs in response to oxygen deprivation and there is insufficient energy available for recovery. During ischemia, OGD results in cell damage such as dendritic beading and cell death, forming an

ischemic infarct. AD is often termed “terminal depolarization” due to the severity of tissue damage, which is highly dependent on vasculature (Obeidat and Andrew, 1998; Joshi and Andrew, 2001; Somjen, 2001). Peri-infarct depolarization’s (PIDs) are spontaneous SDs that expand the ischemic infarct, further contributing to cell damage and death during OGD (Fabricius et al. 2005).

Several compounds have been shown to block the initiation of CSD, including NMDA receptor antagonists and gap junction inhibitors, but once a wave of CSD is evoked its propagation is insensitive to a number of NMDA receptor antagonists and channel inhibitors. Increased $[K^+]_o$ in combination with low energy allows $[K^+]_o$ to diffuse forward along its concentration gradient and propagate across cortex (due to the inability to clear $[K^+]_o$) (Takano, 2007). The inability to identify a transmitter system responsible for propagation of CSD does indirectly support the notion that K^+ and hypoxia drive the forward movement of CSD (Takano, 2007). Studies suggest opening of intercellular gap junctions as a mechanism of SD propagation in vertebrates (Nedergaard et al. 1995; Largo et al. 1997; Thompson et al. 2006). Involvement of gap junction hemichannels may be a mechanism of propagation in the insect CNS as well in which glia are involved in ion homeostasis, function, and development of the insect brain (Kretzschmar and Pflugfelder, 2002).

In this thesis I monitored $[K^+]_o$ increases and propagation within the locust CNS as an indicator of SD in the locust. An interesting question is whether or not SD-like events can be interpreted as being adaptive. Susceptibility to migraine is determined by genetic

factors and given that recurrent, severe headache is prevalent among humans it is possible that this disorder could confer a reproductive or survival advantage (Loder, 2002). An interesting evolutionary explanation for migraine is that migraine may represent a trade-off between the benefits and costs of the disorder, i.e. the benefit of enhanced CNS excitability in migraine-prone individuals outweighs the cost of severe headache and disability (Loder, 2002). Ofcourse, heterozygotes or individuals who inherit some of the genes associated with migraine would have several survival advantages that outweigh the disadvantages experienced by homozygotes who inherit too many or too few of these genes (Loder, 2002). Throughout my thesis I provide evidence for an adaptive role for SD-like events in the locust.

1.5 Preconditioning of neural circuits in locust

In the natural habitat of locusts ambient temperature can fluctuate daily by 45°C (Uvarov, 1977) and during extremes in temperature neuronal function can be impaired. Locusts are routinely exposed to ambient temperatures >40°C, and during vigorous activity such as flight the temperature in the thorax can be as much as 10°C above ambient (Weis-Fogh, 1956). Since locusts are poikilothermic, their internal temperature is vulnerable to temperature fluctuations in their environment. Adaptations exist that allow continued neural functions of locusts and other insect species during acute heat stress and it is well established that locusts can be preconditioned to better tolerate such stresses. Exposure to a heat shock pre-treatment (HS: 3 hours, 45°C) protects several important neural properties in locusts such that neural function is improved during exposure to subsequent high temperature stress (Robertson, 2004a). Extensions in the operating range of crucial

neural circuits in the locust occur within hours following HS pre-treatment and can last for several weeks (Robertson et al. 1996), indicating that induction of a heat shock response (HSR) involves long-term physiological changes. *Locusta migratoria* adults exposed to 45°C for 3 hours experienced coincident enhanced heat shock protein (Hsp) expression and improved thermotolerance during a subsequent, normally lethal temperature stress (Whyard et al. 1986). Expression of Hsps is a universal response to several forms of cellular stress, including high temperature, oxidative, and anoxic stresses (Parsell et al. 1993; Kiang and Tsokos, 1998; Feder and Hofmann, 1999; Sharp et al. 1999; Dalle-Donne et al. 2001; Wu et al. 2002). Hsps have a number of roles in mitigating cellular damage in the nervous system, including protein chaperoning, refolding proteins to their native states, and stabilization of the cytoskeleton (Feder, 1996; Liang and MacRae, 1997; Feder and Hofmann, 1999; Sharp et al. 1999; Klose et al. 2004). The mechanisms by which environmental variables induce adaptive phenotypic changes of crucial neural circuits are also believed to involve induction of neuromodulators such as serotonin and octopamine (Armstrong and Robertson, 2006; Armstrong et al. 2006). A short bout of full anoxia protects neural function against subsequent high temperature stress in the locust, possibly via activation of similar cellular responses (Wu et al. 2002). It is not yet known how prior energetic stress affects subsequent tolerance to low energy stress, and this poses an interesting question for future research.

The protective effects of HS preconditioning have been well established in locust preparations. For example, following HS treatment the operating range of the flight CPG

was extended by 6-7 °C (Robertson et al. 1996). Exposure to HS pre-treatment induced protection of the hindleg neuromuscular system at high temperatures by increasing the temperature at which neuromuscular transmission failed by ~8°C, reducing the time to recovery following heat-induced failure, and decreasing the thermosensitivity of muscle contraction (Barclay and Robertson, 2000). There is evidence that HS-induced synaptic thermoprotection in *Locusta migratoria* extensor tibiae muscle is conferred through cytoskeletal stabilization (Klose et al. 2004). The locust descending contralateral movement detector (DCMD) relays vital information about the looming approach of predators from the brain to the thorax. Following HS preconditioning, peak firing frequency was increased and axonal action potential properties of DCMD such as half-width duration, amplitude, and membrane potential, were maintained with increased temperature (Money et al. 2005; Money et al. 2006). Given the essential nature of the vCPG, it is not surprising that HS pre-treatment also protects this neuronal circuit against high temperature stress. HS-mediated thermoprotection of the vCPG results in sustained operation at higher temperatures than control preparations and a decrease in the length of time taken to recover from heat-induced coma (Armstrong et al. 2006).

The increased ability for the vCPG of heat shocked locusts to function during high temperature stress may reflect an adaptive effect of HS in maintaining ion flow across membranes and ionic gradients necessary for proper functioning. In the locust there is evidence that the HS protective mechanism may induce adaptive modification of ion channel properties. It has been shown that prior stress reduced whole cell K⁺ currents from neuronal somata in locust metathoracic ganglion slices (Ramirez et al. 1999; Wu et

al. 2002). Also, pharmacological block of K^+ channels with tetraethylammonium chloride (TEA) mimics the thermoprotective effects of a prior HS and prior anoxic stress on action potentials in locust flight motoneurons (Wu et al. 2001, 2002). Downregulation of K^+ currents would be protective by increasing the duration of action potentials and preventing the accumulation of $[K^+]_o$. Given all of this evidence it is reasonable to suspect that HS preconditioning acts by stabilizing K^+ homeostasis.

1.6 Energy status

At extremes, abiotic stressors such as high temperature and low oxygen induce failure of neuronal function, an abrupt rise in $[K^+]_o$, and neuronal depolarization. A subsequent period of electrical activity silence ensues that we have defined as a stress-induced coma. Removal of the stressor shortly following coma onset results in recovery of neuronal function. vCPG operation fully recovers, i.e. the animal generates rhythmic ventilatory movements, following failure induced by high temperature and anoxic stressors. It is not clear whether irreparable neuronal damage occurs as a consequence of anoxia in locusts as is the case with ischemic mammalian cortical tissue. The fact that locusts behave normally following hours of whole animal exposure to N_2 gas suggests that the metabolic response to anoxia involves mechanisms that prevent complete energy depletion and irreversible cellular damage. A well-known pathway involved in detecting and prioritizing cellular energy resources is the AMP-activated protein kinase (AMPK) pathway. It was of interest to determine if stress-induced comas in the locust coincide with AMPK activation and if this activation alters energy utilization at the expense of neuronal performance.

Possession of AMPK complexes is a universal feature of eukaryotes (Hardie et al. 2003) and we thus reasoned that AMPK may be involved in the stress response of the locust. The energy available to drive anabolic processes is due to the maintenance of intracellular ATP:ADP within tight limits and it is believed that the AMPK cascade is involved in this process (Hardie et al. 2003). This enzyme is activated both by phosphorylation by an upstream kinase and allosterically by AMP (Lindsley and Rutter, 2004). When ATP is depleted by cellular stresses such as glucose deprivation, ischemia, hypoxia, oxidative stress, and hyperosmotic stress, rising AMP coupled with falling ATP results in an increased AMP:ATP ratio and AMPK activation (Hardie et al. 2003). Upon activation AMPK increases cellular energy levels by arresting nonessential ATP-utilizing functions and stimulating available ATP-generating pathways (Lindsley and Rutter, 2004). In the locust, the AMPK pathway could be triggered well before ATP levels are depleted, signaling metabolic stress before complete energy deprivation. Activation of AMPK and conservation of energy in response to stress may trigger changes in energy usage upon recovery from stress-induced comas that affect vCPG output. Clearly energy is available upon recovery from stress-induced comas, but an important question is what effect energy rationing has on the function of neurons in the vCPG circuit. An important question is whether or not trade-offs exist between energy conservation and neuronal performance. vCPG function is vital to survival, however the vCPG circuit is highly energetically costly. Action potential generation and maintenance of ionic homeostasis by the Na^+/K^+ -ATPase to which 50-60% of neuronal ATP levels are devoted (Erecinska and Silver, 1994). I ended off my PhD thesis by investigating the potential role of the

AMPK in stress-induced comas in the locust, and if changed performance of the vCPG could be linked to induction of AMPK.

1.7 Thesis overview

The locust presents an interesting model for studying the effects of heat and anoxia on the nervous system. Locusts are extremely tolerant of both high temperature and low oxygen conditions and their nervous system is easily accessible while the animal is intact and behaving. This has allowed me to use a variety of electrophysiological and pharmacological techniques to manipulate the vCPG and assess tolerance to cellular stressors. The underlying theme of my PhD thesis is the description of SD in the locust ventilatory neuropile and the mechanisms that suppress or attenuate locust SD-like events. This thesis consists of three data chapters presented in chronological order.

I simultaneously monitored the ventilatory motor pattern and $[K^+]_o$ changes within the metathoracic neuropile of the vCPG during hyperthermia, anoxia, and treatments that disturb the K^+ equilibrium (ouabain, neuropile injections of KCl). In the first data chapter I used the above treatments to induce vCPG arrest and coincident $[K^+]_o$ changes within the MTG and made the case that these $[K^+]_o$ events and associated electrical activity silence resemble SD in mammalian cortical tissue. I concluded that stress-induced $[K^+]_o$ events in the locust are “SD-like” and further investigated their similarity to SD in mammalian cortical tissue using Na^+ and K^+ channel inhibitors, more complex heat and anoxia manipulations, and measurements of ATP levels and total Na^+/K^+ -ATPase activity within the MTG. It was of interest to determine if HS preconditioning

affects SD-like events in the locust. I examined $[K^+]_o$ properties during hyperthermia-induced SD-like events before and after HS pre-treatment to determine if HS acts by stabilizing K^+ homeostasis. In the second data chapter I further investigated the role of the Na^+/K^+ -ATPase and voltage-gated K^+ channels in locust SD-like events. SD-like events induced by ouabain presented an interesting paradigm and it was of interest to more thoroughly characterize SD-like events induced by Na^+/K^+ -ATPase inhibition. In the first two data chapters I suggested that SD-like events in the locust may be an adaptive response to conserve energy and prevent neuronal excitotoxicity before complete energy loss. In the final data chapter I was interested in further substantiating this idea and whether the energy sensor AMPK is activated during SD-like events in the locust. I pharmacologically manipulated AMPK to test the involvement of AMPK in vCPG recovery following chemical anoxia using sodium azide (NaN_3). I also manipulated AMPK to determine if AMPK activation and inhibition had modulatory effects on ouabain-induced SD-like events in the locust.

Together, these three chapters describe the occurrence of SD-like events in the locust, modulation of these events by HS preconditioning, and the role of the Na^+/K^+ -ATPase, ion channels, and AMPK in the locust stress response.

1.8 References

Aitken PG, Tombaugh GC, Turner DA, Somjen GG (1998) Similar propagation of SD and hypoxic SD-like depolarization in rat hippocampus recorded optically and electrically. *J Neurophysiol* 80:1514-1521.

Albrecht FO (1953) *The anatomy of the migratory locust*. University of London. The Athlone Press.

Armstrong GAB, Robertson RM (2006) A role for octopamine in coordinating thermoprotection of an insect nervous system. *J Thermal Biol* 31:149-158.

Armstrong GAB, Rodgers CI, Money TGA, Robertson RM (2009) Suppression of spreading depression-like events in locusts by inhibition of the NO/cGMP/PKG pathway. *J Neurosci* 29:8225-8235.

Armstrong GAB, Shoemaker KL, Money TGA, Robertson RM (2006) Octopamine mediates thermal preconditioning of the locust ventilatory central pattern generator via a cAMP/protein kinase A signaling pathway. *J Neurosci* 26:12118-12126.

Balestrino M, Young J, Aitken PG (1999) Block of $(\text{Na}^+, \text{K}^+)\text{ATPase}$ with ouabain induced spreading depression-like depolarization in hippocampal slices. *Brain Res* 838:37-44.

Barclay JW, Robertson RM (2000) Heat shock induced thermoprotection of hindleg motor control in the locust. *J Exp Biol* 203:941-950.

Basarasky TA, Duffy SN, Andrew RD, MacVicar BA (1998) Imaging spreading depression and associate intracellular calcium waves in brain slices. *J Neurosci* 18:7189-7199.

Bickler PE, Buck LT (2007) Hypoxia tolerance in reptiles, amphibians, and fishes: life with variable oxygen availability. *Annu Rev Physiol* 69:145-70.

Burrows M (1996) *The neurobiology of an insect brain*. Oxford University Press, Oxford.

Bustami HP, Hustert R (2000) Typical ventilatory pattern of the intact locust is produced by the isolated CNS. *J Insect Physiol* 46:1285-1293.

Chapman RF (1958) A field study of the potassium concentration in the blood of the red locust *Nomadacris septemfasciata* (Serv.), in relation to its activity. *Anim Behav* 6:60-67.

Czéh G, Aitken PG, Somjen GG (1993) Membrane currents in CA1 pyramidal cells during spreading depression (SD) and SD-like hypoxic depolarization. *Brain Res* 632:195-208.

Czéh G, Somjen GG (1990) Hypoxic failure of synaptic transmission in the isolated spinal cord, and the effects of divalent cations. *Brain Res* 527:224-233.

Dalle-Donne I, Rossi R, Milzani A, Di Simplicio P, Colombo R (2001) The actin cytoskeleton response to oxidants: from small heat shock protein phosphorylation to changes in the redox state of actin itself. *Free Radic Biol Med* 31:1624–1632.

Dawson-Scully K, Armstrong GAB, Kent C, Robertson RM, Sokolowski MB (2007) Natural variation in the thermotolerance of neural function and behavior due to a cGMP-dependent protein kinase. *PLoS ONE* 2:e773 (doi:10.1371/journal.pone.0000773).

Erecinska M, Silver IA (1994) Ions and energy in mammalian brain. *Prog Neurobiol* 43:37-71.

Fabricius M, Fuhr S, Bhatia R, Boutelle M, Hashemi P, Strong AJ, Lauritzen M (2005) Cortical spreading depression and peri-infarct depolarization in acutely injured human cerebral cortex. *Brain* 129:778-790.

Feder ME (1996) Ecological and evolutionary physiology of stress proteins and the stress response: the *Drosophila melanogaster* model. In: *Animals and temperature: phenotypic and evolutionary adaptation*, pp79-102. Cambridge, UK: Cambridge University Press.

Feder ME, Hofmann GE (1999) Heat-shock proteins, molecular chaperones, and the stress response: evolutionary and ecological physiology. *Annu Rev Physiol* 61:243–282.

Gorji A, Scheller D, Straub H, Tegtmeier F, Köhling R, Höhling J-M, Tuxhorn I, Ebner A, Wolf P, Panneck HW, Ooppel F, Speckmann E-J (2001) Spreading depression in human neocortical slices. *Brain Res* 906:74-83.

Grafstein B (1956) Mechanism of spreading cortical depression. *J Neurophysiol* 19:154-171.

Hadjikhani N, Sanchez Del Rio M, Wu O, Schwartz D, Bakker D, Fischl B, Kwong KK, Cutrer FM, Rosen BR, Tootell RB, Sorensen AG, Moskowitz MA (2001) Mechanisms of migraine aura revealed by functional MRI in human visual cortex. *Proc Natl Acad Sci* 98:4687-4692.

Haglund MM, Schwartzkroin PA (1990) Role of Na-K pump potassium regulation and IPSPs in seizures and spreading depression in immature rabbit hippocampal slices. *J Neurophysiol* 63:225-239.

Hardie DG, Scott JW, Pan DA, Hudson ER (2003) Management of cellular energy by the AMP-activated protein kinase system. *FEBS Letters* 546:113-120.

Hoback WW, Stanley DW (2001) Insects in hypoxia. *J Insect Physiol* 47:533-542.

Hoyle G (1952) High blood potassium in insects in relation to nerve conduction. *Nature* 169:281-282.

Hull CD, Van Harreveld A (1964) Absence of conduction of spreading depression through cortical region damaged by asphyxiation. *Am J Physiol* 207:921-924.

Hustert R (1975) Neuromuscular coordination and proprioceptive control of rhythmical abdominal ventilation in intact *Locusta migratoria migratorioides*. *J Comp Physiol A* 97:159-179.

Huxley AF, Stämpfli R (1951) Effect of potassium and sodium on resting and action potentials of single myelinated nerve fibers. *J Physiol* 112:496-508.

Jiang C, Agulian S, Haddad GG (1992) Cl^- and Na^+ homeostasis during anoxia in rat hypoglossal neurons: intracellular and extracellular *in vitro* studies. *J Physiol* 448:697-705.

Joshi I, Andrew RD (2001) Imaging anoxic depolarization during ischemia-like conditions in the mouse hemi-brain slice. *J Neurophysiol* 84:414-424.

- Kiang JG, Tsokos GC (1998) Heat shock protein 70 KDa: molecular biology, biochemistry and physiology. *Pharmac Ther* 80:183-201.
- Klose M, Armstrong G, Robertson RM (2004) A role for the cytoskeleton in heat shock-mediated thermoprotection of locust neuromuscular junctions. *J Neurobiol* 60:453-462.
- Kretschmar D, Pflugfelder GO (2002) Glia in development, function, and neurodegeneration of the adult insect brain. *Brain Res Bull* 57:121-131.
- Krnjević K (2008) Electrophysiology of cerebral ischemia. *Neuropharmacol* 55: 319-333.
- Largo C, Tombaugh GC, Aitken PG, Herreras O, Somjen GG (1997) Heptanol but not fluoroacetate prevents the propagation of spreading depression in rat hippocampal slices. *J Neurophysiol* 77:9-16.
- Leão AAP (1944) Spreading depression of activity in the cerebral cortex. *J Neurophysiol* 7: 359-390.
- Leão AAP, Morrison RS (1945) Propagation of spreading cortical depression. *J Neurophysiol* 8:33-45.
- Leis JA, Bekar LK, Walz W (2005) Potassium homeostasis in the ischemic brain. *Glia* 50:407-416.

Liang P, MacRae TH (1997) Molecular chaperones and the cytoskeleton. *J Cell Sci* 110:1431-1440.

Lindsley JE, Rutter J (2004) Nutrient sensing and metabolic decisions. *Comp Biochem Physiol B Biochem Mol Biol* 139:543-559.

Loder E (2002) What is the evolutionary advantage of migraine? *Cephalalgia* 22:624-632.

Love S (2003) Apoptosis and brain ischaemia. *Prog Neuropsychopharmacol Biol Psychiatry* 27:267-282.

Menna G, Tong CK, Chesler M (2000) Extracellular pH changes and accompanying cation shifts during ouabain-induced spreading depression. *J Neurophysiol* 83:1338-1345.

Milton SL, Prentice HM (2007) Beyond anoxia: The physiology of metabolic downregulation and recovery in the anoxia-tolerant turtle. *Comp Biochem Physiol A* 147:277-290.

Money TGA*, Anstey ML*, Robertson RM (2005) Heat stress-mediated plasticity in a locust looming-sensitive visual interneuron. *J Neurophysiol* 93:1908-1919.

- Money TGA, De Carlo CA, Robertson RM (2006) Temperature-sensitive gating in a descending visual interneuron, DCMD. *J Comp Physiol A* 192:915-925.
- Müller M, Ballanyi K (2003) Dynamic recording of cell death in the in vitro dorsal vagal nucleus of rats in response to metabolic arrest. *J Neurophysiol* 89:551-561.
- Müller M, Somjen GG (2001) Intrinsic optical signals in rat hippocampal slices during hypoxia-induced spreading depression-like depolarization. *J Neurophysiol* 82:1818-1831.
- Nedergaard M, Cooper AJL, Goldman SA (1995) Gap junctions are required for the propagation of spreading depression. *J Neurobiol* 28:433-444.
- Newman AEM, Foerster M, Shoemaker KL, Robertson RM (2003) Stress-induced thermotolerance of ventilatory motor pattern generation in the locust, *Locusta migratoria*. *J Insect Physiol* 49:1039-1047.
- Nicholson C, Ten Bruggencate G, Stöckle H, Steinberg R (1978) Calcium and potassium changes in extracellular microenvironment of cat cerebellar cortex. *J Neurophysiol* 41:1026-1039.
- Obeidat AS, Andrew RD (1998) Spreading depression determines acute cellular damage in the hippocampal slice during oxygen/glucose deprivation. *Euro J Neurosci* 10:3451-3461.

Parsell DA, Taulien J, Lindquist S (1993) The role of heat-shock proteins in thermotolerance. *Philos Trans R Soc Lond B Biol Sci* 339:279–285.

Pedgley DE (1979) Weather during desert locust plague upsurges. *Phil Trans R Soc Lond B* 287:387.

Pétillon J, Montaigne W, Renault D (2009) Hypoxic coma as a strategy to survive inundation in a salt-marsh inhabiting spider. *Biol Lett* 5:442-445.

Prange HD (1990) Temperature regulation by respiratory evaporation in grasshoppers. *J Exp Biol* 154:463-474.

Prange HD (1996) Evaporative cooling in insects. *J Insect Physiol* 42:493-499.

Rainey RC (1951) Weather and the movements of locust swarms: a new hypothesis. *Nature* 168:1057.

Ramirez JM, Elsen FP, Robertson RM (1999) Long-term effects of prior heat shock on neuronal potassium currents recorded in a novel insect ganglion slice preparation. *J Neurophysiol* 81:795-802.

Robertson RM (2004a) Modulation of neural circuit operation by prior environmental stress. *Integr Comp Biol* 44:21-27.

Robertson RM (2004b) Thermal stress and neural function: adaptive mechanisms in insect model systems. *J Therm Biol* 29:351-358.

Robertson RM, Xu H, Shoemaker K, Dawson-Scully K (1996) Exposure to heat shock affects thermosensitivity of the locust flight system. *J Neurobiol* 29:367-383.

Rodgers CI, Shoemaker KL, Robertson RM (2006) Photoperiod-induced plasticity of thermosensitivity and acquired thermotolerance in *Locusta migratoria*. *J Exp Biol* 209:4690-4700.

Rounds HD (1967) KCl-induced 'spreading depression' in the cockroach. *J Insect Physiol* 13:869-872.

Sharp FR, Massa SM, Swanson RA (1999) Heat-shock protein protection. *Trends Neurosci* 22:97-99.

Snider BJ, Gottron FJ, Choi DW (1999) Apoptosis and necrosis in cerebrovascular disease. *Ann N Y Acad Sci* 893:243-253.

Snow RW, Taylor CP, Dudek FE (1983) Electrophysiological and optical changes in slices of rat hippocampus during spreading depression. *J Neurophysiol* 50:561-572.

Somjen GG (2001) Mechanisms of spreading depression and hypoxic spreading depression-like depolarization. *Physiol Rev* 81:1065-1096.

Somjen GG (2002) Ion regulation in the brain: implications for pathophysiology. *Neuroscientist* 8:254-267.

Stige LC, Chan K-S, Zhang Z, Frank D, Stenseth NC (2007) Thousand-year-long Chinese time series reveals climatic forcing of decadal locust dynamics. *Proc Natl Acad Sci USA* 104:16188.

Storey KB, Storey JM (2004) Metabolic rate depression in animals: transcriptional and translational controls. *Biol Rev* 79:207-233.

Takano T, Tian G-F, Peng W, Lou N, Lovatt D, Hansen AJ, Kasischke KA, Nedergaard M (2007) Cortical spreading depression causes and coincides with tissue hypoxia. *Nat Neurosci* 10:754-762.

Thompson RJ, Zhou N, MacVicar BA (2006) Ischemia opens neuronal gap junction hemichannels. *Science* 312:924-927.

Treherne JE, Schofield PK (1981) Mechanisms of ionic homeostasis in the central nervous system of an insect. *J Exp Biol* 95:61-73.

Uvarov B (1977) Grasshoppers and locusts: a handbook of general acridology. Vol 2. University Press, Cambridge.

Van Harreveld A, Khattab FI (1967) Changes in cortical extracellular space during spreading depression investigated with the electron microscope. *J Neurophysiol* 30:911-927.

Van Harreveld A, Stamm JS, Christensen E (1956a) Spreading depression in rabbit, cat and monkey. *Am J Physiol* 184:312-320.

Van Harreveld A, Terres G, Dernburg EA (1956b) Cortical discontinuity and propagation of spreading depression. *Am J Physiol* 184:233-238.

Vyskočil F, Kříž N, Bureš J (1972) Potassium-selective microelectrodes used for measuring the extracellular brain potassium during spreading and anoxic depolarization in rats. *Brain Res* 39:255-259.

Waloff Z (1963) Field studies on solitary and *transiens* desert locusts in the Red sea area. *Anti-Locust Bull* 40:1-93.

Wegener G (1993) Hypoxia and posthypoxic recovery in insects: physiological and metabolic aspects. In: Surviving hypoxia: mechanisms of control and adaptation, pp417-434. Boca Raton FL: CRC Press, Inc.

Wehner R, Marsh AC, Wehner S (1992) Desert ant on a thermal tightrope. *Nature* 357:586-587.

Weis-Fogh T (1956) Biology and physics of locust flight. II. Flight performance of the desert locust (*Schistocerca gregaria*). *Philos Trans R Soc Lond B* 239:459–510.

Whyard S, Wyatt GR, Walker VK (1986) The heat shock response in *Locusta migratoria*. *J Comp Physiol B* 156:813-817.

Wu BS, Lee JK, Thompson KM, Walker VK, Moyes CD, Robertson RM (2002) Anoxia induces thermotolerance in the locust flight system. *J Exp Biol* 205:815-827.

Wu BS, Walker VK, Robertson RM (2001) Heat shock-induced thermoprotection of action potentials in the locust flight system. *J Neurobiol* 49:188-199.

Wu J, Fisher RS (2000) Hyperthermic spreading depressions in the immature rat hippocampal slice. *J Neurophysiol* 84:1355-1360.

Xiong ZQ, Stringer JL (2000) Sodium pump activity, not glial spatial buffering, clears potassium after epileptiform activity induced in the dentate gyrus. *J Neurophysiol* 83:1443-1451.

Chapter 2

Stress preconditioning of spreading depression in the locust CNS.

2.1 Abstract

Cortical spreading depression (CSD) is closely associated with important pathologies including stroke, seizures and migraine. The mechanisms underlying SD in its various forms are still incompletely understood. Here we describe SD-like events in an invertebrate model, the ventilatory central pattern generator (CPG) of locusts. Using K^+ -sensitive microelectrodes, we measured extracellular K^+ concentration ($[K^+]_o$) in the metathoracic neuropile of the CPG while monitoring CPG output electromyographically from muscle 161 in the second abdominal segment to investigate the role K^+ in failure of neural circuit operation induced by various stressors. Failure of ventilation in response to different stressors (hyperthermia, anoxia, ATP depletion, Na^+/K^+ ATPase impairment, K^+ injection) was associated with a disturbance of CNS ion homeostasis that shares the characteristics of CSD and SD-like events in vertebrates. Hyperthermic failure was preconditioned by prior heat shock (3h, 45°C) and induced-thermotolerance was associated with an increase in the rate of clearance of extracellular K^+ that was not linked to changes in ATP levels or total Na^+/K^+ ATPase activity. Our findings suggest that SD-like events in locusts are adaptive to terminate neural network operation and conserve energy during stress and that they can be preconditioned by experience. We propose that they share mechanisms with CSD in mammals suggesting a common evolutionary origin.

2.2 Introduction

Neural function under stressful conditions is contingent upon maintaining ion gradients across cell membranes, which are essential for neuronal signaling. Hyperthermic failure of neural operation is associated with a loss of ion homeostasis and a major redistribution of ions, including K^+ (Wu and Fisher, 2000; Robertson, 2004a). This pattern of ionic disturbance, monitored by an abrupt rise in extracellular potassium ($[K^+]_o$) and depression of electrical activity, shares many characteristics of cortical spreading depression (CSD (Leão, 1944)). In mammalian tissue CSD has been associated with several important pathologies including stroke, seizures and migraine (Somjen, 2001; Somjen, 2002; Smith et al. 2006). In an insect model system, the onset of hyperthermic failure can be preconditioned by prior stress (Newman et al. 2003). Preconditioning resulting in ischaemic tolerance is considered an evolutionarily conserved phenomenon of cerebral plasticity, evident in invertebrates and vertebrates including humans (Gidday, 2006). Here we characterize stress-induced neural depression of ventilatory central pattern generation in the migratory locust to determine its similarity to CSD and we tested the role of the Na^+/K^+ ATPase in mediating the preconditioning effects of prior heat shock (HS) on hyperthermic neural failure.

Ventilation in locusts is under the control of a reliable central pattern generator (CPG) located in the metathoracic ganglion (MTG) (Hustert, 1975; Bustami and Hustert, 2000) which is sensitive to several forms of stress including changes of internal CO_2 (Gulinson and Harrison, 1996; Henderson et al. 1998), pH (Snyder et al. 1980) and temperature (Banks et al. 1975; Lighton and Lovegrove, 1990; Henderson et al. 1998; Newman et al.

2003). In particular, increased temperature elevates the cycle frequency of the ventilatory motor pattern from 1 cycle/s at room temperature to 3 cycles/s just prior to hyperthermic failure at 38-40 °C (Newman et al. 2003). A subsequent return to room temperature permits recovery of pattern generation within 2 to 3 minutes. Several important neural properties are protected by prior HS (for review, see Robertson, 2004a; Robertson, 2004b). HS-mediated thermoprotection of the ventilatory CPG results in an increase in the failure temperature and a decrease in the time taken to recover, and can be mimicked by octopamine acting through a cAMP signaling pathway (Armstrong et al. 2006). Given that circulating octopamine increases after heat stress in locusts (Davenport and Evans, 1984), that octopamine reduces K^+ conductances and increases activity of the Na^+/K^+ ATPase (Walther and Zittlau, 1998) and that HS reduces whole cell K^+ currents in locust metathoracic neurons (Ramirez et al. 1999), we hypothesized that HS preconditioning acts by stabilizing K^+ homeostasis.

We compared the dynamics of $[K^+]_o$ during failure of motor pattern generation induced by different stressors (hyperthermia, anoxia, ATP depletion, K^+ injection) and used ouabain (a specific Na^+/K^+ ATPase toxin) both to induce repetitive, propagating waves of ionic disturbance and to test the role of the Na^+/K^+ ATPase in HS-mediated thermoprotection. We demonstrate that the surges of $[K^+]_o$ associated with cessation of ventilatory motor patterning represent SD-like phenomena whose occurrence can be interpreted as an adaptive response to conserve energy in the locust, rather than the culmination of cellular collapse. Using TTX and TEA we show that SD-like behaviour is not activity-dependent and that some part of the $[K^+]_o$ surge is via TEA-sensitive K^+

channels. Finally we show that the hyperthermic SD-like event can be preconditioned by a prior HS acting to increase the rate of $[K^+]_o$ clearance, and that the effect of HS is not obviously mediated by the Na^+/K^+ ATPase.

2.3 Results

Stress-induced failure of the ventilatory motor pattern correlates with a sharp rise in extracellular potassium

Ventilatory motor pattern activity and extracellular potassium ion concentrations in the MTG were measured during treatment with various cellular stressors in order to establish a relationship between stress-induced circuit failure and an extracellular build-up of potassium ions (Figures 2.1 and 2.2). Hyperthermic failure of the ventilatory CPG was reliably associated with an abrupt increase in $[K^+]_o$, which occurred in 100% of CON preparations (Figure 2.1A) and of all preparations irrespective of preconditioning or pharmacological treatment ($N_{total} = 85$). When the temperature was allowed to return to baseline levels, $[K^+]_o$ remained elevated before gradually decreasing (Figure 2.1A). Post-stress recovery of the ventilatory central pattern generator correlated with restoration of $[K^+]_o$ to initial levels (Figure 2.1A). In addition, abrupt surges in $[K^+]_o$ were reliably triggered by ATP depletion using $10^{-3}M$ sodium azide (NaN_3) and anoxia (100% N_2) (Figure 2.1B and C). Peak $[K^+]_o$ reached during surges induced by hyperthermia (52 ± 2 mM), NaN_3 (85 ± 2 mM) and anoxia (79 ± 3 mM) were different (one-way ANOVA, $P < 0.001$, $F_{(2,38)} = 43.634$). The peak $[K^+]_o$ induced by hyperthermia was lower than the $[K^+]_o$ peaks induced by NaN_3 and anoxia (*post hoc* Tukey tests, $P < 0.05$). The recovered motor pattern was robust but not identical to the pre-stress motor pattern (see e.g. Figure 2.1Ci and ii).

Abrupt surges in $[K^+]_o$ were reliably triggered by Na^+/K^+ ATPase inhibition using $10^{-4}M$ ouabain and by locally increased $[K^+]_o$ within the ganglion (Figure 2.2). Continuous bath

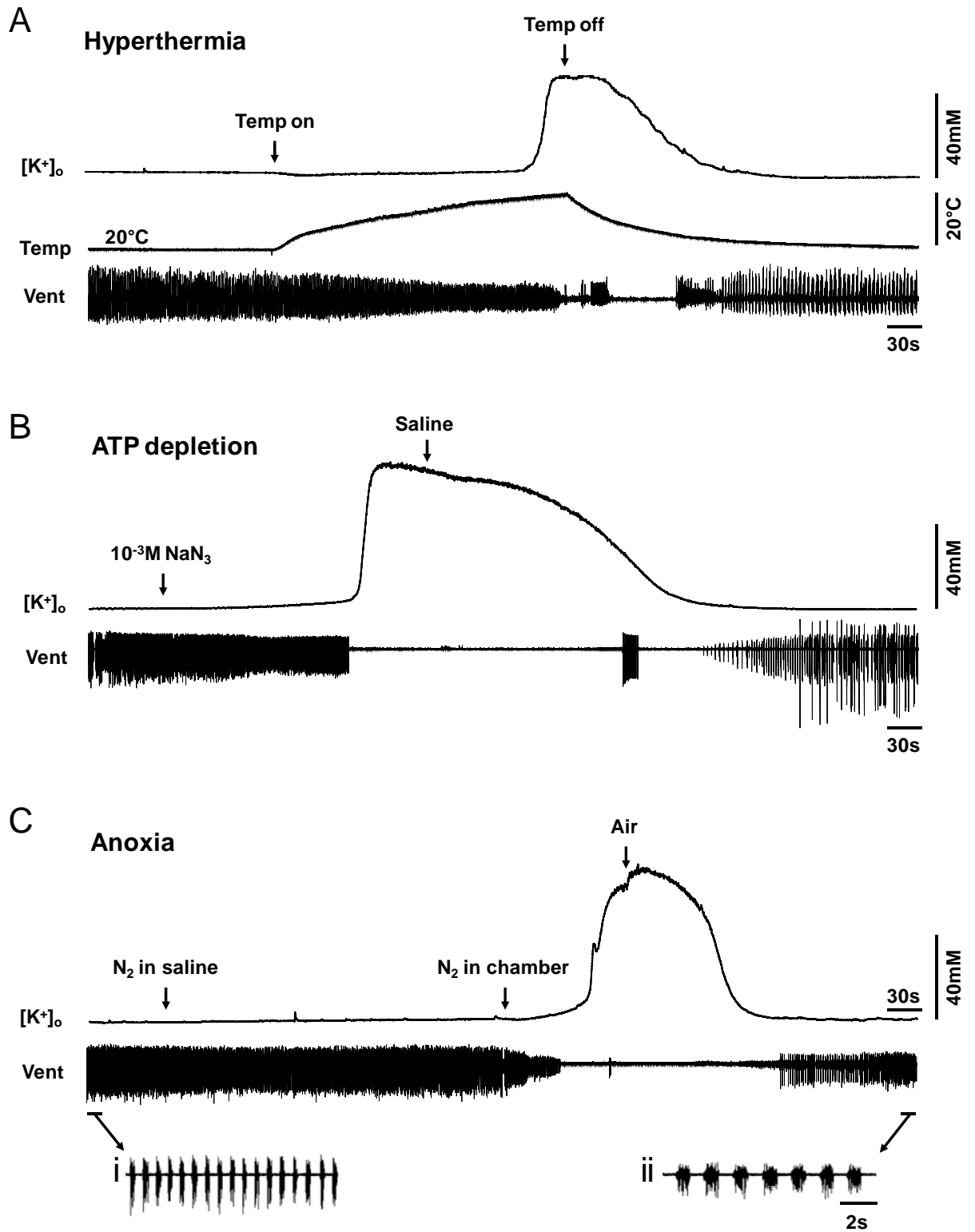


Figure 2.1

Figure 2.1. Stress-induced motor pattern failure is associated with surges of $[K^+]_o$. Simultaneous recordings of the ventilatory motor pattern (Vent), the temperature of the superfusing saline at the MTG (Temp in **A**) and the extracellular potassium concentration ($[K^+]_o$). **A.** An abrupt increase in $[K^+]_o$ was reliably associated with heat-induced failure of the ventilatory motor pattern, which occurred in 100% of preparations (N=17). $[K^+]_o$ was restored to normal baseline levels if heat was removed and this was associated with recovery of ventilatory motor patterning. **B.** $10^{-3}M$ NaN_3 was bath-applied until 1 minute post-failure (N=6). $[K^+]_o$ gradually decreased and the motor pattern recovered upon superfusion of standard locust saline. **C.** N_2 was bubbled into the superfusing saline for 5 minutes, then blown over the preparation until 1 minute post-failure (N=18). Re-oxygenation resulted in $[K^+]_o$ clearance and recovery of the motor pattern. **i** and **ii** show expansions of the motor pattern trace pre- and post-stress to show more clearly the ventilatory motor pattern. In **B** and **C** the temperature was constant at room temperature ($\sim 22^\circ C$).

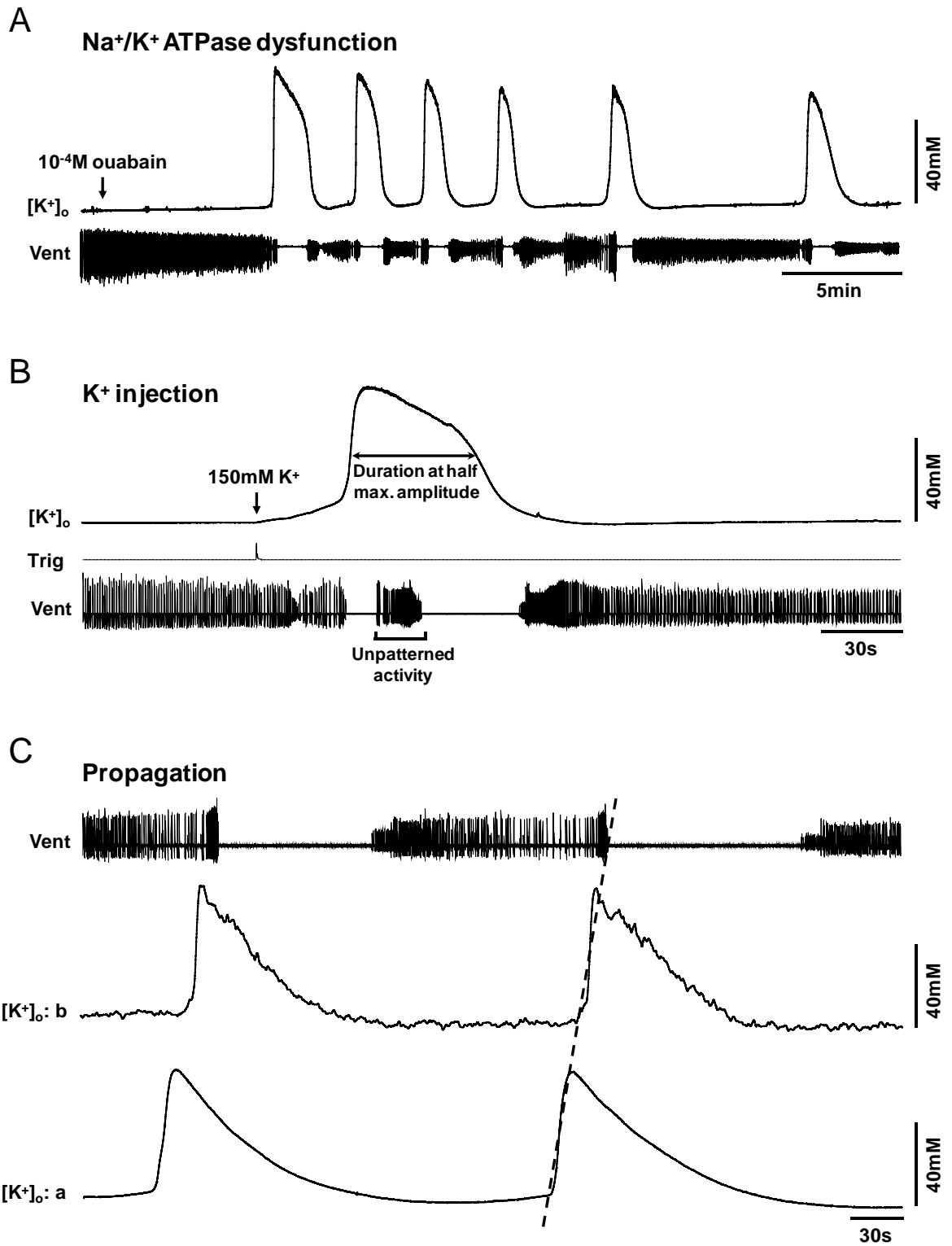


Figure 2.2

Figure 2.2. Characteristics of $[K^+]_o$ surges. Simultaneous recordings of the ventilatory motor pattern (Vent), a monitor of pressure-injection of a bolus of K^+ within the MTG (Trig in **B**) and the extracellular potassium concentration ($[K^+]_o$). **A.** Continuous bath application of $10^{-4}M$ ouabain elicited multiple surges in $[K^+]_o$ (N=13). In the experiment shown here it took 434 seconds for $10^{-4}M$ ouabain to penetrate the MTG and induce failure of motor pattern generation. **B.** A 35nl pressure-injection of locust saline containing a 15-fold higher $[K^+]$ (150mM compared to 10mM) into the MTG neuropile was sufficient to bring $[K^+]_o$ to threshold and induce an abrupt surge (N=18). **C.** Two K^+ -sensitive microelectrodes were inserted in different regions of the MTG (**a** and **b**) to illustrate propagation (dotted line). In this experiment the propagation speed was 1.9 mm/min.

application of 10^{-4} M ouabain elicited multiple surges in $[K^+]_o$ where the rise and fall of $[K^+]_o$ was associated with failure and recovery of the ventilatory motor pattern, respectively (Figure 2.2A). The time from ouabain application to the midpoint of the initial $[K^+]_o$ increase was 557 ± 43 seconds. The average $[K^+]_o$ surge period from the first to the second surge was 217 ± 16 seconds. $[K^+]_o$ increased to a mean peak of 63 ± 5 mM during the initial surge induced by 10^{-4} M ouabain and subsequently returned to a mean baseline level of 10 ± 0.2 mM. $[K^+]_o$ clearance always coincided with recovery of motor pattern generation, however the ventilatory rhythm frequency and duration became more variable following each $[K^+]_o$ surge (Figure 2.2A). A 35nl injection of locust saline containing a 15-fold higher $[K^+]$ (150mM compared to 10mM) was sufficient to bring $[K^+]_o$ to threshold for induction of an abrupt surge (Figures 2.2B and 2.S1). The peak $[K^+]_o$ reached during surges induced by K^+ injection was 63 ± 8 mM. The average duration of the $[K^+]_o$ surge, measured at half the maximum amplitude, was 64 ± 9 seconds. It was of interest to determine if the repetitive ionic disturbance is localized to one area in the MTG, or if, similar to CSD, there is propagation across different areas of the locust nervous system. To investigate this we measured $[K^+]_o$ simultaneously at two different locations in the MTG ~ 0.4 to 0.6 mm apart (Figure 2.2C). Abrupt surges in $[K^+]_o$ generated by injection of high $[K^+]$ saline into the extracellular space spread locally to other areas of the MTG at a speed of 2.4 ± 0.04 mm/min (Figure 2.2C), but did not propagate through the connectives to the mesothoracic ganglion and vice versa (N=3; data not shown).

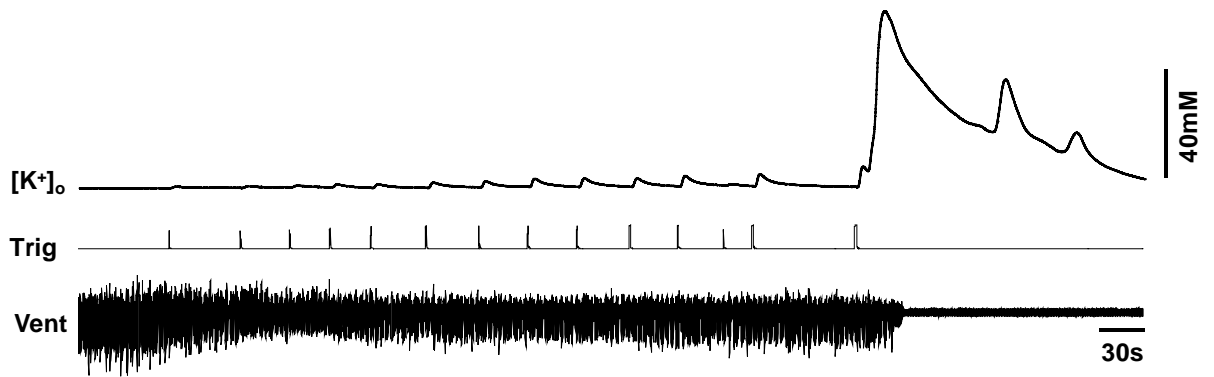


Figure 2.S1. Gradual increases in the volume of K^+ injected triggered a tissue response. Simultaneous recordings of the ventilatory motor pattern (Vent), pressure-injection of a bolus of K^+ within the MTG (Trig) and the extracellular potassium concentration ($[K^+]_o$). Injection of very small volumes of high K^+ saline triggered a tissue response, however ignition of the all-or-none $[K^+]_o$ event occurred only when a threshold was reached.

The hyperthermic $[K^+]_o$ event does not represent complete collapse of the K^+ gradient

To determine if the peak $[K^+]_o$ represented complete collapse of the $[K^+]_o$ gradient during hyperthermia, temperature was increased beyond failure of the motor pattern until a second $[K^+]_o$ plateau was reached at $\sim 60^\circ\text{C}$ (100 ± 7 mM; Figure 2.3A). The motor pattern did not recover upon return to room temperature and $[K^+]_o$ remained elevated. Hyperthermia following anoxic arrest of the motor pattern eliminated the hyperthermic $[K^+]_o$ event and only the second plateau (113 ± 6 mM) was evident without recovery (Figure 2.3B) suggesting that these different stressors converge on the same tissue response. There was no difference in the ultimate $[K^+]_o$ at $\sim 60^\circ\text{C}$ between the two treatment groups (hyperthermia alone and anoxia-induced failure of the motor pattern prior to hyperthermia) (t -test, $t = -1.370$, $P = 0.185$, d.f. = 21).

The hyperthermic $[K^+]_o$ event is delayed by Na^+ channel block and diminished by K^+ channel block

We used voltage-gated Na^+ and K^+ channel blockers (TTX and TEA, respectively) to determine if the hyperthermic SD-like event in the locust is dependent on neural activity and if K^+ efflux is at least in part via TEA-sensitive K^+ channels. Bath application of 10^{-6} M TTX quickly abolished electrical activity from ventilatory muscle 161 while $[K^+]_o$ remained stable at ~ 10 mM for 15 minutes prior to the temperature ramp (Figure 2.4A). However, occurrence of the hyperthermic $[K^+]_o$ event was TTX-resistant; there was no difference in the peak $[K^+]_o$ level between CON and TTX locusts (52 ± 2 mM and 50 ± 4 mM respectively; t -test, $t = 0.334$, $P = 0.741$, d.f. = 30). The abrupt rise in $[K^+]_o$ was delayed in TTX-treated locusts, occurring at higher temperatures during the continuous

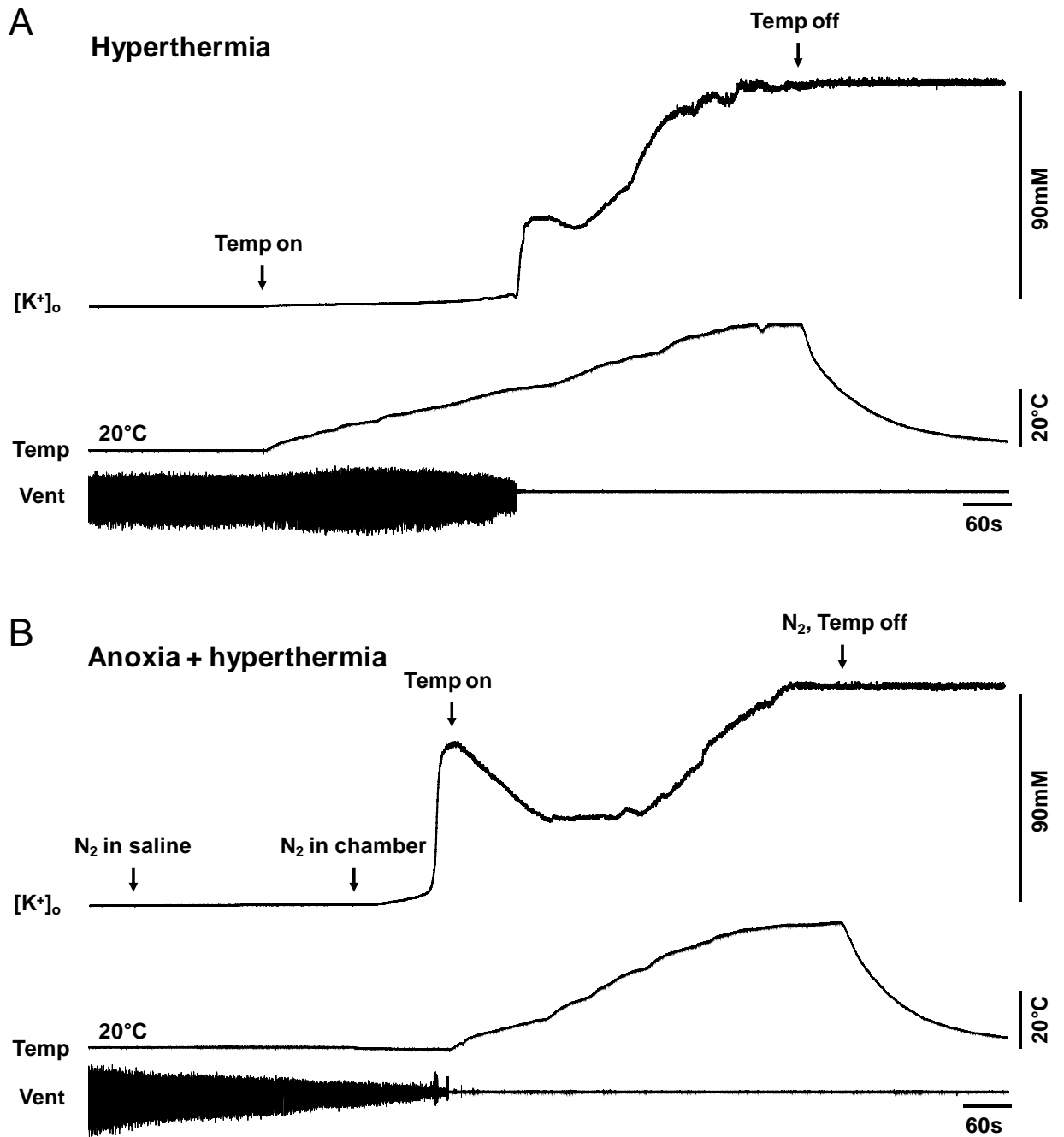


Figure 2.3

Figure 2.3. The hyperthermic $[K^+]_o$ event is not representative of complete collapse of the K^+ gradient. **A.** During a continuous increase of temperature $[K^+]_o$ increased sharply at $\sim 40^\circ\text{C}$ coincident with motor pattern failure and continued to rise until a second plateau was reached at $\sim 60^\circ\text{C}$. When the heater was turned off $[K^+]_o$ remained elevated and motor pattern generation failed to recover (N=11). **B.** Only the second plateau was evident during temperature increase to $\sim 60^\circ\text{C}$ following prior anoxic arrest of motor pattern generation. When the N_2 was turned off and internal temperature returned to room temperature $[K^+]_o$ remained elevated and motor pattern generation failed to recover (N=12).

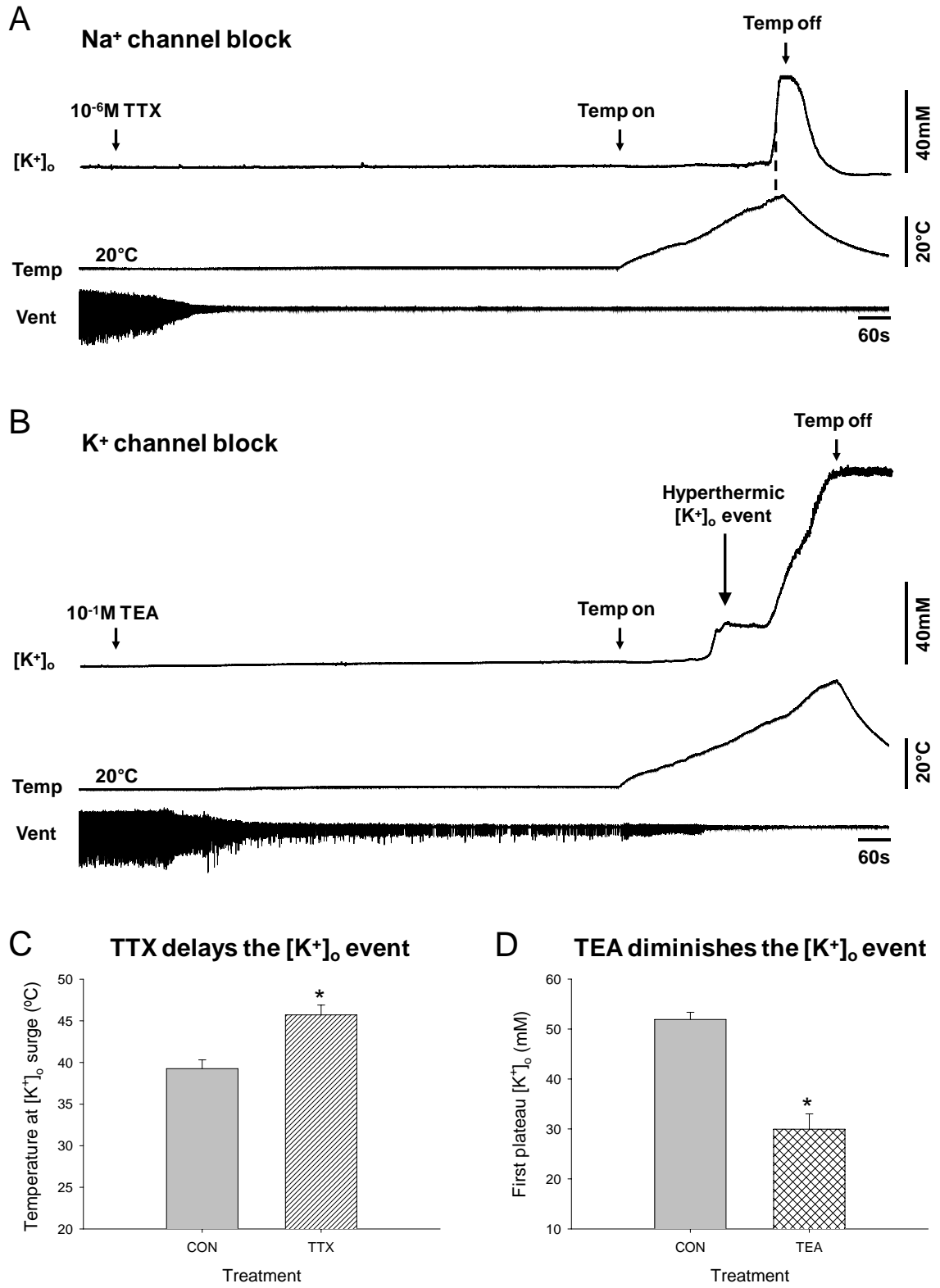


Figure 2.4

Figure 2.4. The hyperthermic $[K^+]_o$ event is delayed by blocking Na^+ channels and neural activity using TTX and is diminished by blocking K^+ channels using TEA. **A.** 10^{-6} M TTX abolished electrical activity within minutes while $[K^+]_o$ remained stable. The abrupt rise in $[K^+]_o$ was not significantly diminished by TTX. The hyperthermic $[K^+]_o$ event occurred at a significantly higher temperature (measured at dotted line) in the absence of electrical activity ($46 \pm 1^\circ C$) compared to CON locusts ($39 \pm 1^\circ C$) (**C**) ($N_{CON} = 17$; $N_{TTX} = 15$). **B.** 10^{-1} M TEA significantly reduced the hyperthermic $[K^+]_o$ event ($N_{CON} = 17$; $N_{TEA} = 6$) (**D**). $[K^+]_o$ increased with continued temperature increase to $\sim 60^\circ C$.

ramp increase than in CON locusts (46 ± 1 °C versus 39 ± 1 °C; *t*-test, $t = -4.541$, $P < 0.001$, d.f. = 30) (Figure 2.4C). Due to the effectiveness of the sheath enclosing the contents of the MTG, bath application of a high concentration of TEA (10^{-1} M) was required to successfully abolish motor pattern generation, although electrical activity was still detected from muscle 161. The hyperthermic $[K^+]_o$ event occurred at 38.9 ± 0.6 °C in locusts treated with 10^{-1} M TEA compared to 39.3 ± 0.9 °C (no significant difference) in CON locusts (Figure 2.4B) but was reduced in amplitude (30 ± 3 mM versus 52 ± 2 mM; *t*-test, $t = 5.429$, $P < 0.001$, d.f. = 21) (Figure 2.4D). With continued temperature increase to ~ 60 °C $[K^+]_o$ reached a higher second plateau in TEA-treated locusts (109 ± 9 mM) that was not different from the second plateau in CON locusts (*t*-test, $t = -0.755$, $P = 0.462$, d.f. = 15).

Initiation of $[K^+]_o$ surges are not correlated with ATP levels within the ganglion

Cell energetics may play a role in the initiation of, and recovery from, the $[K^+]_o$ event induced by various cellular stressors. ATP levels in the MTG taken from locusts subjected to hyperthermia before and after heat shock preconditioning (CON and HS), 10^{-4} M ouabain, 10^{-3} M sodium azide, and anoxia (100% N₂) were compared prior to stress, at failure and at subsequent recovery of the motor pattern (Figure 2.5A). Ganglionic ATP levels were depressed at failure induced by anoxia, hyperthermia (CON), and NaN₃ and at subsequent recovery in NaN₃-treated locusts (*post hoc* Dunnett's test, $P < 0.05$). Stress treatment and the state of motor pattern generation, i.e. failure vs. recovery, both affected ATP levels (two-way ANOVAs: $P < 0.001$, $F_{(4,75)} = 17.435$; $P = 0.002$, $F_{(1,75)} = 10.193$). At failure of the motor pattern, NaN₃-treated locusts

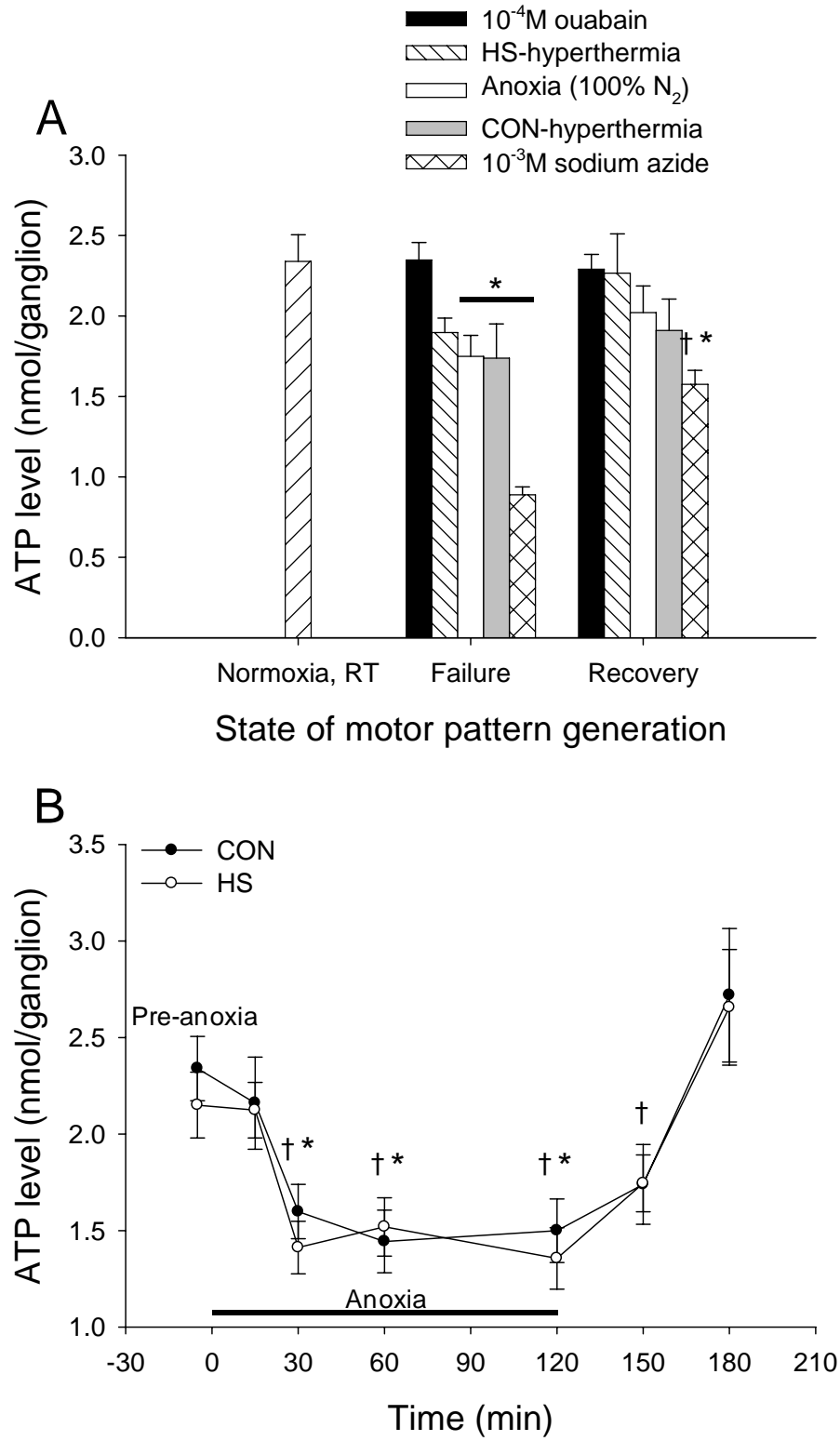


Figure 2.5

Figure 2.5. Failure and recovery of the CPG are not dependent on MTG ATP and HS preconditioning does not confer protection by improving ATP availability. **A.** ATP levels did not differ from the pre-stress level (Normoxia at room temperature; N=16) in locusts treated with 10^{-4} M ouabain or hyperthermia (HS) at failure or recovery, or in all other groups at recovery following stress-induced failure with the exception of NaN_3 -treated locusts. There was a main effect of treatment driven by significant differences among groups within failure and recovery (not indicated by symbols). There was no effect of HS pre-treatment on ATP levels at failure or recovery of motor pattern generation. Asterisks indicate significant differences from the pre-stress level and daggers indicate significantly different ATP levels at failure and recovery in ganglia of NaN_3 -treated locusts. Sample sizes (failure, recovery): $N_{\text{Ouabain}}=10,11$; $N_{\text{HS-hyperthermia}}=8,8$; $N_{\text{Anoxia}}=9,8$; $N_{\text{CON-hyperthermia}}=7,7$; $N_{\text{Sodium azide}}=8,9$. **B.** CON and HS locusts did not have significantly different ATP levels during anoxia-induced coma or subsequent recovery. ATP levels dropped in both CON and HS locusts after 30 minutes of anoxia and remained stable until locusts were removed from the anoxic environment. ATP levels increased to around pre-anoxia values after one hour in normally oxygenated air. Sample sizes (CON, HS): $N_{0\text{min}}=16,16$; $N_{15\text{min}}=12,11$; $N_{30\text{min}}=11,11$; $N_{60\text{min}}=9,9$; $N_{120\text{min}}=12,11$; $N_{150\text{min}}=11,12$; $N_{180\text{min}}=10,10$. Asterisks indicate significant differences from 0 and 15 minutes and daggers indicate significant differences from 180 minutes (or 60 minutes recovery) according to *post hoc* Tukey tests ($P < 0.05$).

had lower ganglionic ATP levels than all other groups. Locusts subjected to anoxia and hyperthermia (CON) had lower ATP levels than locusts treated with 10^{-4} M ouabain (*post hoc* Tukey tests, $P < 0.05$). At recovery of the motor pattern NaN_3 -treated locusts had lower ganglionic ATP levels than locusts subjected to 10^{-4} M ouabain and hyperthermia (HS) suggesting that recovery was independent of metabolic state (*post hoc* Tukey tests, $P < 0.05$). ATP levels in ganglia at failure and recovery of the motor pattern were not different except in NaN_3 -treated locusts (*post hoc* Tukey tests, $P < 0.05$). Notably, HS preconditioning did not increase ATP levels at hyperthermic failure or subsequent recovery of the motor pattern compared to CON-hyperthermia locusts (Figure 2.5A). The lack of effect of HS on MTG ATP levels was also evident during and after two hours of whole animal anoxia (Figure 2.5B). HS pre-treatment did not affect ATP levels prior to anoxia, at 15, 30, 60, and 120 minutes of anoxia exposure, and at 30 and 60 minutes post-anoxia (two-way ANOVA, $P = 0.467$, $F_{(1,147)} = 0.531$). Anoxia exposure affected ganglionic ATP (two-way ANOVA, $P < 0.001$, $F_{(6,147)} = 11.418$). Anoxia (15 minutes) did not affect ATP levels in either CON or HS locusts, even though locusts entered anoxic coma within 1 minute. ATP levels dropped after 30 minutes of anoxia and remained stable for 90 minutes in CON and HS locusts (*post hoc* Tukey tests, $P < 0.05$). Following 2 hours in an anoxic environment, ATP increased after 60 minutes of normoxia in CON and HS locusts (*post hoc* Tukey tests, $P < 0.05$).

HS pre-treatment changed $[K^+]_o$ homeostasis in the MTG

We used 10^{-5} M ouabain to test whether increased Na^+/K^+ ATPase activity could underlie the increased thermotolerance conferred by HS pre-treatment (Newman et al. 2003). 10^{-

5M ouabain is not normally sufficient to induce the SD-like events of Figure 2.2A but is sufficient to inhibit the Na^+/K^+ ATPase (see below). HS pre-treatment and 10^{-5}M ouabain bath application affected $[\text{K}^+]_o$ before and during a temperature ramp (Figure 2.6). Heat shock pre-treatment increased initial $[\text{K}^+]_o$ measured after 10 minutes of bath application with standard locust saline (t -test, $t = -3.195$, $P = 0.002$, d.f. = 49; Figure 2.6A). Changes in extracellular potassium ($\Delta[\text{K}^+]_o$) were examined after 15 minutes of ouabain treatment at room temperature and in response to the initial 5°C increase of the temperature ramp to determine the effects of HS pre-treatment and 10^{-5}M ouabain treatment on K^+ homeostasis (Figure 2.6B and C). HS pre-treatment had no effect on $\Delta[\text{K}^+]_o$ after 15 minutes of bath application, however there was an effect of 10^{-5}M ouabain treatment (two-way ANOVAs: $P = 0.407$, $F_{(1,43)} = 0.703$; $P < 0.001$, $F_{(1,43)} = 42.772$) (Figure 2.6B). CON-OUA and HS-OUA locusts had a greater increase in $[\text{K}^+]_o$ than CON and HS locusts after 10^{-5}M ouabain bath application for 15 minutes (*post hoc* Tukey tests, $P < 0.05$). HS pre-treatment affected $\Delta[\text{K}^+]_o$ after a 5°C increase in temperature, however there was no effect of 10^{-5}M ouabain treatment (two-way ANOVAs: $P < 0.001$, $F_{(1,43)} = 15.584$; $P = 0.988$, $F_{(1,43)} = 0.000223$) (Figure 2.6C). CON and CON-OUA locusts had a greater $\Delta[\text{K}^+]_o$ than HS and HS-OUA locusts (*post hoc* Tukey tests, $P < 0.05$).

Time to recovery is correlated with failure temperature in control and HS locusts

HS preconditioning delayed the onset of the $[\text{K}^+]_o$ event and subsequently hastened recovery and re-establishment of normal $[\text{K}^+]_o$ (Figure 2.7). However HS had no effect on the amplitude of the $[\text{K}^+]_o$ event at failure (Figure 2.S2) and there was no correlation

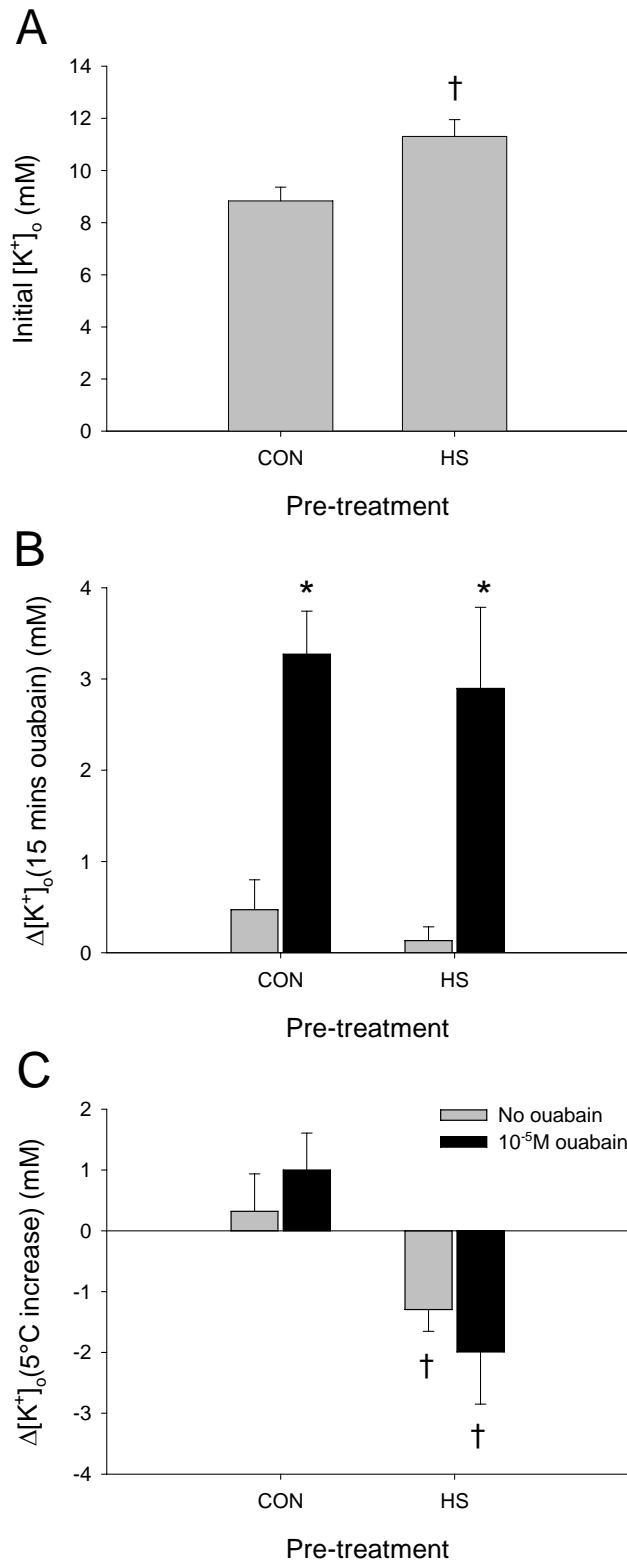


Figure 2.6

Figure 2.6. HS and ouabain affect $[K^+]_o$. **A.** Heat shock preconditioning resulted in a significantly higher $[K^+]_o$ in HS locusts compared to CON locusts. All animals pooled: $N_{CON} = 25$; $N_{HS} = 26$. **B.** CON-OUA and HS-OUA locusts had a significantly greater increase in $[K^+]_o$ after 15 minutes of bath application with $10^{-5}M$ ouabain compared to CON and HS locusts. HS pre-treatment did not have an effect on $\Delta[K^+]_o$ over this 15 minute period ($N_{CON} = 12$; $N_{CON-OUA} = 10$; $N_{HS} = 17$; $N_{HS-OUA} = 8$). **C.** CON and HS locusts had a markedly different $\Delta[K^+]_o$ in response to a $5^\circ C$ increase in temperature. $\Delta[K^+]_o$ was positive in CON locusts and negative in HS locusts after only one minute of temperature increase. There was no effect of $10^{-5}M$ ouabain treatment on $\Delta[K^+]_o$ one minute into the temperature ramp ($N_{CON} = 12$; $N_{CON-OUA} = 10$; $N_{HS} = 17$; $N_{HS-OUA} = 8$). Asterisks indicate a significant effect of ouabain and daggers indicate a significant effect of pre-treatment according to *t*-test (**A**) and *post hoc* Tukey tests ($P < 0.05$) (**B,C**).

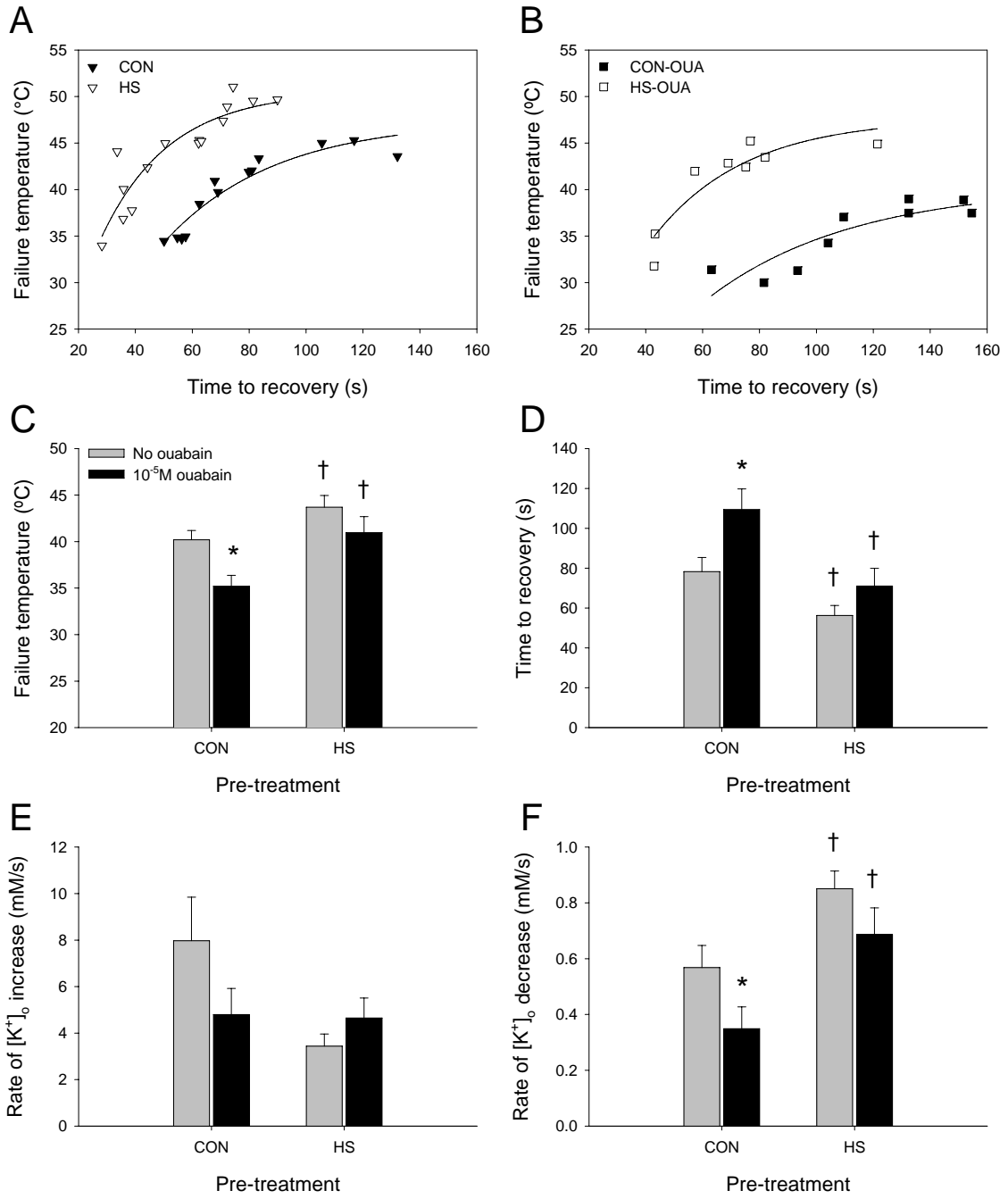


Figure 2.7

Figure 2.7. HS delays the $[K^+]_o$ event and speeds recovery by increasing the rate of $[K^+]_o$ clearance. **A.** Time to recovery was positively correlated with failure temperature in CON and HS locusts ($N_{CON} = 13$; $N_{HS} = 15$). Animals whose ventilatory motor pattern failed at a higher temperature had a longer time to recovery when temperature returned to normal levels. **B.** The correlations seen in CON and HS animals were shifted in animals treated with $10^{-5}M$ ouabain ($N_{CON-OUA} = 9$; $N_{HS-OUA} = 8$). The relationship between failure temperature and time to recovery in HS-OUA animals resembled CON animals. Data points for each group were fitted with exponential curves that rise to a plateau (**A**, **B**). **C.** Ventilatory motor pattern generation in HS locusts failed at a significantly higher temperature than in CON locusts with and without $10^{-5}M$ ouabain treatment. There was a significant effect of ouabain on the ability to withstand high temperature stress in CON locusts but not in HS locusts ($N_{CON} = 15$; $N_{CON-OUA} = 9$; $N_{HS} = 17$; $N_{HS-OUA} = 8$). **D.** Ventilatory motor pattern generation in HS locusts took significantly less time to recover following heat-induced failure than in CON locusts with and without ouabain treatment. CON-OUA locusts took significantly more time to recover than CON locusts, however there was no significant effect of ouabain treatment on time to recovery in HS locusts ($N_{CON} = 13$; $N_{CON-OUA} = 10$; $N_{HS} = 15$; $N_{HS-OUA} = 8$). **E.** Overall there were no main effects of HS pre-treatment or ouabain treatment on the rate of $[K^+]_o$ increase (mM/s) associated with failure of the motor pattern ($N_{CON} = 15$; $N_{CON-OUA} = 10$; $N_{HS} = 18$; $N_{HS-OUA} = 7$). **F.** The rate of $[K^+]_o$ decrease (mM/s) associated with recovery of the motor pattern was significantly greater in HS locusts than in CON locusts and this effect of pre-treatment was conserved in ouabain-treated locusts. Ouabain treatment significantly decreased the rate of $[K^+]_o$ clearance in CON locusts but not in HS locusts ($N_{CON} = 15$;

$N_{\text{CON-OUA}} = 10$; $N_{\text{HS}} = 18$; $N_{\text{HS-OUA}} = 8$). Asterisks indicate a significant effect of ouabain and daggers indicate a significant effect of pre-treatment according to *post hoc* Tukey tests ($P < 0.05$) (C-F).

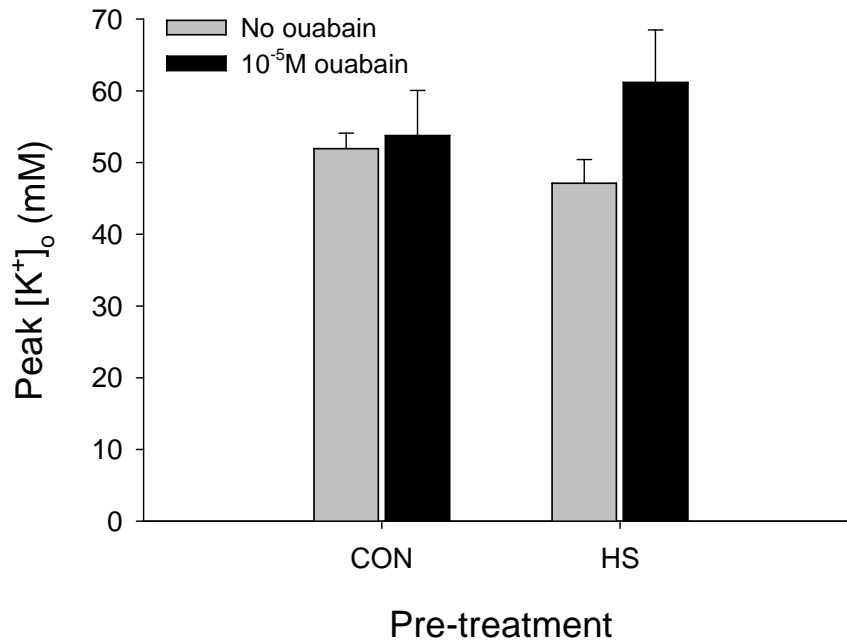


Figure 2.S2. The degree of the [K⁺]_o disturbance was the same in CON and HS locusts. There were no main effects of HS pre-treatment or 10⁻⁵M ouabain treatment on the peak [K⁺]_o associated with failure of the motor pattern ($N_{\text{CON}} = 17$; $N_{\text{CON-OUA}} = 10$; $N_{\text{HS}} = 18$; $N_{\text{HS-OUA}} = 8$).

between time to recovery and peak $[K^+]_o$ in C and HS locusts (data not shown) indicating that the effect of HS on rate of recovery was not due to a decrease in the initial ionic disturbance. There was a strong positive correlation between time to recovery and failure temperature in control locusts that was shifted by HS and by 10^{-5} M ouabain (Pearson Product Moment Correlations: CON, $r = 0.91$, $P < 0.0001$; HS, $r = 0.90$, $P < 0.0001$; CON-OUA, $r = 0.88$, $P = 0.00172$; HS-OUA, $r = 0.85$, $P = 0.00785$) (Figure 2.7A and B). Thus high failure temperatures were correlated with slower recovery under all conditions. HS improved performance by increasing failure temperatures and speeding recovery whereas ouabain impaired performance of both CON and HS preparations.

HS pre-treatment increases failure temperature and decreases time to recovery

HS pre-treatment increased the upper temperature limit and shortened time to recovery when these measures were examined independently (Figure 2.7C and D). HS pre-treatment and 10^{-5} M ouabain treatment affected failure temperature though there was no interaction between treatments suggesting that the effect of ouabain did not depend on the pre-treatment (two-way ANOVAs: $P = 0.001$, $F_{(1,45)} = 11.777$; $P = 0.007$, $F_{(1,45)} = 8.140$) (Figure 2.7C). HS increased failure temperatures compared with CON, and ouabain decreased failure temperatures in CON but not HS preparations (*post hoc* Tukey tests, $P < 0.05$). HS pre-treatment and 10^{-5} M ouabain treatment also affected time to recovery of the motor pattern with a similar lack of interaction (two-way ANOVAs: $P < 0.001$, $F_{(1,42)} = 15.302$; $P = 0.005$, $F_{(1,42)} = 8.823$) (Figure 2.7D). HS decreased time to recovery compared with CON, and ouabain increased time to recovery in CON but not HS preparations (*post hoc* Tukey tests, $P < 0.05$).

HS pre-treatment increases the rate of $[K^+]_o$ clearance following hyperthermic failure

Rates of $[K^+]_o$ increase and clearance associated with hyperthermic failure and subsequent recovery of the ventilatory motor pattern were compared among groups to determine if preconditioning improves $[K^+]_o$ stabilization and to test the role of the Na^+/K^+ ATPase in this preconditioning (Figure 2.7E and F). Neither HS pre-treatment nor $10^{-5}M$ ouabain treatment affected the rate of $[K^+]_o$ increase associated with failure of the motor pattern (two-way ANOVAs: $P = 0.098$, $F_{(1,46)} = 2.846$; $P = 0.482$, $F_{(1,46)} = 0.502$) (Figure 2.7E). However HS pre-treatment and $10^{-5}M$ ouabain treatment did affect the rate of $[K^+]_o$ decrease associated with recovery of the motor pattern (two-way ANOVAs: $P < 0.001$, $F_{(1,47)} = 14.395$; $P = 0.024$, $F_{(1,47)} = 5.478$) (Figure 2.7F) though there was no interaction between the treatments. HS increased the $[K^+]_o$ clearance rate compared with CON, and ouabain decreased this measure in CON but not in HS preparations (*post hoc* Tukey tests, $P < 0.05$). Thus the proportion of the $[K^+]_o$ clearance rate sensitive to the $10^{-5}M$ ouabain treatment was halved by HS from ~40% in control preparations to ~20% after HS.

HS preconditioning does not increase Na^+/K^+ ATPase activity in the MTG

To complement the results obtained by ouabain treatment on $[K^+]_o$ clearance rates we also measured steady-state Na^+/K^+ ATPase activity within the MTG. Na^+/K^+ ATPase activity (i.e. the ouabain-sensitive fraction of total MTG ATPase activity) was 144 ± 12 nmol ATP/min/mg protein in CON ganglia compared to 133 ± 9 nmol ATP/min/mg protein in HS ganglia (no significant difference; *t*-test, $t = 0.755$, $P = 0.468$, d.f. = 10;

$N_{\text{CON}}=6$, $N_{\text{HS}}=6$). In the presence of phosphatase inhibitors, Na^+/K^+ ATPase activity was 120 ± 7 nmol ATP/min/mg protein in CON ganglia compared to 116 ± 10 nmol ATP/min/mg protein in HS ganglia (no significant difference; *t*-test, $t = 0.430$, $P = 0.672$, d.f. = 18; $N_{\text{CON}}=10$, $N_{\text{HS}}=10$). This suggests that total Na^+/K^+ ATPase activity is not a target for protection by HS preconditioning.

2.4 Discussion

In a central pattern generator controlling ventilation in the locust, we have shown that hyperthermic failure and recovery of neural function are tightly correlated with an abrupt rise in $[K^+]_o$ and its subsequent restoration when temperature is allowed to return to normal. Anoxia and ATP depletion evoked similar tissue responses, which could also be induced when we disturbed the ionic equilibrium by impairing Na^+/K^+ ATPase activity using ouabain or by local neuropile injections of high $[K^+]$ saline. The fact that a prior anoxia-induced $[K^+]_o$ surge occluded the hyperthermic event suggests that these different stressors converged on the same mechanism. In addition, the nature of these events as large ionic disturbances propagating throughout the MTG neuropile makes it unlikely that different stressors would have additive effects. The amplitude of the hyperthermic $[K^+]_o$ surge was smaller than those induced by either anoxia or ATP depletion and we attribute this partly to the confounding effect of its occurrence at high temperatures ($>40^\circ C$). This is supported by further analysis that shows a significant negative correlation between the failure temperature during hyperthermia (for CON, HS, CON-OUA, HS-OUA preparations) and $[K^+]_o$ at its peak (Pearson Product Moment Correlation; $r = -0.3$, $P = 0.03$; $N = 47$, one outlier removed), and may be due to the fact that at the point of hyperthermic failure $[K^+]_o$ increased from its room temperature level (t -test, $t = -5.085$, $P < 0.001$, d.f. = 104) thereby reducing the driving force on K^+ ions. We conclude that the different stressors converged on a single tissue mechanism.

CSD occurs in vertebrate grey matter and is characterized by a rapid and nearly complete depolarization of neurons that propagates at 2-5 mm/min as a wave across the cortex.

This propagating wave is due to a disordered regulation of ionic homeostasis evident as a massive redistribution of ions across neuronal membranes, including large increases of $[K^+]_o$ (Somjen, 2001). Each wave results in neuronal hyperexcitation followed by suppression of electrical activity because of spike inactivation. SD events can be evoked by hypoxia (Wu and Fisher, 2000; Somjen, 2001; Kager et al. 2002), ouabain (Balestrino et al. 1999; Wu and Fisher, 2000; Somjen, 2001), simulated ischemia (Anderson et al. 2005), and increased $[K^+]_o$ (Wu and Fisher, 2000; Somjen, 2001; Kager et al. 2002) with normal temperature, as well as hyperthermia (Wu and Fisher, 2000). The locust responses: 1) were all-or-none events of similar magnitude (at least with respect to $[K^+]_o$), 2) were induced by the same stimuli, 3) were not activity-dependent, 4) occurred as repetitive waves with ouabain, 5) propagated at around 2mm/min, 6) did not cross between ganglia through the connectives (equivalent to white matter) and 7) were associated with complete depression of neural activity manifest by failure of ventilatory pattern generation. Thus the locust tissue response, reflected in the all-or-none surge of $[K^+]_o$, shares most, if not all, of the essential characteristics of CSD.

The biophysical mechanism of the extensive redistribution of ions causing CSD is incompletely understood. It nevertheless seems clear that SD-like events in mammals are triggered by positive feedback processes involving an initial ionic disturbance reaching a threshold and caused by neuronal overexcitation or by treatments or conditions that impair ionic homeostasis (e.g. Grafstein, 1956; van Harrevald, 1978; Balestrino et al. 1999; Somjen, 2001). In a model hippocampal pyramidal neuron, SD-like events can be triggered by manipulating ion clearance mechanisms or levels of excitation, causing the

net current in the apical dendrites to turn inward (Kager et al. 2002). The locust responses were triggered by treatments that cause a reduction in energy (i.e. ATP depletion and anoxia). However disruption of energy status was not essential since similar events were triggered by impairment of the Na^+/K^+ ATPase (10^{-4}M ouabain) and by local injection of high $[\text{K}^+]$ saline into the neuropile. Moreover there was no correlation between the occurrence of motor pattern failure and recovery with levels of ATP in the MTG. Energy status of a cell (e.g. phosphorylation potential) can change and activate signaling pathways without measureable effects on ATP (Hardie et al. 2006; Evans, 2006), but the size of the sample precluded measurement of any adenylate but ATP. Hyperthermia caused a drop in metathoracic ATP but also increased levels of neuronal excitation in the ganglion. There was an interesting trade-off in our measures of thermotolerance for ventilatory pattern generation such that early failure (i.e. low failure temperature) was associated with shorter times to recovery. This suggests that the triggered event is adaptive and represents a neural off-switch to conserve energy and to prevent hyperexcitation during stressful conditions. In contrast to the insect system, CSD in mammals is associated with local tissue hypoxia and neuronal swelling due to energy consumption that is not met with adequate oxygen supply (Takano et al. 2007). The recovery of motor function was closely associated with the return of $[\text{K}^+]_o$ to near normal levels and thus the time taken to recover was related to the rate of clearance of extracellular K^+ ions. Treatment with 10^{-5}M ouabain rendered preparations more thermosensitive by decreasing failure temperature and increasing recovery time concomitant with a decrease in the rate of extracellular K^+ ion clearance during the recovery period. This indicates an important role for the Na^+/K^+ ATPase pump, as in

vertebrate SD-like phenomena. The $[K^+]_o$ disturbance induced by injection of high $[K^+]_o$ saline propagated within the locust MTG at a similar rate as the depolarizing wave in mammalian brain slices during CSD. Studies suggest opening of intercellular gap junctions as a mechanism of SD propagation in vertebrates (Nedergaard et al. 1995; Largo et al. 1997). Similar mechanisms may exist in the insect CNS in which glia are involved in ion homeostasis, function, and development of the insect brain (Kretzschmar and Pflugfelder, 2002).

Our findings show that the events we recorded in locust ganglia are SD-like ionic disturbances similar to CSD and possibly induced by common mechanisms, which in theory would suggest that these mechanisms have been evolutionarily conserved. Moreover in the locust there is evidence that this is an adaptive event to conserve energy and prevent complete cellular collapse. In the case of hyperthermia this was evident when temperature was increased to the point at which $[K^+]_o$ levels reached a high plateau and motor pattern recovery was precluded.

We found that prior HS preconditioned neural function in the metathoracic ganglion, allowing the ventilatory pattern generator to operate at higher temperatures and to recover more rapidly from hyperthermic failure on return to normal temperatures. Such preconditioning significantly protects neural function and has been well established in insect preparations (Robertson, 2004a; Robertson, 2004b). HS signals a change to more extreme environmental conditions and it has pleiotropic effects to prepare cells, tissues and organisms for such a change. The shift to higher temperatures of the neural off-

switch described here would be appropriate for an organism that has put protective mechanisms in place with a robust HS response (Whyard et al. 1986; Qin et al. 2003). Here we show that at least part of the beneficial effect of HS was on the rate of clearance of extracellular K^+ ions with no change in the initial disturbance. There was no evidence that this was due to improvements of energy status or management; ATP levels in the MTG after HS were not different from control either at rest, during anoxic stress or during hyperthermic stress. Given the thermoprotective effect of a heat shock protein (Hsp70) on mammalian muscle sarco/endoplasmic reticulum Ca^{2+} ATPase (Tupling et al. 2004) we suspected that the SD-like event in the locusts might have been shortened by a protective effect of HS on the activity of the Na^+/K^+ ATPase pump. However measurement of ouabain-sensitive ATPase activity in a biochemical assay of the metathoracic ganglion was not different after HS, with or without the presence of phosphatase inhibitors. Measurements of Na^+/K^+ ATPase activity were made on ganglia of CON and HS locusts at rest, and it is possible that examination of pump activity when stimulated by a rise in $[K^+]_o$ would yield different results suggesting a role for the pump. In addition, this result does not rule out the possibility that HS affected the trafficking of Na^+/K^+ ATPase complexes in neuronal and glial membranes. Nevertheless an effective concentration of ouabain ($10^{-5}M$) did not prevent the protective effects of HS on K^+ clearance in the MTG. Indeed the ouabain-sensitive proportion of extracellular K^+ ion clearance was reduced by HS suggesting either that HS somehow rendered membrane-bound Na^+/K^+ ATPase less sensitive to ouabain or that HS was acting via a different mechanism such as glial buffering via inwardly rectifying K^+ channels. This issue is currently unresolved.

In summary we conclude that in locust CNS different stressors converge on an adaptive SD-like event that can be preconditioned by prior HS to delay its occurrence until higher temperatures. We believe that the mechanisms underlying this event are much like those underlying CSD and other SD-like phenomena in mammals and a conserved genetic component to this thermotolerance pathway in insects has recently been demonstrated (Dawson-Scully et al. 2007). It is therefore an intriguing possibility that this phenomenon in the locust and migraine in humans (Lauritzen, 2001; Loder, 2002; van den Maagdenberg et al. 2007) have common evolutionary origins.

2.5 Materials and Methods

Animals

Adult male locusts, *Locusta migratoria migratorioides* (R. and F.), 4-6 weeks past the imaginal ecdysis, were randomly chosen from a crowded colony maintained in the Department of Biology at Queen's University. The animals were housed in cages within the colony under a 12 h:12 h light:dark cycle. Each cage was individually lit with a 40 W fluorescent light bulb. Room temperature was maintained at $25 \pm 1^\circ\text{C}$, with a constant humidity of $23 \pm 1\%$. Animals were provided with wheat seedlings and carrot slices once daily and an *ad libitum* mixture of 1 part skim milk powder, 1 part torula yeast, and 13 parts bran, by volume. All animals were collected from the colony at the same time each morning and were placed in a two litre ventilated plastic container for 4-8 hours prior to experimentation.

Heat shock pre-treatment

Locusts designated for control (CON) and HS pre-treatments were separated into different containers. HS locusts were placed in a humid incubator (45°C) for 3 hours followed by 1-5 hours of recovery at room temperature ($21 \pm 2^\circ\text{C}$). CON animals were held at room temperature for 4-8 hours.

Preparation of potassium-sensitive microelectrodes

$[\text{K}^+]_o$ was measured with K^+ -sensitive microelectrodes. The K^+ -sensitive microelectrodes were made from unfilamented glass pipettes (0.1mm diameter; World Precision Instruments Inc., Sarasota, FL, USA) that were cleaned with methanol (99.9%)

and dried on a hot plate, then pulled to form a low resistance (5-7M Ω) tip. The microelectrodes were silanized by exposure to dichlorodimethylsilane (99%) (Sigma-Aldrich) vapor while baking on a hot plate (100°C) for one hour. After cooling, the microelectrodes were filled at the tip with Potassium Ionophore I - Cocktail B (5% Valinomycin; Sigma-Aldrich) to form an artificial membrane and then back-filled with 500mM KCl. The tips of the K⁺-sensitive microelectrodes were suspended in distilled water until experimentation. Reference electrodes were made by pulling a filamented pipette (0.1mm diameter; World Precision Instruments Inc.) to form a low resistance (5-7M Ω) tip and were filled with 3M KCl.

Semi-intact preparation

Following removal of legs, wings and pronotum, the nervous system and ventilatory muscle 161 were exposed by making a dorsal midline incision and pinning the locust open onto a cork board, dorsal side up. The gut, air sacs and fat bodies were removed. A Peri-Star peristaltic pump (World Precision Instruments Inc.) was used for perfusion of standard locust saline into the thoracic and abdominal cavities which contained (in mM) 147 NaCl, 10 KCl, 4 CaCl₂, 3 NaOH, and 10 HEPES buffer (pH 7.2) (all chemicals were from Sigma-Aldrich). The saline flow was directed onto the MTG where the ventilatory CPG is located and exited through an incision in the posterior abdominal wall. The tissue covering the MTG was removed as well as the cuticle and attached muscle tissue situated between the connectives. A metal plate was inserted below the MTG to stabilize it. Nerves five and seven of the MTG were cut on both sides to allow saline and

pharmacological agents to permeate the ganglion. The preparation was grounded by placing a silver wire in the posterior tip of the abdomen.

Electromyographic recording of the motor pattern

An extracellular recording of the ventilatory motor pattern was obtained by placing a 0.1mm diameter copper wire, insulated except at the tip, onto abdominal muscle 161. The recording was digitized using a DigiData 1200 Series Interface (Axon Instruments Inc., Union City, CA, USA) and displayed using AxoScope 9.0 software (Axon Instruments Inc.). Ventilation can be monitored as a series of rhythmic electrical bursts in the abdominal muscles (e.g. Figure 2.1D and E). Failure was characterized as the cessation of electrical activity in the extracellular recording and the lack of visible contractions of the ventilatory muscles. Recovery was defined as the first visible sign of rhythmical abdominal contractions coincident with resumption of rhythmic electrical activity.

Extracellular potassium recording

K^+ -sensitive microelectrodes were connected to a pH/Ion amplifier (Model 2000; A-M Systems Inc., Carlsborg, WA, USA) by an electrode holder with a chloride-coated silver wire. Preceding each experiment, a K^+ -sensitive and a reference electrode were calibrated at room temperature ($\sim 21^\circ\text{C}$) using 15mM and 150mM KCl solutions to determine the voltage change, or 'slope', which was needed for determination of $[K^+]_o$ (mM) using the Nernst equation. Electrode sensitivities ranged from 54 to 58mV for a 10-fold change in $[K^+]$. A reference and K^+ -sensitive electrode pair were discarded if the

slope did not fall within this range or if the voltage reading exhibited atypical sensitivities. The K^+ -sensitive microelectrode was inserted through the sheath of the MTG adjacent to the reference electrode in the area of the ventilatory CPG.

The voltage of the K^+ -sensitive electrode is logarithmically related to the potassium concentration which was obtained by transforming the $[K^+]_o$ trace in mV to mM using the Nernst equation:

$$E_K = RT / zF \cdot \ln[K^+]_o / [K^+]_i.$$

In the above equation, E_K is the membrane potential at which K^+ is at equilibrium, R is the gas constant ($8.315 \text{ J} \cdot \text{K}^{-1} \cdot \text{mol}^{-1}$), T is the temperature in ° Kelvin ($T_{\text{Kelvin}} = 273.16 + T_{\text{Celsius}}$), F is Faraday's constant ($96,485 \text{ C} \cdot \text{mol}^{-1}$), z is the valence of the ion, and $[K^+]_o$ and $[K^+]_i$ are the concentrations of K^+ outside and inside the cell, respectively. For a membrane permeable only to K^+ at room temperature (20°C), substituting the appropriate numbers and converting natural log (\ln) into log base 10 (\log_{10}) results in the equation:

$$E_K = 58.2 \log_{10}[K^+]_o / [K^+]_i.$$

The K^+ -sensitive electrode voltage recording was set to zero in a stock solution of 15mM KCl and the following conversion of the above equation was used for determination of extracellular potassium concentrations (corrections for temperature differences were made when appropriate):

$$[K^+]_o = 15 \cdot 10^{\text{voltage} / \text{slope}(-58.2)}.$$

Hyperthermia

Preparations were bathed for 25 minutes with saline before starting the temperature ramp to allow the ventilatory rhythm to stabilize and the $[K^+]_o$ to settle at around 10mM. Saline passed through a glass pipette wrapped in NichromeTM wire, and the temperature of the saline was controlled by varying the amount of current passed through the wire. Temperature at the ganglion was monitored using a thermocouple connected to a digital thermometer (BAT-12; Physitemp Instruments Inc., Clifton, NJ, USA). Internal temperature was raised in a ramped manner 5°C per minute from room temperature (~20°C) until failure of the motor pattern (Figure 2.1A, Figure 2.6C, and Figure 2.7), until the abrupt rise in $[K^+]_o$ was observed (Figure 2.4A), or raised beyond the first $[K^+]_o$ plateau (not necessarily in a ramped manner) until a second plateau was reached (Figure 2.3 and Figure 2.4B). At this time, the heater was switched off allowing the saline temperature to return to ambient levels and the motor pattern to recover.

Anoxia

The locust preparation was enclosed in a sealed chamber. Nitrogen gas (N₂) was first bubbled into the superfusing saline for 5 minutes then blown over the preparation within the chamber. 100% N₂ was maintained until 1 minute post-failure of the motor pattern at which point the preparation was re-oxygenated.

Pharmacological treatments

All drugs were dissolved in standard locust saline and bath-applied in semi-intact preparations as described above (all drugs were obtained from Sigma-Aldrich).

Preparations were bathed in standard locust saline for a 10 minute stabilization period prior to pharmacological treatment. Drugs were bath-applied continuously for the full duration of each experiment with the exception of 10^{-3} M sodium azide (NaN_3), an electron transport chain inhibitor that prevents cells from using oxygen, which was bath-applied until 1 minute post-failure. 10^{-4} M ouabain, a Na^+/K^+ ATPase toxin, was bath-applied continuously for 1 hour. 10^{-6} M tetrodotoxin (TTX), a Na^+ channel blocker, and 10^{-1} M tetraethylammonium chloride (TEA), a voltage-gated K^+ channel blocker, were bath-applied for 15 minutes prior to a ramped increase in temperature (5°C per minute). For TTX experiments, the heater was turned off once the $[\text{K}^+]_o$ surge was observed and the temperature at the $[\text{K}^+]_o$ surge was taken as the temperature at half the maximum amplitude of the $[\text{K}^+]_o$ increase. For TEA experiments, the temperature ramp was continued beyond the first $[\text{K}^+]_o$ plateau until a second plateau was reached, at which point the heater was turned off.

CON and HS locusts were treated with 10^{-5} M ouabain to determine the role of ouabain-sensitive Na^+/K^+ ATPase activity in thermotolerance and $[\text{K}^+]_o$ homeostasis. Animals were divided into four groups: 1) CON, N = 17; 2) HS, N = 18; 3) CON locusts treated with 10^{-5} M ouabain (CON-OUA), N = 10; 4) HS locusts treated with 10^{-5} M ouabain (HS-OUA), N = 8. Experiments on animals receiving different (pre-) treatments were interspersed over time with each other. All preparations were bathed for 25 minutes with saline before starting the temperature ramp. For 10^{-5} M ouabain treatment, the ganglion was bathed with standard locust saline for 10 minutes, and then with 10^{-5} M ouabain for 15 minutes prior to the temperature ramp. At 25 minutes, internal temperature was raised

in a ramped manner 5°C per minute until failure of the motor pattern. Failure temperature (°C) and time to recovery (s) were scored as the temperature at which rhythmical ventilator activity ceased and the length of time taken to recover motor pattern function, respectively. In order to determine the nature of the relationships between time to recovery and failure temperature for each group, values were log-transformed to make the relationships linear, which allowed accurate statistical analyses of the data. The correlations are shown in Figure 2.7 as scatterplots of the untransformed data fit with exponential curves that rise to a plateau. Rates of $[K^+]_o$ increase and decrease associated with hyperthermic failure and recovery of the motor pattern were also determined. Rate of $[K^+]_o$ increase (mM/s) was calculated as the slope between the baseline at the inflection point of the $[K^+]_o$ increase and the maximum peak $[K^+]_o$. Rate of $[K^+]_o$ decrease (mM/s) was calculated as the slope between the maximum peak $[K^+]_o$ and the baseline $[K^+]_o$ inflection point. The sample sizes for each analysis varied depending on the ability to measure parameters in some or all locusts within each group.

To locally increase $[K^+]_o$ in the MTG neuropile we pressure-injected using a PicoSpritzer III (INTRACEL, Shepreth, UK) a small volume (35nl) of locust saline containing a 15-fold higher $[K^+]_o$ (147mM NaCl, 150mM KCl, 4mM CaCl₂, 3mM NaOH, 10mM HEPES buffer, pH 7.2). Two K^+ -sensitive microelectrodes were inserted into the MTG, one next to the injection point and another in a different region of the ganglion. The distance between the recording electrodes (~0.4 to 0.6mm) was determined as well as the time to onset of the $[K^+]_o$ surge measured by each electrode. Using these values the speed of

propagation (mm/s) of the $[K^+]_o$ disturbance between the two recording electrodes was calculated.

ATP extraction and assay for locust ganglia

Metathoracic ganglia were removed from locust preparations prior to stress, at stress-induced failure, and at recovery of the motor pattern for ATP measurement. ATP levels in the ventilatory neuropile of HS locusts at hyperthermic failure and subsequent recovery of the motor pattern were also measured in order to determine if preconditioning confers protection by increasing energy availability. In addition, metathoracic ganglia were removed from CON and HS locusts at normal oxygen levels (pre-anoxia) and at 15, 30, 60, and 120 minutes of anoxia exposure. Locusts were then removed from the anoxic environment and ganglia were removed at 30 and 60 minutes post-anoxia for ATP measurement.

Immediately after removal, each ganglion was added to 220 μ l of ice-cold 3.5% perchloric acid in a 1.5ml centrifuge tube. The ganglion was homogenized thoroughly with a pestle and the solution was centrifuged for 5 minutes at maximum speed. Then, 200 μ l of the supernatant were transferred to a new centrifuge tube on ice containing 20 μ l Tris (saturated), 20 μ l KCl (2M), 10 μ l phenol red (0.005%), and 120 μ l KOH (1M) to neutralize the sample. The neutralized sample was stored at -80°C until the ATP assays were performed. At that time, samples were thawed and centrifuged for five minutes at maximum speed. A volume of 2.5 μ l of supernatant was used for the ATP assay.

ATP was quantified using a luciferin-luciferase reaction in which ATP is consumed and light is emitted when firefly luciferase catalyzes the oxidation of D-luciferin. Since ATP is the limiting reagent, the light emitted is proportional to the ATP present, measured by an L_{\max} luminometer (Molecular Devices, Sunnyvale, CA, USA). A reaction mix was prepared by diluting one volume of luciferin-luciferase ATP Assay Mix (lyophilized powder containing luciferin, luciferase, $MgSO_4$, DTT, EDTA Na_4 , BSA, and tricine buffer salts dissolved in 5ml of sterile water) with 100 volumes of ATP Assay Mix Dilution Buffer (250ml: 300mg $MgSO_4$, 4mg DTT, 100mg EDTA Na_4 , 250mg BSA, 2.25g tricine buffer salts, pH 7.5). The diluted luciferin-luciferase reaction mix was added by auto injector in 200 μ l aliquots to 2.5 μ l of sample, pre-dispensed in a 96-well microplate. Light was collected for 20 seconds. Measures of light intensity were compared to a standard curve generated using known quantities of ATP prepared in water, acidified and neutralized as were samples.

Assay of Na^+/K^+ ATPase activity in locust MTG

The Na^+/K^+ ATPase activity was assessed using a pyruvate kinase/lactate dehydrogenase assay in the presence or absence of ouabain. Single metathoracic ganglia from control and HS locusts were homogenized on ice in 300 μ L of lysis buffer (150mM sucrose, 10mM EDTA, 50mM imidazole and 0.1% deoxycholate, pH 7.3). In one experiment, inhibitors of phosphorylation and dephosphorylation were also added to the lysis buffer to prevent changes in the phosphorylation status of the ATPase. The additional compounds included (in mM) 10 EGTA, 50 NaF, 10 tetrasodium pyrophosphate, 1 phospho-serine, 1 phospho-threonine, and 1 phospho-tyrosine. After homogenization,

0.01 volumes of 100mM PMSF (dissolved in isopropanol) were added to the homogenate.

The measurement of ATPase activity was measured as the production of NADH spectrophotometrically for 10 minutes at 340 nm. Each sample was assayed in six wells on the 96 well plate, three containing ouabain. Each well contained a 300 μ L reaction mixture consisting of the following solutions (in order): 228 μ L of assay buffer (50mM imidazole, 100mM NaCl, 20mM KCl, and 5mM MgCl₂), 3 μ L each of 0.2mM NADH, 0.5mM PEP, 10U/mL LDH, and 10U/mL PK, 15 μ L of either ouabain (0.5mM) or assay buffer, and 30 μ L sample homogenate. The reaction was started with the addition of 15 μ L ATP (3mM). The slope of absorbance over 10 minutes was compared between samples with and without ouabain to give a value for activity of only Na⁺/K⁺ ATPase. This value was normalized to total protein within the sample, which was measured from each homogenate using a standard protocol based on the Bradford method (Bradford, 1976).

Statistical analyses

Data were plotted using SigmaPlot 8.0 (SPSS Inc., Chicago, IL, USA) and results are reported as the mean \pm standard error (s.e.m.). Data were analyzed using SigmaStat 3.0 statistical analysis software (SPSS Inc.) and statistical differences were determined using appropriate parametric tests as indicated in the text. A 95% confidence interval was used to determine significance among means.

2.6 References

Anderson TR, Jarvis CR, Biedermann AJ, Andrew RD (2005) Blocking the anoxic depolarization: neuroprotection without functional compromise following simulated stroke in cortical brain slices. *J Neurophysiol* 93: 963-979.

Armstrong GAB, Shoemaker KL, Money TGA, Robertson RM (2006) Octopamine mediates thermal preconditioning of the locust ventilatory central pattern generator via a cAMP/protein kinase A signaling pathway. *J Neurosci* 26: 12118-12126.

Balestrino M, Young J, Aitken PG (1999) Block of (Na⁺,K⁺)ATPase with ouabain induced spreading depression-like depolarization in hippocampal slices. *Brain Res* 838: 37-44.

Banks WM, Bruce AS, Peart HT (1975) The effects of temperature, sex and circadian rhythm on oxygen consumption in two species of cockroaches. *Comp Biochem Physiol* 52A: 223-227.

Bradford MM (1976) A rapid and sensitive method for the quantitation of microgram quantities of protein utilizing the principle of protein-dye binding. *Anal Biochem* 72: 248-254.

Bustami HP, Hustert R (2000) Typical ventilatory pattern of the intact locust is produced by the isolated CNS. *J Insect Physiol* 46: 1285-1293.

Davenport AP, Evans PD (1984) Stress-induced changes in the octopamine levels of insect haemolymph. *Insect Biochem* 14: 135-143.

Dawson-Scully K, Armstrong GAB, Kent C, Robertson RM, Sokolowski MB (2007) Natural variation in the thermotolerance of neural function and behavior due to a cGMP-dependent protein kinase. *PLoS ONE* 2: e773 (doi:10.1371/journal.pone.0000773).

Evans AM (2006) AMP-activated protein kinase and the regulation of Ca²⁺ signalling in O₂-sensing cells. *J Physiol* 574: 113-123.

Gidday JM (2006) Cerebral preconditioning and ischaemic tolerance. *Nat Neurosci* 7: 437-448.

Grafstein B (1956) Mechanism of spreading cortical depression. *J Neurophysiol* 19: 154-171.

Gulinson SL, Harrison JF (1996) Control of resting ventilation rate in grasshoppers. *J Exp Biol* 199: 379-389.

Hardie DG, Hawley SA, Scott JW (2006) AMP-activated protein kinase - development of the energy sensor concept. *J Physiol* 574: 7-15.

Henderson DR, Johnson SM, Prange HD (1998) CO₂ and heat have different effects on directed ventilation behaviour of grasshoppers *Melanoplus differentialis*. *Respir Physiol* 114: 297-307.

Hustert R (1975) Neuromuscular coordination and proprioceptive control of rhythmical abdominal ventilation in intact *Locusta migratoria migratorioides*. *J Comp Physiol A* 97: 159-179.

Kager H, Wadman WJ, Somjen GG (2002) Conditions for the triggering of spreading depression studied with computer simulations. *J Neurophysiol* 88: 2700-2712.

Kretschmar D, Pflugfelder GO (2002) Glia in development, function, and neurodegeneration of the adult insect brain. *Brain Res Bull* 57: 121-131.

Largo C, Tombaugh GC, Aitken PG, Herreras O, Somjen GG (1997) Heptanol but not fluoroacetate prevents the propagation of spreading depression in rat hippocampal slices. *J Neurophysiol* 77: 9-16.

Lauritzen M (2001) Cortical spreading depression in migraine. *Cephalalgia* 21: 757-60.

Leão AAP (1944) Spreading depression of activity in the cerebral cortex. *J Neurophysiol* 7: 359-390.

Lighton JRB, Lovegrove BG (1990) A temperature-induced switch from diffusive to convective ventilation in the honeybee. *J Exp Biol* 154: 509-516.

Loder E (2002) What is the evolutionary advantage of migraine? *Cephalalgia* 22: 624-632.

Nedergaard M, Cooper AJL, Goldman SA (1995) Gap junctions are required for the propagation of spreading depression. *J Neurobiol* 28: 433-444.

Newman AEM, Foerster M, Shoemaker KL, Robertson RM (2003) Stress-induced thermotolerance of ventilatory motor pattern generation in the locust, *Locusta migratoria*. *J Insect Physiol* 49: 1039-1047.

Qin W, Tyshenko MG, Wu BS, Walker VK, Robertson RM (2003) Cloning and characterization of a member of the Hsp70 gene family from *Locusta migratoria*, a highly thermotolerant insect. *Cell Stress Chaperones* 8: 144-52.

Ramirez JM, Elsen FP, Robertson RM (1999) Long-term effects of prior heat shock on neuronal potassium currents recorded in a novel insect ganglion slice preparation. *J Neurophysiol* 81: 795-802.

Robertson RM (2004a) Modulation of neural circuit operation by prior environmental stress. *Integr Comp Biol* 44: 21-27.

Robertson RM (2004b) Thermal stress and neural function: adaptive mechanisms in insect model systems. *J Therm Biol* 29: 351-358.

Smith JM, Bradley DP, James MF, Huang CL (2006) Physiological studies of cortical spreading depression. *Biol Rev Camb Philos Soc* 81: 457-481.

Snyder GK, Ungerman G, Breed M (1980) Effects of hypoxia, hypercapnia, and pH on ventilation rate in *Nauphoeta cinerea*. *J Insect Physiol* 26: 699-702.

Somjen GG (2001) Mechanisms of spreading depression and hypoxic spreading depression-like depolarization. *Physiol Rev* 81: 1065-1096.

Somjen GG (2002) Ion regulation in the brain: implications for pathophysiology. *Neuroscientist* 8: 254-267.

Takano T, Tian G-F, Peng W, Lou N, Lovatt D, et al. (2007) Cortical spreading depression causes and coincides with tissue hypoxia. *Nat Neurosci* 10: 754-762.

Tupling AR, Gramolini AO, Duhamel TA, Kondo H, Asahi M, et al. (2004) HSP70 binds to the fast-twitch skeletal muscle sarco(endo)plasmic reticulum Ca^{2+} -ATPase (SERCA1a) and prevents thermal inactivation. *J Biol Chem* 279: 52382-52389.

van den Maagdenberg AM, Haan J, Terwindt GM, Ferrari MD (2007) Migraine: gene mutations and functional consequences. *Curr Opin Neurol* 20: 299-305.

van Harrevald A (1978) Two mechanisms for spreading depression in the chicken retina. *J Neurobiol* 9: 419-431.

Walther C, Zittlau KE (1998) Resting membrane properties of locust muscle and their modulation. II. Actions of the biogenic amine octopamine. *J Neurophysiol* 80: 785-797.

Whyard S, Wyatt GR, Walker VK (1986) The heat shock response in *Locusta migratoria*. *J Comp Physiol B* 156: 813-817.

Wu J, Fisher RS (2000) Hyperthermic spreading depressions in the immature rat hippocampal slice. *J Neurophysiol* 84: 1355-1360.

Chapter 3

K⁺ homeostasis and central pattern generation in the metathoracic ganglion of the locust.

3.1 Abstract

Stress-induced arrest of ventilatory motor pattern generation is tightly correlated with an abrupt increase in extracellular potassium concentration ($[K^+]_o$) within the metathoracic neuropil of the locust, *Locusta migratoria*. Na^+/K^+ -ATPase inhibition with ouabain elicits repetitive surges of $[K^+]_o$ that coincide with arrest and recovery of motor activity. Here we show that ouabain induces repetitive $[K^+]_o$ events in a concentration-dependent manner. $10^{-5}M$, $10^{-4}M$, and $10^{-3}M$ ouabain was bath-applied in semi-intact locust preparations. $10^{-4}M$ and $10^{-3}M$ ouabain reliably induced repetitive $[K^+]_o$ events whereas $10^{-5}M$ ouabain had no significant effect. In comparison to $10^{-4}M$ ouabain, $10^{-3}M$ ouabain increased the number and hastened the time to onset of repetitive $[K^+]_o$ waves, prolonged $[K^+]_o$ event duration, increased resting $[K^+]_o$, and diminished the absolute value of $[K^+]_o$ waves. Recovery of motor patterning following $[K^+]_o$ events was less likely in $10^{-3}M$ ouabain. In addition, we show that K^+ channel inhibition using TEA suppressed the onset and decreased the amplitude of ouabain-induced repetitive $[K^+]_o$ waves. Our results demonstrate that ventilatory circuit function in the locust CNS is dependent on the balance between mechanisms of $[K^+]_o$ accumulation and $[K^+]_o$ clearance. We suggest that with an imbalance in favour of accumulation the system tends towards a bistable state with transitions mediated by positive feedback involving voltage-dependent K^+ channels.

3.2 Introduction

Potassium (K^+) plays an important role in the nervous system and therefore disruption of K^+ homeostasis can have important consequences for neuronal function. Prior research using both invertebrate and vertebrate models has demonstrated that stress-induced failure of neural function coincides with a loss in K^+ homeostasis (Rounds, 1967; Erulkar and Weight, 1977; Balestrino et al., 1999; Wu and Fisher, 2000; Xiong and Stringer, 2000; Rodgers et al., 2007). In the locust (*Locusta migratoria*) stress-induced arrest of ventilation is tightly correlated with an abrupt increase in extracellular potassium concentration ($[K^+]_o$) within the ventilatory neuropil (Rodgers et al., 2007), however the cellular mechanisms involved in the initiation of and recovery from stress-induced ventilatory arrest and the associated increases in $[K^+]_o$ in the locust are not known. We investigated the role of the Na^+/K^+ pump and K^+ channel conductances in ventilatory arrest and recovery.

The migratory locust provides an exceptional model system for characterizing the relationship between neural circuit function and K^+ ion homeostasis. This invertebrate provides a rare opportunity as its vital neural circuitry is experimentally accessible for simultaneous, comprehensive studies at both cellular and systemic levels (Robertson, 2004). We are able to monitor potassium ion disturbances within the neuropil while simultaneously monitoring failure and recovery of an intact neural circuit. Ventilation is a key motor behaviour necessary for the circulation, supply, and removal of respiratory gases. Due to its important nature it is imperative that functioning remains intact, as prolonged loss of function could lead to oxygen starvation and ultimately death.

Ventilation, defined as the contraction and expansion of the thoracic and abdominal cavities, is represented by two different forms in the locust: discontinuous and continuous (Harrison, 1997; Bustami and Hustert, 2000). Whereas discontinuous ventilation commonly occurs during undisturbed states or rest (Harrison, 1997), stress causes the ventilatory pattern to become continuous, making ventilatory muscles contract in a more constant and predictable fashion (Bustami and Hustert, 2000). Control of ventilatory motor activity in locusts is accomplished by a central pattern generator (CPG) situated in the metathoracic ganglion (MTG) (Ramirez and Pearson, 1989; Bustami and Hustert, 2000). Although incomplete, current knowledge indicates that the ventilatory CPG (“vCPG”) is composed primarily of a network of interneurons (Ramirez and Pearson, 1989), which are connected to the motor neurons relaying neuronal signals to the thoracic and abdominal muscles responsible for ventilation (Bustami and Hustert, 2000).

Neuronal membranes become depolarized when $[K^+]_o$ increases (Huxley and Stämpfli, 1951; Somjen, 2002). Initially, a neuron can become hyperexcitable as its firing threshold is approached during minor depolarization (Balestrino et al., 1999; Somjen, 2002). Further depolarization however can depress excitability as some voltage-gated Na^+ and Ca^{2+} channels inactivate, which increases firing threshold, decreases action potential amplitude, and can also limit neurotransmitter release (Erulkar and Weight, 1977; Somjen, 2002). $[K^+]_o$ levels are largely regulated by glial cells which form the superficial layer of the insect CNS, also referred to as the sheath of the ganglion (Kretzschmar and Pflugfelder, 2002). Glial cells utilize multiple different ion channels that are capable of K^+ uptake from the interstitial space. The $Na^+/K^+/2Cl^-$ co-transporter,

for instance, picks up a K^+ ion from the extracellular space in exchange for a Na^+ ion and two Cl^- ions (Walz, 1987), while inwardly rectifying potassium channels have been shown to display an increase in conduction during rises in $[K^+]_o$ (Newman, 1993; Leis et al., 2005). In addition, gap junctions between glial cells provide a network that acts as a “spatial buffer” for K^+ (Orkand et al. 1966; Leis et al., 2005). The Na^+/K^+ -ATPase is essential for cellular function due to its role in maintenance of ionic concentration gradients across the membrane. The Na^+/K^+ -ATPase has a hyperpolarizing effect in cells by pumping three Na^+ ions out of the cell for every two K^+ ions into the cell and this requires the expenditure of energy (ATP hydrolysis). 50-60% of neuronal ATP levels are devoted to driving the Na^+/K^+ pump (Erecinska and Silver, 1994) indicating its important role in the maintenance of ion homeostasis.

Previously we have shown that in the locust abrupt increases in $[K^+]_o$ are reliably triggered in response to multiple cellular stressors, namely hyperthermia, anoxia (N_2), ATP depletion (NaN_3), and Na^+/K^+ -ATPase impairment (ouabain) (Rodgers et al., 2007). The increase in $[K^+]_o$ associated with arrest of the ventilatory motor pattern occurs within the locust MTG surrounding the vCPG and is not modest, increasing by approximately 40-60mM at arrest induced by anoxia, ATP depletion, and Na^+/K^+ -ATPase inhibition (Rodgers et al., 2007). $[K^+]_o$ gradually decreases when the stress is removed and this coincides with recovery of ventilatory motor pattern generation (Rodgers et al., 2007). Interestingly, inhibition of the Na^+/K^+ pump induces repetitive arrest of the vCPG (Rodgers et al., 2007). Continuous bath application of $10^{-4}M$ ouabain elicits multiple surges in $[K^+]_o$ where the rise and fall of $[K^+]_o$ are associated with arrest and recovery of

the ventilatory motor pattern, respectively (Rodgers et al., 2007). One explanation for the repetitive nature of the arrest induced by 10^{-4} M ouabain is that it critically depends on the balance between the processes of $[K^+]_o$ accumulation and clearance. If this hypothesis is true then manipulation of these processes should affect the occurrence and characteristics of repetitive ventilatory arrest.

In this paper we characterize ouabain-induced repetitive $[K^+]_o$ events in the locust ventilatory neuropil and the associated vCPG arrest in detail. We show that the time to initiation as well as the severity of this phenomenon, i.e. number of $[K^+]_o$ events, $[K^+]_o$ event duration, pre- and post-surge resting $[K^+]_o$ levels, slope of $[K^+]_o$ increase, and likelihood of vCPG recovery following $[K^+]_o$ surges, is dependent on the magnitude of ouabain-induced inhibition of $[K^+]_o$ clearance (varying ouabain concentration). We also show that the onset and severity of repetitive $[K^+]_o$ events induced by ouabain is dependent on the level of $[K^+]_o$ accumulation through K^+ channels (inhibition of voltage-dependent K^+ channels with tetraethylammonium chloride).

3.3 Materials and Methods

Animals

Adult male locusts, *L. migratoria migratorioides* (R. and F.), aged approximately 3-5 weeks past imaginal ecdysis, were randomly selected from a crowded colony located in the Animal Care Facility of the Biosciences Complex at Queen's University. The colony was reared under a 12h:12h light:dark photoperiod at a room temperature of $30 \pm 1^\circ\text{C}$ during light hours and $26 \pm 1^\circ\text{C}$ during dark hours. Humidity was maintained at $23 \pm 1\%$. Animals were provided with carrots, wheat seedlings and an ad libitum mixture of 1 part skim milk powder, 1 part torula yeast, and 13 parts bran, by volume.

Preparation of potassium-sensitive microelectrodes

K^+ -sensitive microelectrodes were made from 1 mm diameter unfilamented capillary tubes (World Precision Instruments Inc., Sarasota, FL, USA) that were cleaned with methanol (99.9%) and dried on a hot plate before being pulled to form a low resistance (5-7 M Ω) tip. The inner glass surface of the microelectrodes was made hydrophobic by exposure to dichlorodimethylsilane (99%) (Sigma-Aldrich) vapor while baking on a hot plate (100°C) for 1 h. The microelectrodes were allowed to cool, then filled at the tip with Potassium Ionophore I-Cocktail B (5% valinomycin; Sigma-Aldrich) and back-filled with 500mM KCl. Reference microelectrodes were made from 1 mm diameter filamented capillary tubes (World Precision Instruments Inc., Sarasota, FL, USA) that were pulled to form a low resistance (5-7 M Ω) tip, then filled with 3M KCl. Microelectrode tips were suspended in distilled water until experimentation.

Semi-intact preparation

Appendages and pronotum were removed and a dorsal midline incision was made. A corkboard was used to pin open the locust dorsal side up, allowing the gut, fatty tissue and air sacs to be removed, exposing the metathoracic ganglion (MTG) and ventilatory muscle 161 (M161) found in the second abdominal segment (A2). This provided a semi-intact preparation as utilized by Newman et al. (2003).

Standard locust saline containing (in mM): 147 NaCl, 10 KCl, 4 CaCl₂, 3 NaOH, and 10 HEPES buffer (pH 7.2) was perfused into the thoracic cavity through a glass pipette using a Peri-Star peristaltic pump (World Precision Instruments Inc., Sarasota, FL, USA). The saline flow was directed onto the MTG where the vCPG is located with overflow draining out of the posterior abdomen. The tissue covering the MTG was removed, followed by the cuticle and attached muscle tissue situated between the connectives, rostral to the metathoracic ganglion. A metal plate was placed beneath the MTG to stabilize it, and a silver wire was inserted into the caudal portion of the abdomen to ground the preparation.

Electromyographic recording of the motor pattern

An electromyographical (EMG) recording of the ventilatory motor pattern was obtained by resting the non-insulated tip of a 0.1 mm diameter insulated copper wire onto the ventilatory muscle 161 located in the second abdominal segment (A2). A DigiData 1200 Series Interface (Axon Instruments Inc., Union City, CA, USA) was used to digitize the

ventilation recordings which were then displayed and recorded using AxoScope 9.0 software (Axon Instruments Inc.).

Extracellular potassium recording

K⁺-sensitive and reference microelectrodes were connected to a pH/ion amplifier (Model 2000; A-M Systems Inc., Carlsborg, WA, USA). A K⁺-sensitive and reference microelectrode pair was calibrated at room temperature (~21°C) using 15mM and 150mM KCl solutions to obtain the voltage change, or 'slope', which was required for determination of [K⁺]_o (mM). A 10-fold change in [K⁺] resulted in a voltage change of ~58 mV and only electrode pairs with slope values very close to 58 mV (± 4 mV) were accepted for experimental use. Following calibration, the K⁺-sensitive and reference microelectrodes were inserted through the sheath of the MTG side-by-side in the region of the vCPG (Burrows, 1996). Specifically, the microelectrodes were placed centrally in the region of the first three abdominal neuromeres, which are fused to the metathoracic neuromere, forming the MTG. [K⁺]_o changes spread to other regions of the MTG (but not through the connectives), therefore placement of microelectrodes precisely at the vCPG was important to accurately measure the timing of [K⁺]_o disturbances surrounding the vCPG relative to arrest of the ventilatory motor pattern.

The [K⁺]_o was obtained by transforming the recorded [K⁺]_o trace in mV to mM using the Nernst equation:

$$E_K = RT / zF \cdot \ln[K^+]_o / [K^+]_i.$$

The following conversion of the above equation was used for determination of $[K^+]_o$ (mM):

$$[K^+]_o = 15 \cdot 10^{\text{voltage} / \text{slope}(\sim 58)}$$

Pharmacological treatments

Drugs (Sigma-Aldrich) were dissolved in standard locust saline and bath-applied in semi-intact preparations as described above. Ouabain solutions were kept in opaque coverings to prevent exposure to light. All preparations were bathed in standard locust saline for a 10 min stabilization period prior to bath application of drugs. To examine the effects of different concentrations of ouabain $10^{-5}M$, $10^{-4}M$, and $10^{-3}M$ ouabain solutions were bath-applied in preparations for a minimum of 30 min. To examine the effects of potassium channel block $10^{-3}M$ TEA was bath-applied alone for 5 min followed by bath application of $10^{-3}M$ TEA in combination with $10^{-4}M$ ouabain for a minimum of 30 min.

The time to the initial $[K^+]_o$ event was calculated as the time from ouabain or TEA/ouabain application to the inflection point of the first abrupt increase in $[K^+]_o$. $[K^+]_o$ event duration was measured at half of the maximum amplitude and period was measured as the time from the upward inflection point of one $[K^+]_o$ event to the upward inflection point of the subsequent event. $[K^+]_o$ was calculated prior to the upward inflection point of the first surge as well as every 5 min thereafter to determine pre- as well as post-surge values. These values are termed “non-surge $[K^+]_o$ ”. The closest non-surge $[K^+]_o$ was chosen if time points coincided with an $[K^+]_o$ event. The maximum $[K^+]_o$ peak value during $[K^+]_o$ events was also measured. $[K^+]_o$ event amplitudes were calculated by

subtracting pre-surge $[K^+]_o$ from peak $[K^+]_o$. The change in extracellular $[K^+]$ during $[K^+]_o$ events is characterized by three distinct phases (Fig. 3.2D). The increase in $[K^+]_o$ from non-surge to peak values consists of one positive $[K^+]_o$ change referred to as the “up-slope”. Once peak $[K^+]_o$ is reached there is a slow $[K^+]_o$ decrease referred to as the “top-slope”. Finally, there is a switch from the slow top-slope phase to a steeper $[K^+]_o$ decrease termed the “down-slope”. The up-, top-, and down-slopes for the first $[K^+]_o$ event were calculated at the point of greatest change during these phases. The probability of ventilatory motor pattern recovery following $[K^+]_o$ events was determined for preparations treated with $10^{-3}M$ and $10^{-4}M$ ouabain.

Statistical analyses

Data were plotted using SigmaPlot 9.0 (SPSS Inc., Chicago, IL, USA) and presented as the mean and standard error (S.E.). Statistical analyses were performed using SigmaStat 3.0 statistical analysis software (SPSS Inc.). *t*-Tests were used to determine if there were statistically significant differences in overall means between treatment groups ($10^{-4}M$ vs. $10^{-3}M$ ouabain and $10^{-4}M$ ouabain alone vs. $10^{-4}M$ ouabain in combination with $10^{-3}M$ TEA). Two-way repeated measures (RM) ANOVAs were used to determine if there were statistically significant differences in mean measurements repeatedly taken over the duration of experiments between treatment groups. A two-way ANOVA was used to determine if there were significantly different mean slopes of $[K^+]_o$ increase and decrease during the first $[K^+]_o$ surge between treatment groups (two subject factors: $10^{-4}M$ vs. $10^{-3}M$ ouabain and up-, top-, or down-slope). *Post hoc* Tukey tests were performed to determine which groups drove the main effects. A Kaplan-Meier Survival Analysis was

conducted in order to determine if there were significant differences in the ability of the vCPG to recover following $[K^+]_o$ surges induced by $10^{-4}M$ vs. $10^{-3}M$ ouabain. A z-test was used to compare the proportion of preparations treated with $10^{-4}M$ ouabain alone vs. $10^{-4}M$ ouabain in combination with $10^{-3}M$ TEA that had at least one $[K^+]_o$ event. A 95% confidence interval was used to determine significance.

3.4 Results

Ouabain-induced inhibition of the Na^+/K^+ -ATPase elicits repetitive $[\text{K}^+]_o$ events

Ventilatory motor pattern activity and extracellular potassium ion concentration surrounding the vCPG were measured during treatment with different doses of the Na^+/K^+ -ATPase inhibitor ouabain (Fig. 3.1). It was shown previously that continuous bath application of 10^{-4}M ouabain elicits multiple surges in $[\text{K}^+]_o$ where the rise and fall of $[\text{K}^+]_o$ are associated with arrest and recovery of the vCPG, respectively (Rodgers et al., 2007). It was of interest to further explore this phenomenon and characterize the concentration-dependence of the effect of ouabain. A relationship between repetitive $[\text{K}^+]_o$ surges in the locust MTG and the concentration of ouabain in the bathing saline would indicate that the level of inhibition of Na^+/K^+ transporters and thus the rate of clearance of $[\text{K}^+]_o$ plays a role in vCPG arrest and the associated $[\text{K}^+]_o$ surge. We found that continuous bath application of two different concentrations of ouabain, 10^{-4}M and 10^{-3}M , elicited multiple abrupt surges in $[\text{K}^+]_o$ (Fig. 3.1A and B). 10^{-5}M ouabain was bath-applied in a total of four preparations and induced a single $[\text{K}^+]_o$ event in only one of these preparations (data not shown). During 10^{-4}M ouabain application the arrest and recovery of the ventilatory motor pattern were associated with the rise and fall of $[\text{K}^+]_o$, respectively (Fig. 3.1A). $[\text{K}^+]_o$ clearance always coincided with recovery of motor pattern generation, however the ventilatory rhythm frequency and duration became more variable following each $[\text{K}^+]_o$ surge (Fig. 3.1A). During 10^{-3}M ouabain application complete loss of the ventilatory motor pattern was eventually seen (Fig. 3.1B). $[\text{K}^+]_o$ events were reliably induced during both 10^{-4}M ($N = 8$) and 10^{-3}M ($N = 9$) ouabain treatment, with 100% of preparations ($N_{\text{total}} = 17$) having at least one $[\text{K}^+]_o$ event,

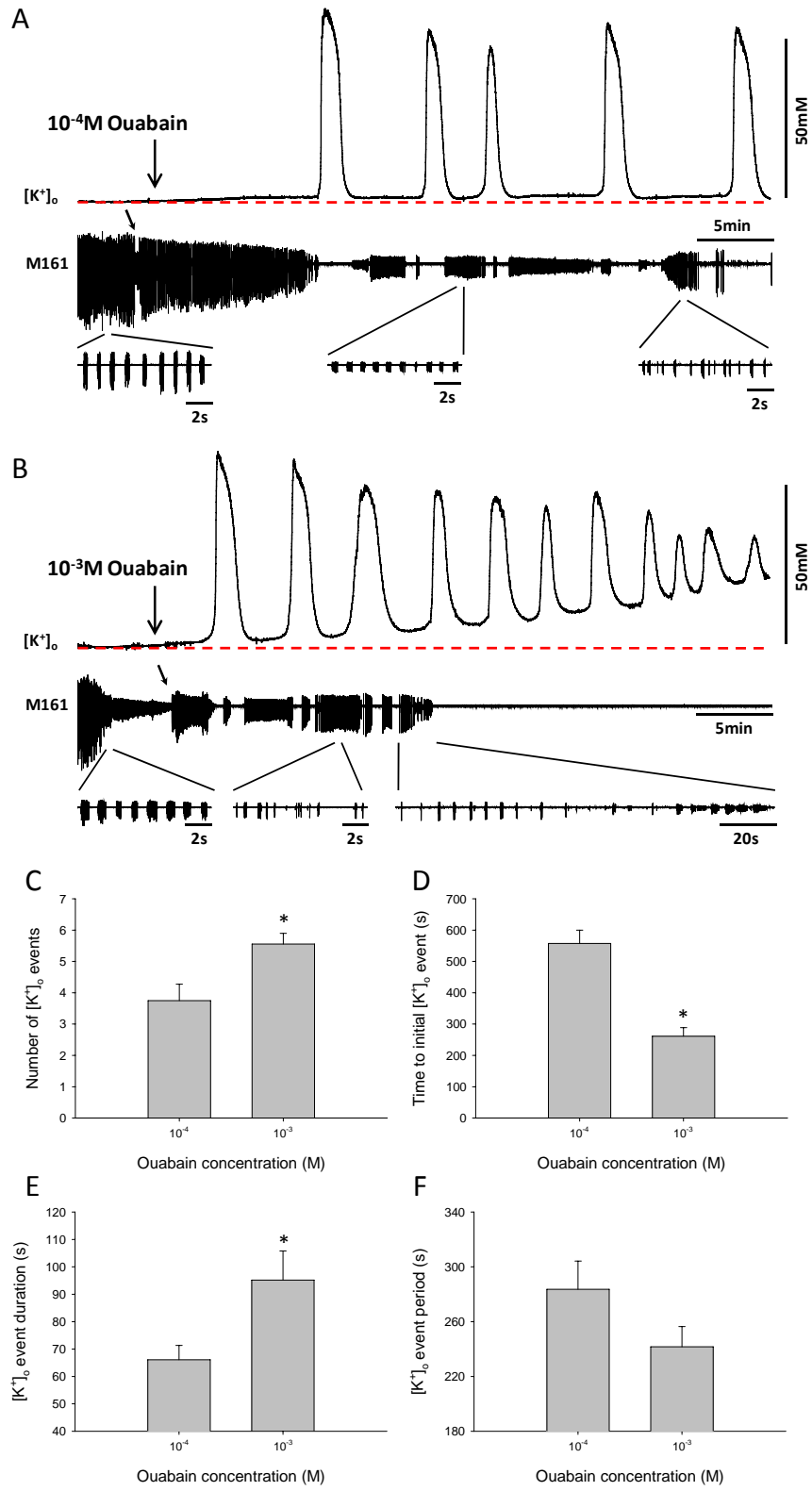


Figure 3.1

Figure 3.1. Simultaneous recordings of electrical activity from muscle 161 (M161) in the second abdominal segment and the extracellular potassium concentration ($[K^+]_o$) surrounding the ventilatory CPG. Continuous bath application of both $10^{-4}M$ ($N = 8$) and $10^{-3}M$ ($N = 9$) ouabain induced multiple all-or-none increases in $[K^+]_o$. (A) During $10^{-4}M$ ouabain treatment each $[K^+]_o$ event was associated with arrest of the ventilatory motor pattern and a period of depression of electrical activity from M161. Recovery of motor pattern generation was associated with return of $[K^+]_o$ to near pre-surge levels. (B) During $10^{-3}M$ ouabain treatment non-surge $[K^+]_o$ levels progressively increased. An inability to recover motor pattern generation was common during $10^{-3}M$ ouabain treatment. (A and B) There was often a burst of unpatterned electrical activity following arrest of the ventilatory motor pattern during $[K^+]_o$ events. Expanded regions of EMG recordings from ventilatory muscle 161 show increased variability of the motor pattern following multiple $[K^+]_o$ events. Diagonal arrows above M161 recordings indicate anomalies in the motor pattern due to readjustment of the EMG electrode. (C) All preparations treated with ouabain generated repetitive $[K^+]_o$ events, but a significantly greater number of $[K^+]_o$ events were elicited by $10^{-3}M$ ouabain compared to $10^{-4}M$ ouabain. (D) Time to onset of the initial $[K^+]_o$ event (seconds) in response to $10^{-4}M$ ($N = 8$) and $10^{-3}M$ ($N = 9$) ouabain bath application. $10^{-3}M$ ouabain hastened the onset of the first $[K^+]_o$ event in comparison to $10^{-4}M$ ouabain. (E) Mean duration (seconds) of the first $[K^+]_o$ event during $10^{-3}M$ ($N = 9$) ouabain application was significantly longer than during $10^{-4}M$ ($N = 8$) ouabain application. $[K^+]_o$ event durations were calculated using the duration at half the maximum amplitude of each $[K^+]_o$ event. (F) There was no significant difference in the period (seconds) from the first to the second $[K^+]_o$ event

during 10^{-4}M ($N = 8$) and 10^{-3}M ($N = 9$) ouabain application. $[\text{K}^+]_o$ event periods were calculated as the time from the inflection point of the $[\text{K}^+]_o$ increase of the first event to the inflection point of the $[\text{K}^+]_o$ increase of the second event. Data are means \pm S.E. and the asterisks indicate significant differences between 10^{-4}M and 10^{-3}M ouabain treatments.

however preparations treated with 10^{-3} M ouabain had a significantly greater number of $[K^+]_o$ events (*t*-test, $t = -2.955$, $P = 0.010$, d.f. = 15) (Fig. 3.1C).

Timing of repetitive $[K^+]_o$ events during 10^{-4} M and 10^{-3} M ouabain treatment

We examined various parameters related to the timing of $[K^+]_o$ events induced by 10^{-4} M and 10^{-3} M ouabain. Latency to onset of ouabain-induced $[K^+]_o$ surging was measured to determine how the degree of Na^+/K^+ -ATPase inhibition by ouabain affects initiation of repetitive $[K^+]_o$ events, if at all. The time from ouabain application to the initial $[K^+]_o$ event was significantly shorter in preparations treated with 10^{-3} M ouabain compared to 10^{-4} M ouabain (*t*-test, $t = -5.949$, $P < 0.001$, d.f. = 15) (Fig. 3.1D). Duration, measured at half the maximum amplitude of each $[K^+]_o$ event, was analyzed in preparations treated with 10^{-4} M and 10^{-3} M ouabain to characterize the difference in the ability of neuronal tissue to recover from the $[K^+]_o$ disturbance. There was a main effect of ouabain concentration on the duration of the first five $[K^+]_o$ events (two-way RM-ANOVA, $P = 0.008$, $F_{(1,19)} = 14.620$), however $[K^+]_o$ event duration did not change over time (two-way RM-ANOVA, $P = 0.181$, $F_{(4,19)} = 1.699$) (data not shown). The mean duration at half the maximum amplitude of the first $[K^+]_o$ event was significantly longer in preparations treated with 10^{-3} M ouabain compared to those treated with 10^{-4} M ouabain (*t*-test, $t = -2.352$, $P = 0.033$, d.f. = 15) (Fig. 3.1E). $[K^+]_o$ event period, i.e. the time from the upward inflection point of one surge to the upward inflection point of the next surge, was measured to determine if a higher concentration of ouabain increased the frequency of respective $[K^+]_o$ events. There was no main effect of ouabain concentration on the period of the first five $[K^+]_o$ events (two-way RM-ANOVA, $P = 0.705$, $F_{(1,18)} = 0.157$) and $[K^+]_o$

event period did not change over time (two-way RM-ANOVA, $P = 0.222$, $F_{(4,18)} = 1.529$) (data not shown). There was no significant difference between the two concentrations in the mean period from the first to the second $[K^+]_o$ event (t -test, $t = 1.691$, $P = 0.111$, d.f. = 15) (Fig. 3.1F). These results show that there is a shorter latency between the first two $[K^+]_o$ events elicited during $10^{-3}M$ ouabain application compared to during $10^{-4}M$ ouabain application.

Characteristics of $[K^+]_o$ surrounding the vCPG during $10^{-4}M$ and $10^{-3}M$ ouabain treatment

We measured non-surge $[K^+]_o$ prior to the initial $[K^+]_o$ event and every 5 min thereafter in order to determine if the degree of pump inhibition affects the ability to recover $[K^+]_o$ to initial levels over the 30 min duration of ouabain application. There was a main effect of ouabain concentration on pre- and post-surge $[K^+]_o$ during a 30 min bath application (two-way RM-ANOVA, $P < 0.001$, $F_{(1,24)} = 33.179$) (Fig. 3.2A). Preparations treated with $10^{-3}M$ ouabain had significantly higher non-surge $[K^+]_o$ levels measured at 25 and 30 min following initial ouabain application compared to preparations treated with $10^{-4}M$ ouabain (*post hoc* Tukey tests, $P < 0.05$) (Fig. 3.2A). In addition, the non-surge $[K^+]_o$ in preparations treated with $10^{-4}M$ and $10^{-3}M$ ouabain responded differently to increased time of exposure (significant interaction between ouabain concentration and time: two-way RM-ANOVA, $P = 0.003$, $F_{(6,24)} = 4.560$) (Fig. 3.2A). There was a main effect of ouabain concentration on the peak $[K^+]_o$ of the first five $[K^+]_o$ events (two-way RM-ANOVA, $P = 0.003$, $F_{(1,23)} = 5.019$), however peak $[K^+]_o$ did not change over time (two-way RM-ANOVA, $P = 0.134$, $F_{(4,23)} = 2.863$) (data not shown). The average peak $[K^+]_o$,

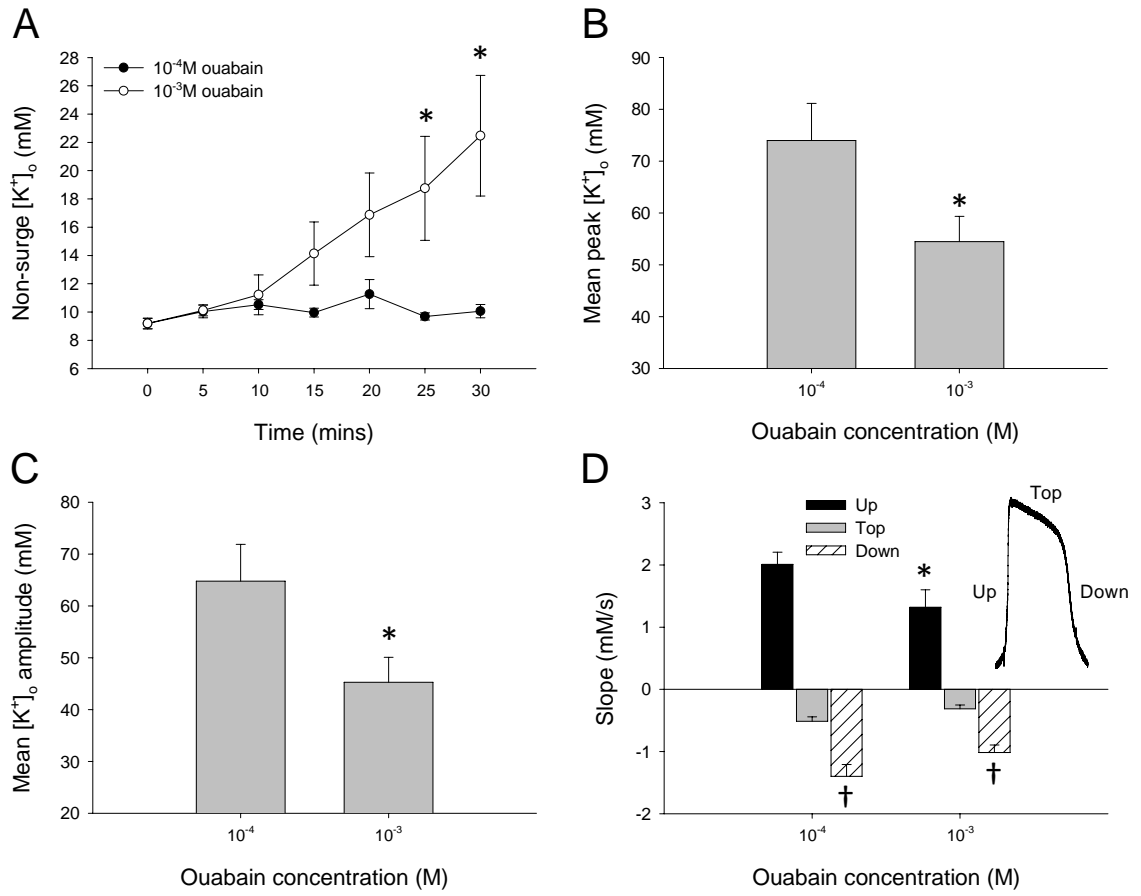


Figure 3.2

Figure 3.2. (A) Mean non-surge $[K^+]_o$ levels (mM) during continuous bath application of $10^{-4}M$ and $10^{-3}M$ ouabain. Non-surge $[K^+]_o$ was measured prior to the first $[K^+]_o$ event (time = 0) and every 5 min thereafter (where possible). $[K^+]_o$ returned to initial levels following each $[K^+]_o$ event during $10^{-4}M$ ouabain application, whereas non-surge $[K^+]_o$ progressively increased during treatment with $10^{-3}M$ ouabain. (B) Mean peak $[K^+]_o$ (mM) of the first $[K^+]_o$ event during $10^{-4}M$ and $10^{-3}M$ ouabain bath application. Peak $[K^+]_o$ of the first $[K^+]_o$ event elicited by $10^{-3}M$ ($N = 9$) ouabain treatment was significantly decreased compared to peak values in preparations treated with $10^{-4}M$ ($N = 8$) ouabain. (C) The amplitude of $[K^+]_o$ increase (mM) was calculated as the difference between the peak $[K^+]_o$ during an $[K^+]_o$ event and the preceding non-surge $[K^+]_o$. The mean amplitude $[K^+]_o$ of the first $[K^+]_o$ event during $10^{-3}M$ ($N = 9$) ouabain application was significantly lower compared to the amplitude of the first $[K^+]_o$ event elicited by $10^{-4}M$ ($N = 8$) ouabain application. (D) Three distinct slopes could be detected during $[K^+]_o$ events, as displayed in the inset: “Up” slope from pre-surge to maximum peak $[K^+]_o$, “Top” slope from maximum peak $[K^+]_o$ to the first downward inflection point, and “Down” slope from the first downward inflection point to post-surge $[K^+]_o$. Up-slopes generated by $10^{-4}M$ and $10^{-3}M$ ouabain were significantly different, however ouabain concentration did not have an effect on top- and down-slopes. Top- and down-slopes were significantly different irrespective of ouabain dose (indicated by daggers). Sample sizes ($10^{-4}M$, $10^{-3}M$): $N_{Up} = 8,9$; $N_{Top} = 8,9$; $N_{Down} = 8,9$. Data are means \pm S.E. and the asterisks indicate significant differences between $10^{-4}M$ and $10^{-3}M$ ouabain treatments.

calculated from the peak values of the first $[K^+]_o$ event, was significantly lower in preparations treated with $10^{-3}M$ ouabain compared to $10^{-4}M$ ouabain (t -test, $t = 2.292$, $P = 0.037$, d.f. = 15) (Fig. 3.2B). There was a main effect of ouabain concentration on the amplitude of $[K^+]_o$ increase during the first five $[K^+]_o$ events (two-way RM-ANOVA, $P < 0.001$, $F_{(1,23)} = 6.960$), however amplitude of $[K^+]_o$ events did not change over time (two-way ANOVA, $P = 0.073$, $F_{(1,23)} = 4.396$ (data not shown)). The mean amplitude of the $[K^+]_o$ increase of the first $[K^+]_o$ event was significantly lower in preparations treated with $10^{-3}M$ ouabain compared to $10^{-4}M$ ouabain (t -test, $t = 2.319$, $P < 0.035$, d.f. = 15) (Fig. 3.2C). There was no main effect of ouabain concentration on the slopes of the $[K^+]_o$ increase and decrease of the first $[K^+]_o$ event elicited by $10^{-4}M$ and $10^{-3}M$ ouabain treatment (two-way ANOVA, $P = 0.813$, $F_{(1,45)} = 0.0565$), however there was a significant interaction between ouabain concentration and the location of slopes (two-way ANOVA, $P = 0.008$, $F_{(2,45)} = 5.456$) (Fig. 3.2D). The up-slopes of the first surges elicited during $10^{-4}M$ and $10^{-3}M$ ouabain application were significantly different (*post hoc* Tukey test, $P < 0.05$) (Fig. 3.2D). A trend occurred during the downward phase of every first $[K^+]_o$ event, as two seemingly different slopes were present. The rate of $[K^+]_o$ decrease was significantly smaller during the top-slope phase compared to the down-slope phase and this difference occurred irrespective of ouabain concentration (*post hoc* Tukey tests, $P < 0.05$) (Fig. 3.2D). When examining top-slopes and down-slopes individually, there was no effect of ouabain concentration on the magnitude of these slopes (*post hoc* Tukey tests, $P > 0.05$) (Fig. 3.2D).

Arrest and recovery of the ventilatory motor pattern

All preparations had a robust ventilatory motor pattern during the initial stages of both 10^{-3}M and 10^{-4}M ouabain application. As time of exposure to ouabain increased and following each $[\text{K}^+]_o$ event there was a concentration-dependent difference in the ability of preparations to recover generation of a motor pattern (data not shown). Overall the probability of motor pattern recovery following $[\text{K}^+]_o$ events during 10^{-3}M ouabain application was significantly lower than during 10^{-4}M ouabain application (Kaplan-Meier Survival Analysis, Gehan-Breslow test statistic = 12.077, $P < 0.001$, d.f. = 1). In one preparation treated with 10^{-3}M ouabain motor pattern recovery did not occur following the first $[\text{K}^+]_o$ event or subsequent $[\text{K}^+]_o$ events. The motor pattern did not recover following the fourth $[\text{K}^+]_o$ event in any preparation treated with 10^{-3}M ouabain. During 10^{-3}M ouabain treatment, the average time to complete ventilatory motor pattern failure was 10.4 ± 1.3 min from initial ouabain application. During 10^{-4}M ouabain application only one preparation exhibited complete ventilatory motor pattern failure which occurred following the fourth $[\text{K}^+]_o$ event.

Effect of potassium channel block on ouabain-induced repetitive ventilatory arrest

10^{-3}M TEA, a nonselective voltage-gated K^+ channel inhibitor, was bath-applied in combination with 10^{-4}M ouabain in order to determine if ouabain-induced $[\text{K}^+]_o$ events are modulated by K^+ conductances (Fig. 3.3A). Bath application of 10^{-3}M TEA in combination with 10^{-4}M ouabain (“OUA/TEA”) significantly reduced the likelihood of producing ouabain-induced $[\text{K}^+]_o$ events compared to preparations treated with 10^{-4}M ouabain alone (“OUA”; Fig. 3.1A) (z -test, $z = 2.028$, $P = 0.043$) (Fig. 3.3B). The

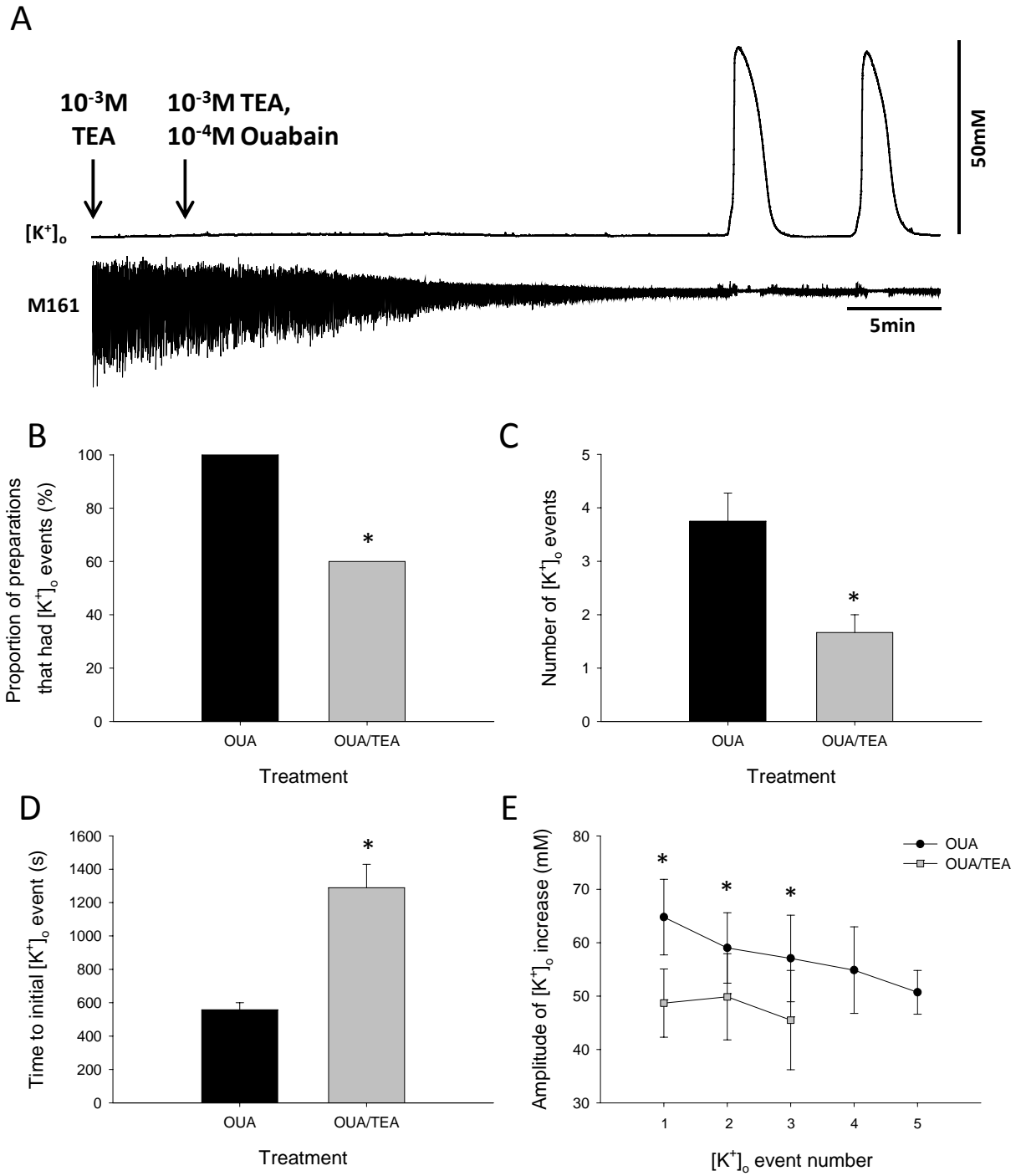


Figure 3.3

Figure 3.3. (A) Simultaneous recording of electrical activity from muscle 161 (M161) and the extracellular potassium concentration ($[K^+]_o$) surrounding the vCPG. 10^{-3} M TEA was bath-applied for 5 min alone, then in combination with 10^{-4} M ouabain for 40 min. In the experiment shown here 10^{-3} M TEA delayed the onset of ouabain-induced $[K^+]_o$ events, thereby reducing the number of events that occurred compared to preparations treated with 10^{-4} M ouabain alone. Note that reduction in amplitude of the EMG recording is attributable to the effect of TEA at the neuromuscular junction. (B-D) Preparations treated with 10^{-4} M ouabain alone are termed “OUA” (Fig. 3.1A) and preparations treated with 10^{-3} M TEA in combination with 10^{-4} M ouabain are termed “OUA/TEA”. (B) Block of voltage-gated potassium channels with TEA significantly reduced the proportion of preparations that had at least one $[K^+]_o$ event ($N_{OUA} = 8$; $N_{OUA/TEA} = 10$). (C) TEA reduced the severity of ouabain-induced $[K^+]_o$ events by significantly decreasing the number of $[K^+]_o$ events ($N_{OUA} = 8$; $N_{OUA/TEA} = 6$). (D) The time from initial ouabain application to the initial $[K^+]_o$ event was increased in preparations that had simultaneous TEA treatment ($N_{OUA} = 8$; $N_{OUA/TEA} = 6$). (E) The amplitude of $[K^+]_o$ events in preparations treated with TEA was reduced compared to preparations treated with ouabain alone ($N_{OUA} = 8$; $N_{OUA/TEA} = 6$). Data are means \pm S.E. and the asterisks indicate significant differences between OUA and OUA/TEA treatments.

proportions of OUA and OUA/TEA preparations that had at least one $[K^+]_o$ event were 1 (8/8) and 0.6 (6/10), respectively (Fig. 3.3B). Of the preparations that had at least one $[K^+]_o$ event, TEA treatment significantly reduced the number of events (*t*-test, $t = 3.079$, $P = 0.010$, d.f. = 12) (Fig. 3.3C). In addition, TEA significantly increased the time to onset of ouabain-induced $[K^+]_o$ events (*t*-test, $t = -2.555$, $P = 0.025$, d.f. = 12) (Fig. 3.3D), and K^+ channel block significantly reduced the absolute value of $[K^+]_o$ increases during the first three $[K^+]_o$ events compared to preparations treated with ouabain alone (two-way RM-ANOVA, $P = 0.001$, $F_{(1,7)} = 23.659$) (Fig. 3.3E).

3.5 Discussion

We found that ouabain-induced Na^+/K^+ -ATPase inhibition elicits repetitive arrest of ventilatory motor pattern generation in the locust. Each period of electrical activity depression occurred simultaneously with abrupt increases in $[\text{K}^+]_o$, where the rise and fall of $[\text{K}^+]_o$ coincided with arrest and recovery of the ventilatory motor pattern, respectively. It is intriguing that Na^+/K^+ -ATPase dysfunction induced repetitive waves of $[\text{K}^+]_o$ increase and decrease as opposed to a gradual increase in $[\text{K}^+]_o$. $[\text{K}^+]_o$ remained fairly stable during the time from initial ouabain bath application to the initial abrupt increase in $[\text{K}^+]_o$, indicating that there is a threshold for the $[\text{K}^+]_o$ disturbance. The Na^+/K^+ -ATPase is under the control of a wide range of regulatory mechanisms and pathways and can be regulated by changes in ions such as Na^+ (Kaplan, 2002). Pump inhibition causes an increase in the intracellular sodium concentration ($[\text{Na}^+]_i$) which in turn stimulates Na^+/K^+ -ATPase complexes free of ouabain block to work more rapidly to expel the excess Na^+ (Kaplan, 2002). We suggest that the threshold for the abrupt $[\text{K}^+]_o$ increase occurs at a point when functioning Na^+/K^+ pumps fail to cope with changing concentration gradients as a result of ouabain. At this point the system enters a positive feedback cycle in which increasing $[\text{K}^+]_o$ causes cellular depolarization that opens voltage-dependent channels and the flux of K^+ ions into the extracellular space. Our model for ouabain-induced cyclic K^+ increases is depicted in Figure 3.4. We hypothesize that spreading depression (SD)-like events in the locust (Rodgers et al., 2007) are triggered by positive feedback processes involving an initial ionic disturbance reaching a threshold and caused by neuronal overexcitation or by treatments or conditions that impair ionic homeostasis (Grafstein, 1956; van Harrevald, 1978; Balestrino et al., 1999;

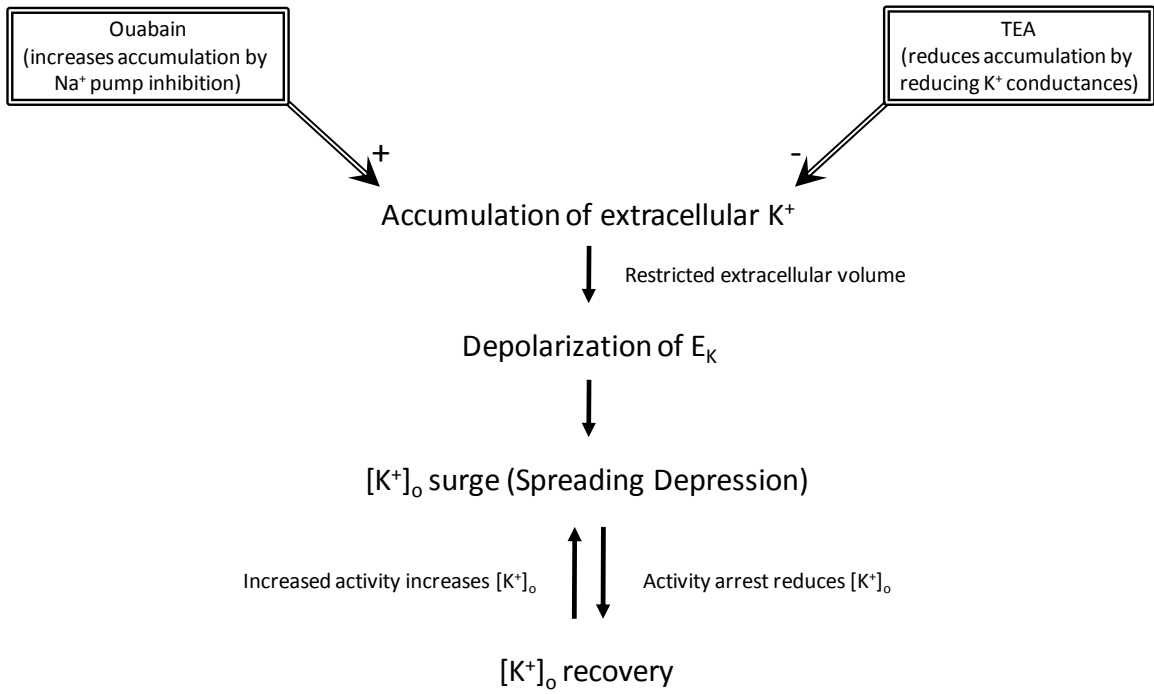


Figure 3.4

Figure 3.4. A model describing a possible mechanism for the abrupt $[K^+]_o$ increase and subsequent $[K^+]_o$ recovery in response to cellular stressors in the locust metathoracic ganglion. $[K^+]_o$ accumulation surrounding the vCPG occurs due to impaired clearance mechanisms (Na^+/K^+ -ATPase dysfunction using ouabain) or increased neuronal activity in an extracellular compartment with small volume. With low concentrations of ouabain or low activity levels pump regulation can accommodate the change in $[K^+]_o$ and maintain concentration gradients (e.g. $10^{-5}M$ ouabain). High concentrations of ouabain impair $[K^+]_o$ clearance sufficiently to change the equilibrium potential for K^+ and depolarize membranes. Depolarization of E_K initiates a positive feedback cycle where depolarization leads to opening of voltage-dependent channels, increased activity, further increases in $[K^+]_o$, leading again to further depolarization. At the peak of the $[K^+]_o$ surge activity ceases due to inactivation of Na^+ channels, allowing remaining $[K^+]_o$ clearance mechanisms to counteract $[K^+]_o$ accumulation. This process leads into another positive feedback cycle at the point at which restoration of the ion gradient begins to hyperpolarize membranes, which in turn closes voltage-dependent K^+ channels and reduces the process of $[K^+]_o$ accumulation. Thus, the repetitive nature of $[K^+]_o$ surges induced by $10^{-4}M$ ouabain depends on the balance of $[K^+]_o$ clearance and accumulation.

Somjen, 2001). We believe that the positive feedback cycle is initiated when processes of $[K^+]_o$ accumulation overwhelm the ability to clear $[K^+]_o$ from a restricted interstitium with limited glial buffering capacity (Somjen and Müller, 2000; Kager et al., 2000, 2002; Somjen, 2002), changing the equilibrium potential for K^+ and depolarizing membranes. The conductances involved in the repetitive $[K^+]_o$ events in the locust are not known, but could be due to opening of voltage-dependent or ATP-sensitive K^+ channels of neurons or glia. Nonselective conductances could also explain the intense outflow of K^+ . In vertebrate pyramidal neurons pannexin 1 (Px1) hemichannels, or half gap junctions, open during ischemic-like conditions (oxygen/glucose deprivation) (Thompson et al., 2006). Interestingly, invertebrate neuronal gap junctions are composed of Px1 proteins (Panchin, 2005), and these nonselective cation channels could be a conduit of K^+ efflux during ouabain-induced repetitive $[K^+]_o$ events in the locust. The mechanisms underlying the repetitive nature of ouabain-induced $[K^+]_o$ events remain to be precisely defined, however we suggest that when activity ceases as a result of a $[K^+]_o$ event, the remaining K^+ clearance mechanisms are sufficient to cause the system to enter another positive feedback cycle whereby decreasing $[K^+]_o$ causes membrane hyperpolarization that closes voltage-dependent K^+ channels and reduces the flux of K^+ across the membrane (Fig. 3.4). Our results demonstrate that the balance of $[K^+]_o$ accumulation and clearance is biased by the degree of Na^+/K^+ -ATPase inhibition by ouabain.

Consistent with this model $10^{-3}M$ ouabain bath application hastened the time to onset of the initial $[K^+]_o$ event and elicited a greater number of $[K^+]_o$ events compared to $10^{-4}M$ ouabain treatment. Following initial ouabain application it took approximately 4 min

(261 ± 27 s) for 10^{-3} M ouabain to generate the initial $[K^+]_o$ event compared to approximately 9 min (557 ± 43 s) in response to 10^{-4} M ouabain application. Differences in latency to onset suggest that the threshold for the initial $[K^+]_o$ disturbance is dependent on the degree of Na^+/K^+ -ATPase saturation by ouabain. Duration, measured at half the maximum amplitude of each $[K^+]_o$ event, was analyzed to determine how fast the neuronal tissue was able to recover from the $[K^+]_o$ disturbance. We found that the $[K^+]_o$ event durations during 10^{-3} M ouabain application were significantly longer than during 10^{-4} M ouabain application. If blocking more Na^+/K^+ -ATPase pumps using a higher concentration of ouabain (10^{-3} M) causes longer duration $[K^+]_o$ events, then it could be suggested that Na^+/K^+ -ATPase transporters play a key role in recovery from this state of homeostatic disruption (Leis et al., 2005). Analysis of the $[K^+]_o$ event period revealed no significant difference between 10^{-4} M and 10^{-3} M ouabain treatments. Thus duration and period data demonstrate that there is a shorter latency between $[K^+]_o$ events elicited during 10^{-3} M ouabain application compared to during 10^{-4} M ouabain application.

During 10^{-4} M ouabain application non-surge extracellular $[K^+]_o$ levels remained relatively stable, with $[K^+]_o$ returning to near initial levels following each abrupt increase.

Application of 10^{-3} M ouabain resulted in a gradual increase in non-surge $[K^+]_o$ following each $[K^+]_o$ event until the mean $[K^+]_o$ at 25 min and 30 min of treatment was significantly higher than the corresponding 10^{-4} M value. In the dentate gyrus of adult rat hippocampal slices application of a relatively high concentration of ouabain prevents the return of $[K^+]_o$ to baseline levels following a surge (Xiong and Stringer, 2000). We suggest that

the gradual rise in $[K^+]_o$ during $10^{-3}M$ ouabain application is indicative of Na^+/K^+ pumps becoming progressively inhibited as more become blocked, causing $[K^+]_o$ to accumulate.

If $[K^+]_o$ clearance mechanisms are impaired, then it would be logical to assume that the rate of $[K^+]_o$ clearance, or down-slope, during $[K^+]_o$ events would be negatively affected (McCarren and Alger, 1987; Xiong and Stringer, 2000). The up-slopes of the first $[K^+]_o$ event during $10^{-4}M$ and $10^{-3}M$ ouabain treatment were significantly different, however there was no significant difference in the down-slopes associated with motor pattern recovery. An interesting characteristic of the initial $[K^+]_o$ event is the two seemingly different slopes during the return of $[K^+]_o$ to baseline values. Although there was no significant difference between the top- or down-slopes of the first $[K^+]_o$ event across ouabain concentrations, the top- and down- slopes were significantly different irrespective of ouabain dose which indicates an abrupt change in $[K^+]_o$ clearance mechanisms. Following an abrupt increase in $[K^+]_o$ and arrest of the ventilatory motor pattern $[K^+]_o$ accumulation will necessarily decrease once neural activity has ceased allowing remaining mechanisms of clearance to predominate until the threshold for rapid recovery is reached. The change in the trajectory of recovery may simply reflect the accelerating nature of a positive feedback mechanism.

In addition to Na^+/K^+ -ATPase impairment other cellular stressors, including hyperthermia, ATP depletion, and anoxia, cause arrest of the ventilatory motor pattern that is associated with abrupt all-or-none type increases in $[K^+]_o$ in the vCPG region of the MTG (Rodgers et al., 2007). These stress-induced $[K^+]_o$ events share many

characteristics with cortical spreading depression (CSD), characterized as a massive redistribution of ions, notably $[K^+]_o$ and $[Na^+]_i$, accompanied by a rapid and nearly complete depolarization of neurons in vertebrate cortical tissue (Leao, 1944; Hansen and Zeuthen, 1981; Gorji, 2001; Somjen, 2001). What is quite intriguing is that the ionic changes during SD trigger surrounding neuronal cells to follow suit (Hansen and Zeuthen, 1981; Somjen, 2001). The end result is a depression of neural activity that arises from a focal point, and spreads throughout the cerebral cortex at a rate of approximately 2-5 mm/min (Leao, 1944). SD events propagate within the locust MTG at a rate similar to that in cortical tissue (2.4 ± 0.04 mm/min) (Rodgers et al., 2007) and the ouabain-induced repetitive SD-like events in our study could represent propagating waves of $[K^+]_o$ increase and decrease passing by the K^+ -sensitive electrode tip. We suggest that arrest of the ventilatory CPG coincides with an abrupt $[K^+]_o$ increase surrounding the CPG that spreads locally to other regions of the neuropil via diffusion across the extracellular space and possibly through gap junctions. Given that $[K^+]_o$ events spread within the locust MTG at a rate of ~ 2 mm/min we conclude that the entire ganglion is affected during the ~ 1 min duration of $[K^+]_o$ events. Several studies have exploited the ability of ouabain in blocking the Na^+/K^+ -ATPase in order to study SD in mammalian brain tissue (Haglund and Schwartzkroin, 1990; Balestrino et al., 1999; Menna et al., 2000; Xiong and Stringer, 2000). It is possible that Na^+/K^+ -ATPase inhibition is primarily responsible for the neural circuitry impairment that occurs in response to cellular stressors in the locust.

We found that block of voltage-gated K^+ channels with TEA suppressed ouabain-induced repetitive ventilatory arrest and the associated $[K^+]_o$ events. TEA blocks voltage-gated K^+ channels in a nonselective manner and it is not known which subtypes of K^+ channels are blocked by TEA at a given concentration in the locust CNS. It has been shown that TEA diminishes the amplitude of hyperthermia-induced $[K^+]_o$ events in the locust (Rodgers et al., 2007), suggesting that at least part of the K^+ leaving cells during the abrupt stress-induced $[K^+]_o$ increase flows through TEA-sensitive channels (Somjen, 2001). TEA also diminished the amplitude $[K^+]_o$ of ouabain-induced $[K^+]_o$ events compared to preparations treated with $10^{-4}M$ ouabain alone. TEA both reduced neuronal K^+ release and prolonged the circling time of self-sustaining circling SD in the chicken retina (RSD) (Scheller et al., 1998). Scheller et al. (1998) concluded that TEA reduced the RSD-mediated neuronal K^+ release, thereby reducing K^+ re-uptake and buffering by glial cells, which resulted in decreased re-initiation of RSD and consequently decreased propagation velocity. We suggest that the TEA-induced reduction of K^+ conductances in our study resulted in reduced $[K^+]_o$ clearance requirements of un-inhibited Na^+/K^+ pumps, allowing these pumps to better maintain K^+ homeostasis (Fig. 3.4).

In conclusion we show that ouabain-induced Na^+/K^+ -ATPase dysfunction elicits repetitive SD-like events that are concentration-dependent. In addition, we provide evidence for a role for K^+ channels in modulation of ouabain-induced repetitive SD-like events in the locust CNS. We propose that our manipulations acted on either side of a balance between processes of accumulation and clearance of extracellular $[K^+]_o$ and that ventilatory arrest occurs when the balance is such that $[K^+]_o$ is able to accumulate

sufficiently to change the potassium equilibrium potential and cause cellular depolarization.

3.6 References

Balestrino, M., Young, J. and Aitken, P., 1999. Block of (Na⁺, K⁺) ATPase with ouabain induces spreading depression-like depolarization in hippocampal slices. *Brain Research* 838 (1-2), 37-44.

Burrows, M., 1996. *The Neurobiology of an Insect Brain*. Oxford University Press, Oxford.

Bustami, H. P. and Hustert, R., 2000. Typical ventilatory pattern of the intact locust is produced by the isolated CNS. *Journal of Insect Physiology* 46 (9), 1285-1293.

Erecinska, M. and Silver, I. A., 1994. Ions and energy in mammalian brain. *Progress in Neurobiology* 43 (1), 37-71.

Erulkar, S. D. and Weight, F. F., 1977. Extracellular potassium and transmitter release at the giant synapse of squid. *Journal of Physiology* 266 (2), 209-218.

Gorji, A., 2001. Spreading depression: a review of the clinical relevance. *Brain Research Reviews* 38 (1-2), 33-60.

Haglund, M. M., and Schwartzkroin, P. A., 1990. Role of Na-K pump potassium regulation and IPSPs in seizures and spreading depression in immature rabbit hippocampal slices. *Journal of Neurophysiology* 63 (2), 225-239.

Hansen, A. J. and Zeuthen, T., 1981. Extracellular ion concentrations during spreading depression and ischemia in the rat brain cortex. *Acta Physiologica Scandinavica* 113 (4), 437-45.

Harrison, J. F., 1997. Ventilatory mechanism and control in grasshoppers. *American Zoologist* 37 (1), 73-81.

Huxley, A. F. and Stämpfli, R., 1951. Effect of potassium and sodium on resting and action potentials of single myelinated nerve fibers. *Journal of Physiology* 112 (3-4), 496-508.

Kaplan, J. H., 2002. Biochemistry of Na,K-ATPase. *Annual Review of Biochemistry* 71, 511-535.

Kretzschmar, D. and Pflugfelder, G. O., 2002. Glia in development, function, and neurodegeneration of the adult insect brain. *Brain Research Bulletin* 57 (1), 121-131.

Leao, A. A. P., 1944. Spreading depression of activity in the cerebral cortex. *Journal of Neurophysiology* 7 (6), 359-390.

Leis, J. A., Bekar, L. K. and Walz, W., 2005. Potassium homeostasis in the ischemic brain. *Glia* 50 (4), 407-416.

McCarren, M. and Alger, B. E., 1987. Sodium-potassium pump inhibitors increase neuronal excitability in the rat hippocampal slice: role of a Ca²⁺-dependent conductance. *Journal of Neurophysiology* 57 (2), 496-509.

Menna, G., Tong, C. K. and Chesler, M., 2000. Extracellular pH changes and accompanying cation shifts during ouabain-induced spreading depression. *Journal of Neurophysiology* 83 (3), 1338-1345.

Newman, A. E. M., Foerster, M., Shoemaker, K. L. and Robertson, R. M., 2003. Stress-induced thermotolerance of ventilatory motor pattern generation in the locust, *Locusta migratoria*. *Journal of Insect Physiology* 49 (11), 1039-1047.

Newman, E. A., 1993. Inward-rectifying potassium channels in retinal glial (Müller) cells. *Journal of Neuroscience* 13 (8), 3333-3345.

Orkand, R. K., Nicholls, J. G. and Kuffler, S. W., 1966. Effect of nerve impulses on the membrane potential of glial cells in the central nervous system of amphibian. *Journal of Neurophysiology* 29 (4), 788-806.

Panchin, Y. V., 2005. Evolution of gap junction proteins – the pannexin alternative. *Journal of Experimental Biology* 208 (8), 1415-1419.

Ramirez, J. M. and Pearson, K. G., 1989. Distribution of intersegmental interneurons that can reset the respiratory rhythm of the locust. *Journal of Experimental Biology* 141 (1), 151-176.

Robertson, R. M., 2004. Thermal stress and neural function: adaptive mechanisms in insect model systems. *Journal of Thermal Biology* 29 (7-8), 351-358.

Rodgers, C. I., Armstrong, G. A. B., Shoemaker, K. L., LaBrie, J. D., Moyes, C. D. and Robertson, R. M., 2007. Stress preconditioning of spreading depression in the locust CNS. *PLoS ONE* 2, e1366, doi:10.1371/journal.pone.0001366.

Rounds, H. D., 1967. KCl-induced 'spreading depression' in the cockroach. *Journal of Insect Physiology* 13, 869-872.

Scheller, D., Tegmeier, F. and Schule, W.-R., 1998. Dose-dependent effects of tetraethylammonium on circling spreading depressions in chicken retina. *Journal of Neuroscience Research* 51 (1), 85-89.

Somjen, G. G., 2001. Mechanisms of spreading depression and hypoxic spreading depression-like depolarization. *Physiological Reviews* 81 (3), 1065-1096.

Somjen, G. G., 2002. Ion regulation in the brain: implications for pathophysiology. *Neuroscientist* 8 (3), 254-267.

Thompson, R. J., Zhou, N. and MacVicar, B. A., 2006. Ischemia opens neuronal gap junction hemichannels. *Science* 312 (5775), 924-927.

Walz, W., 1987. Swelling and potassium uptake in cultured astrocytes. *Canadian Journal of Physiology and Pharmacology* 65 (5), 1051-1057.

Wu, J. and Fisher, R. S., 2000. Hyperthermic spreading depressions in the immature rat hippocampal slice. *Journal of Neurophysiology* 84 (3), 1355-1360.

Xiong, Z. Q. and Stringer, J. L., 2000. Sodium pump activity, not glial spatial buffering, clears potassium after epileptiform activity induced in the dentate gyrus. *Journal of Neurophysiology* 83 (3), 1443-1451.

Chapter 4

Central pattern generation is modulated by AMP-activated protein kinase (AMPK) in response to energy compromise.

4.1 Abstract

The AMP-activated protein kinase (AMPK) senses cellular energy status and signals metabolic stress. In the locust (*Locusta migratoria*) anoxia-induced arrest of ventilation is tightly correlated with an abrupt increase in extracellular potassium concentration ($[K^+]_o$) within the ventilatory neuropile. This $[K^+]_o$ increase resembles cortical spreading depression (CSD), although neuronal depolarization is not complete as with CSD. Using suction electrode recordings from a ventilatory nerve and bath-application of AICAR (AMPK activator) and compound-C (AMPK inhibitor) we addressed whether AMPK is associated with stress-induced ventilatory arrest and SD-like events in the locust.

Ventilatory rate gradually decreased following recovery from chemical anoxia using sodium azide (NaN_3) and the associated SD-like event. We tested the hypothesis that AMPK activation using AICAR would mimic the motor pattern changes induced by NaN_3 . Treatment with either $10^{-3}M$ or $10^{-2}M$ AICAR caused an immediate increase in ventilatory rate, however $10^{-2}M$ AICAR had multiple effects on the ventilatory rhythm, some resembling the recovered motor pattern following NaN_3 -induced arrest.

Application of $10^{-4}M$ compound-C during recovery from NaN_3 -induced arrest and during AICAR-induced disruption of the motor pattern gradually returned burst durations and periods to Control values. Ouabain-induced SD-like events in the locust CNS were suppressed by inhibition of AMPK and exacerbated by its activation. Application of compound-C following initiation of ouabain-induced SD-like events aborted subsequent $[K^+]_o$ surges, suggesting that AMPK inhibition may be involved in $[K^+]_o$ propagation. These results indicate that activation of the AMPK pathway is involved in the onset of and recovery from a stress-induced SD-like shutdown in the locust CNS.

4.2 Introduction

Variation in ambient temperature and oxygen levels can impair vital neuronal circuits and have drastic consequences for an organism's survival. At the cellular level, lack of adequate O₂ results in disruption of protein synthesis, depletion of intracellular energy stores, opening of voltage-gated Ca²⁺ channels, and loss of ionic gradients leading to excitotoxicity and oxidative damage (Snider et al. 1999; Love, 2003). Regulatory mechanisms such as the AMP-activated protein kinase (AMPK) cascade exist to monitor energy and protect against the damaging effects of metabolic stress (Hardie et al. 2003; McCullough et al. 2005) though little is known of how prior energetic stress or AMPK modulate neural circuit operation. We examined the effects of energetic stress on a locust model of CNS function, the operation of the ventilatory central pattern generator (vCPG). We aimed to characterize the stress-induced changes in the activity of the vCPG in response to chemical anoxia using sodium azide (NaN₃) and we tested the role of AMPK in mediating these effects.

Locusts are extremely tolerant of oxygen deprivation and can withstand hours of submersion under water (Armstrong et al. 2009). During this time, they enter a reversible state of electrical silence in the nervous and muscular systems that we interpret as a stress-induced coma. Upon removal from anoxic conditions, neural and muscular systems completely recover and locusts behave normally. Stress-induced coma and arrest of vCPG operation is associated with spreading depression (SD)-like events that share properties of SD in cortical tissue (cortical SD; CSD) (Rodgers et al. 2007; Rodgers et al. 2009; Armstrong et al. 2009). These are characterized by abrupt increases in [K⁺]_o 50-

80mM in amplitude within the ventilatory neuropile that coincide with a shutdown of vCPG activity. The role of SD-like events in the locust CNS remains unclear. Our hypothesis is that stress-induced comas and associated SD-like events in the locust represent a protective strategy to cope with environmental stress by preventing neuronal hyperexcitation and energy collapse that, if allowed to occur, can be detrimental to survival (Rodgers et al. 2010). Conceivably, energy levels would be maintained by entering a state of coma during which energy-utilizing mechanisms to restore ion gradients are suspended (Rodgers et al. 2007). There was no correlation between ganglionic ATP levels and the occurrence of stress-induced motor pattern arrest and subsequent recovery in the locust (Rodgers et al. 2007), however metabolic stresses can trigger the activation of signaling pathways before changes in ATP can be detected (Evans, 2006; Hardie et al. 2006).

AMPK is an evolutionarily conserved homeostatic regulator that senses cellular energy status before ATP levels are depleted (Hardie et al. 2003). AMPK activation in response to stress in the locust may initiate a switch in energy usage that fosters improvement in energy status, thereby affecting any number of energy-intensive neuronal systems. Given that ventilation is both an energy-requiring process and involved in providing oxygen to tissues, it is conceivable that vCPG output would be altered by AMPK activation during stress. We examined the effects of AMPK activation and inhibition using AICAR and compound-C, respectively, on the ventilatory motor pattern to establish a role for AMPK in stress-induced motor pattern changes. We pharmacologically manipulated AMPK activation during SD-like events induced by ouabain to determine whether AMPK

activation and inhibition had modulatory effects on SD-like events. Our results support the hypothesis that SD-like events in the locust represent an adaptive shutdown to conserve energy and suggest a role for the AMPK pathway.

4.3 Materials and Methods

Animals

All experiments were performed on adult male locusts, *Locusta migratoria migratorioides* (R. and F.), aged approximately 3-5 weeks past imaginal ecdysis. Locusts were randomly selected from a crowded colony located in the Animal Care Facility of the Biosciences Complex at Queen's University. The colony was reared under a 12h:12h light:dark photoperiod at a room temperature of $30 \pm 1^\circ\text{C}$ during light hours and $26 \pm 1^\circ\text{C}$ during dark hours. Humidity was maintained at $23 \pm 1\%$. Animals were provided with carrots, wheat seedlings and an ad libitum mixture of 1 part skim milk powder, 1 part torula yeast, and 13 parts bran, by volume.

Semi-intact preparation

Appendages and pronotum were removed and a dorsal midline incision was made. A corkboard was used to pin open the locust dorsal side up, allowing the gut, fatty tissue and air sacs to be removed, exposing the ventral nerve cord, metathoracic ganglion (MTG) and ventilatory nerves. The preparation was set up to prevent leakage and thus maximize the use of very small quantities of drugs. A metal plate was placed beneath the MTG to stabilize it, and nerves 2-5 on both sides of the ganglion were severed at the root to allow saline and drug entry. The MTG was bathed in standard locust saline containing (in mM): 147 NaCl, 10 KCl, 4 CaCl₂, 3 NaOH, and 10 HEPES buffer (pH 7.2), which was applied manually by pipetting into the preparation above the MTG where the ventilatory CPG (vCPG) is located. A silver wire was inserted in the anterior portion of the thorax to ground the preparation.

Motor patterns

A suction electrode (World Precision Instruments) was used to obtain extracellular neurographic recordings of the ventilatory motor pattern. The suction electrode pipette was pulled to form a high resistance tip, then broken to the appropriate size and smoothed to suction onto the median ventilatory nerve originating at the A3 neuromere of the MTG. Signals were amplified using a Model 1600 neuroprobe amplifier (A-M Systems) and digitized using a DigiData 1322A (Molecular Devices). Ventilation recordings were then displayed and recorded using AxoScope 9.0 software (Axon Instruments), and data were analyzed using Clampfit 9.0 (Molecular Devices). Expiratory burst duration and period were measured every 5 minutes over the course of each experiment and averaged to obtain means \pm S.E.

Preparation of potassium-sensitive microelectrodes

K⁺-sensitive microelectrodes were made from 1 mm diameter unfilamented capillary tubes (World Precision Instruments) that were cleaned with methanol (99.9%) and dried on a hot plate before being pulled to form a low resistance (5-7 M Ω) tip. The inner glass surface of the microelectrodes were made hydrophobic by exposure to dichlorodimethylsilane (99%) (Sigma-Aldrich) vapor while baking on a hot plate (100°C) for one hour. The microelectrodes were allowed to cool, then filled at the tip with Potassium Ionophore I-Cocktail B (5% Valinomycin; Sigma-Aldrich) and back-filled with 500mM KCl. Reference microelectrodes were made from 1 mm diameter filamented capillary tubes (World Precision Instruments) that were pulled to form a low

resistance (5-7 M Ω) tip, then filled with 3M KCl. Microelectrode tips were suspended in distilled water until experimentation.

Extracellular potassium recording

K⁺-sensitive and reference microelectrodes were connected to a DUO 773 two-channel intracellular/extracellular amplifier (World Precision Instruments). A K⁺-sensitive and reference microelectrode pair were calibrated at room temperature (~21°C) using 15mM and 150mM KCl solutions to obtain the voltage change, 'or slope', which was required for determination of [K⁺]_o (mM). A 10-fold change in [K⁺] resulted in a voltage change of 54 to 58 mV and only electrode pairs with slope values falling within this range were accepted for experimental use. Following calibration the K⁺-sensitive and reference microelectrodes were inserted through the sheath of the MTG side-by-side in the region of the vCPG. Specifically, the microelectrodes were placed centrally in the region of the first three abdominal neuromeres, which are fused to the metathoracic neuromere, forming the MTG. [K⁺]_o changes spread to other regions of the MTG (but not through the connectives), therefore placement of microelectrodes precisely at the vCPG was important to accurately measure the timing of [K⁺]_o disturbances surrounding the vCPG relative to arrest of the ventilatory motor pattern.

The [K⁺]_o was obtained by transforming the recorded [K⁺]_o trace in mV to mM using the Nernst equation:

$$E_K = RT / zF \cdot \ln[K^+]_o / [K^+]_i.$$

The following conversion of the above equation was used for determination of $[K^+]_o$ (mM):

$$[K^+]_o = 15 \cdot 10^{\text{voltage} / \text{slope}(\sim 58.2)}$$

Pharmacological treatments

All chemicals were obtained from Sigma-Aldrich and dissolved in standard locust saline using a minimum amount of DMSO (0.5 ml/100 ml of saline) and bath-applied to the semi-intact preparation. Each experiment was 1 hour in duration. In all preparations the MTG was bathed in standard locust saline for 20 minutes prior to pharmacological treatment. To examine the effects of chemical anoxia on ventilatory motor pattern generation, $10^{-3}M$ and $5 \times 10^{-4}M$ sodium azide (NaN_3) were bath-applied until 1 minute post-arrest of the ventilatory motor pattern and were washed out with standard locust saline. Lower doses of NaN_3 ($10^{-4}M$ and $10^{-5}M$) were bath-applied for 40 minutes. $10^{-3}M$ 5-aminoimidazole-4-carboxamide ribonucleoside (AICAR), an AMP-activated protein kinase (AMPK) activator, and $10^{-4}M$ compound-C, an AMPK inhibitor, were bath-applied for 40 minutes. A higher dose of AICAR ($10^{-2}M$) was bath-applied for 20 minutes, followed by $10^{-4}M$ compound-C application for 20 minutes. To investigate the effects of compound-C and glucose on the post-stress motor pattern, $10^{-4}M$ compound-C and $10^{-3}M$ glucose were bath-applied 10-12 minutes following recovery from NaN_3 -induced arrest for ~15 minutes. To examine the effects of AMPK activation and inhibition on ouabain-induced repetitive SD-like events, we bath-applied either $10^{-2}M$ AICAR or $10^{-4}M$ compound-C alone for 15 minutes followed by either $10^{-2}M$ AICAR or $10^{-4}M$ compound-C in combination with $10^{-4}M$ ouabain, respectively, for 35 minutes.

4M compound-C in combination with 10^{-4}M ouabain was also bath-applied following the initial ouabain-induced SD-like event. The time to the initial $[\text{K}^+]_o$ event was calculated as the time from ouabain, AICAR/ouabain or compound-C /ouabain application to the inflection point of the first abrupt increase in $[\text{K}^+]_o$.

Statistical analyses

Data were plotted using SigmaPlot 9.0 and presented as the mean and standard error (S.E.). Statistical analyses were performed using SigmaStat 3.0 statistical analysis software and significant differences among means were determined using appropriate parametric tests as indicated in the text. A 95% confidence interval was used to determine significance.

4.4 Results

Altered ventilatory motor pattern behaviour post-recovery from NaN₃-induced coma is not the result of damage to the vCPG

The ventilatory motor pattern following recovery from NaN₃-induced vCPG arrest is robust but not identical to the pre-stress motor pattern (Rodgers et al. 2007). As in cortical SD we presume that the likelihood and quality of recovery depends on the severity of anoxia and energy deprivation, and this has yet to be investigated in the locust. Here we examined ventilatory burst durations and periods following recovery from a NaN₃-induced vCPG shutdown to determine if this stress results in an altered ventilatory pattern or long-term damage to the vCPG (Figs. 4.1 – 4.3). Application of 10⁻³M NaN₃ after 20 minutes of standard saline application induced vCPG arrest within 5 minutes and this coincided with an abrupt surge in [K⁺]_o (Fig. 4.1A, B). Control animals had consistent (unchanging) burst durations and periods over one hour of standard saline bath application (Fig. 4.1C, D). Following recovery from NaN₃-induced arrest burst durations and periods gradually increased over time, i.e. the ventilatory motor pattern gradually slowed and deviated from the pre-stress motor pattern (Fig. 4.1B, C, D). There was a main effect of 10⁻³M NaN₃ treatment on normalized burst durations compared to Control (two-way RM-ANOVA, $P < 0.001$, $F_{(1,81)} = 72.938$), and burst durations of Control and NaN₃-treated preparations responded differently over time (statistically significant interaction: two-way RM-ANOVA, $P < 0.001$, $F_{(11,81)} = 25.313$) (Fig. 4.1C). There was also a main effect of 10⁻³M NaN₃ treatment on normalized burst periods compared to Control (two-way RM-ANOVA, $P < 0.001$, $F_{(1,82)} = 24.445$), and burst periods of Control and NaN₃-treated preparations also responded differently over time (statistically

Figure 4.1. The duration and period of expiratory bursts post-recovery from anoxia-induced vCPG arrest progressively increased over time. **A.** Simultaneous recording of electrical activity from the median ventilatory nerve originating at the A3 neuromere of the MTG (“Suct. Elec.”) and the extracellular potassium concentration ($[K^+]_o$) surrounding the vCPG. An abrupt rise in $[K^+]_o$ was reliably triggered by ATP depletion using sodium azide ($10^{-3}M NaN_3$; N=10). Following 20 minutes of standard locust saline bath-application, $10^{-3}M NaN_3$ was bath-applied until 1 minute post-arrest of the motor pattern. $[K^+]_o$ reached a plateau of 77 ± 3 mM on average. $[K^+]_o$ gradually decreased and the motor pattern recovered upon superfusion of standard locust saline. **B.** The motor pattern post-recovery from NaN_3 -induced arrest was not identical to the pre-stress motor pattern. In the experiment shown here, burst duration and period increased by 0.9 and 1.7 seconds, respectively, at 2 minutes post-recovery (“recovery (2 min)”) and burst duration and period increased by 2.1 and 3.5 seconds, respectively, at 30 minutes post-recovery from NaN_3 -induced arrest (“recovery (30 min)”). Relative duration (**C**) and relative period (**D**) over 1 hour in Control preparations and those treated with $10^{-3}M NaN_3$. **C.** There was a main effect of $10^{-3}M NaN_3$ on relative burst duration over time following vCPG recovery. **D.** There was also a main effect of $10^{-3}M NaN_3$ on relative burst period following vCPG recovery. The data points at a relative duration and relative period of 0 represent vCPG arrest coinciding with the $[K^+]_o$ event. Error bars represent SEM.

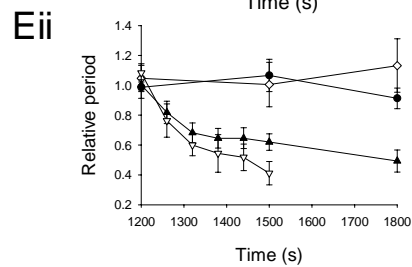
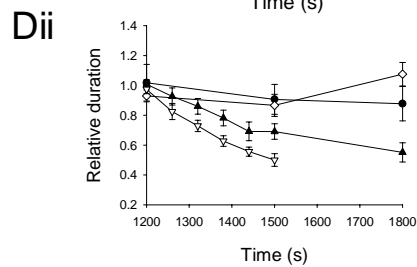
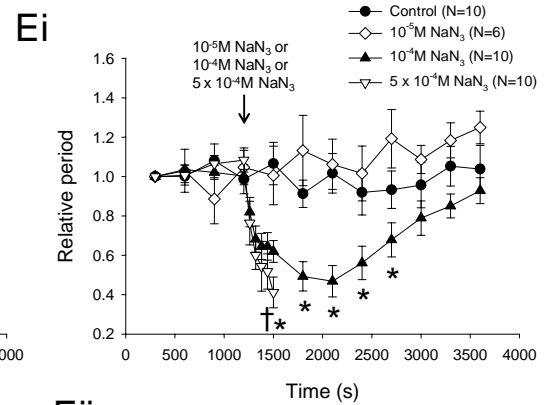
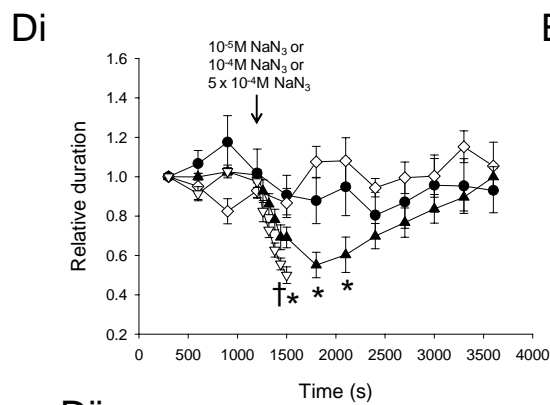
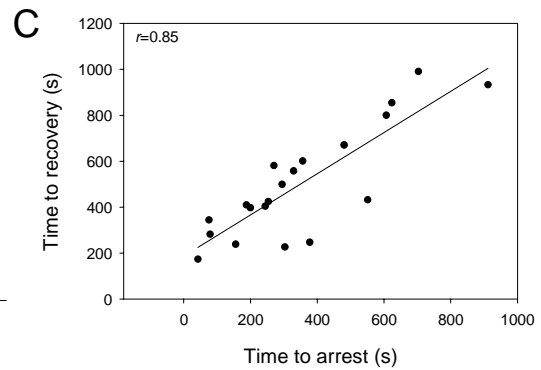
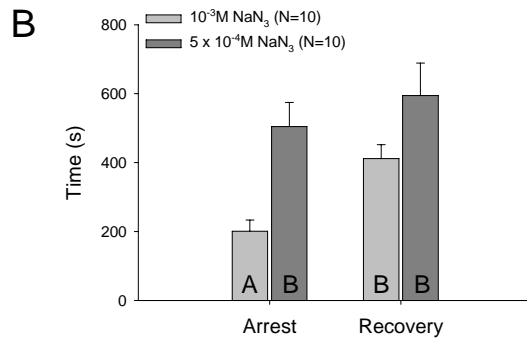
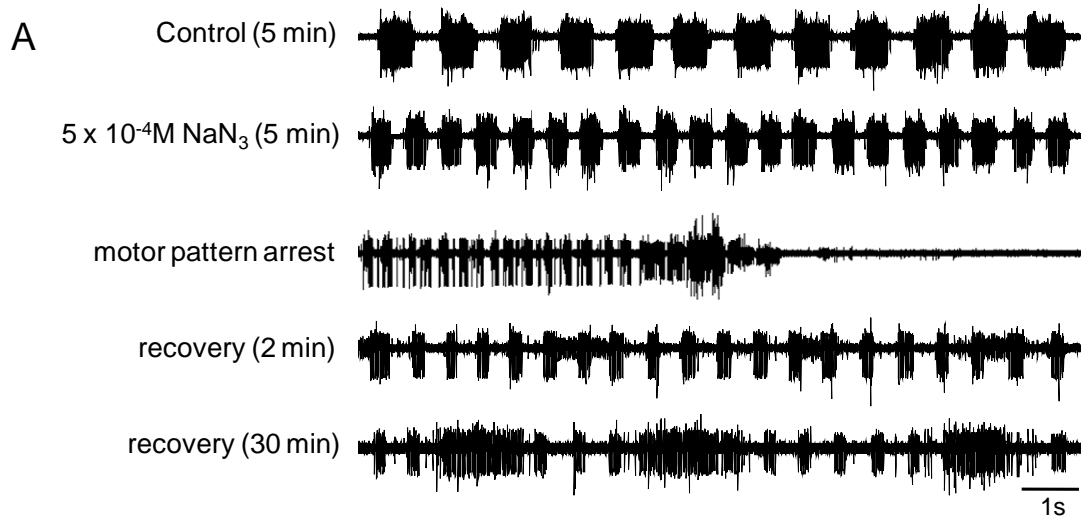


Figure 4.2

Figure 4.2. There was a concentration-dependent effect of NaN₃ treatment both initially, during the first 5 minutes of NaN₃ application, and post-recovery from NaN₃-induced arrest. **A.** The motor pattern post-recovery from arrest induced by 5x10⁻⁴M NaN₃ was not identical to the pre-stress motor pattern, however there was not a complete switch to the long duration and long period motor pattern as with 10⁻³M NaN₃. **B.** Preparations treated with 5x10⁻⁴M NaN₃ had a significantly longer time to vCPG arrest compared to preparations treated with 10⁻³M NaN₃, however there was not a significant difference in the time taken to recover motor pattern generation between treatments. Letters in histogram bars represent statistical groupings whereby bars with different letters (A, B) are significantly different using a *post hoc* Tukey test (*P*<0.05). **C.** Time to vCPG arrest in response to NaN₃ treatment was significantly correlated to the time taken for motor pattern generation to recover. Preparations that had a longer time to arrest also took longer to recover vCPG operation following arrest and the associated [K⁺]_o event. **Di, Ei.** 10⁻⁵M NaN₃ did not induce vCPG arrest, and continuous application for 40 min did not alter the motor pattern compared to Control preparations. 10⁻⁴M NaN₃ application also did not induce vCPG arrest, but there was an initial increase in ventilatory frequency that stabilized and burst durations and periods returned to the Control motor pattern by 40 minutes of application. **Dii, Eii.** The first 10 minutes of NaN₃ application were expanded to show the concentration-dependent effect of NaN₃ treatment on the initial increase in ventilatory rate. Ventilatory burst durations and periods shortened (ventilatory frequency increased) in response to 10⁻⁴M NaN₃, and there was a stronger increase in ventilatory frequency in response to 5x10⁻⁴M NaN₃ within the first 5 minutes of treatment. Asterisks indicate a significant difference from Control and 10⁻⁵M NaN₃-

treated preparations and daggers indicate a significant difference from 10^{-4} M NaN₃-treated preparations (*post hoc* Tukey tests, $P < 0.05$). Error bars represent SEM.

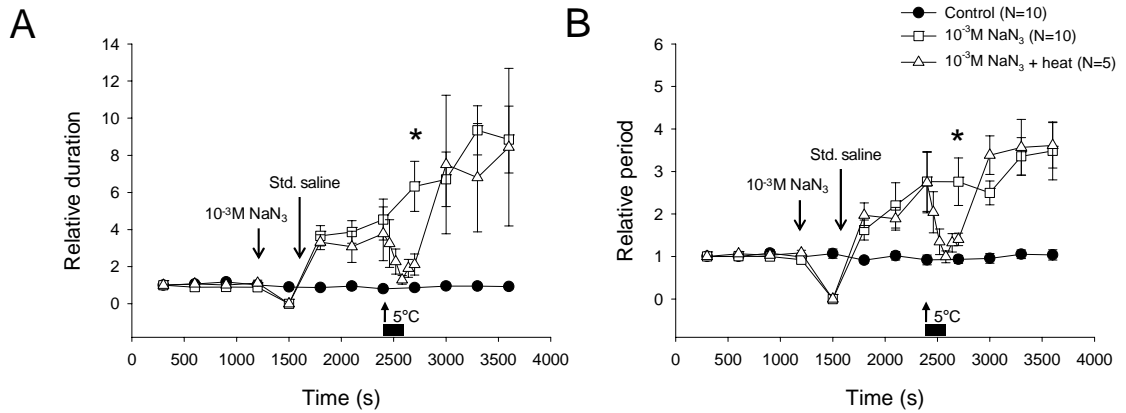


Figure 4.3. Increased burst duration and period over time following recovery from NaN_3 -induced arrest does not appear to be a consequence of permanent damage to vCPG function. **A, B.** Ventilatory burst durations and periods returned to the Control motor pattern when internal temperature was raised 5°C 10-15 minutes following recovery from NaN_3 -induced vCPG arrest (black box). Asterisks indicate significantly different relative burst durations and periods compared to NaN_3 -treated preparations without an increase in internal temperature following recovery (*post hoc* Tukey tests, $P < 0.05$). Error bars represent SEM.

significant interaction: two-way RM-ANOVA, $P < 0.001$, $F_{(11,82)} = 11.737$) (Fig. 4.1D).

vCPG arrest and the associated abrupt increase in $[K^+]_o$ induced by artificially increasing $[K^+]_o$ within the MTG (Rodgers et al. 2007) also resulted in decreased ventilatory frequency, increased burst durations and increased burst periods following vCPG recovery as seen following recovery from NaN_3 -induced arrest ($N=10$, data not shown).

There was a concentration-dependence to the effect of NaN_3 treatment on ventilatory motor pattern generation (Fig. 4.2). Application of $10^{-3}M$ and $5 \times 10^{-4}M$ NaN_3 (as opposed to $10^{-4}M$ and $10^{-5}M$ NaN_3) induced shutdown of vCPG operation and an associated surge in $[K^+]_o$ (Figs. 4.1 and 4.2). $5 \times 10^{-4}M$ NaN_3 induced arrest of the vCPG, but time to arrest was longer and there was not a complete switch to the long duration and period motor pattern post-recovery from NaN_3 -induced arrest as with $10^{-3}M$ NaN_3 (Fig. 4.2A, B).

There was a main effect of NaN_3 concentration ($10^{-3}M$ vs. $5 \times 10^{-4}M$ NaN_3) on time to vCPG arrest and time to subsequent recovery (two-way ANOVA, $P < 0.001$, $F_{(1,36)} = 14.352$) (Fig. 4.2B). Time to vCPG arrest was significantly longer in preparations treated with $5 \times 10^{-4}M$ NaN_3 compared to preparations treated with $10^{-3}M$ NaN_3 , however there was not a significant difference in time to subsequent recovery between preparations treated with the two NaN_3 doses (*post hoc* Tukey tests, $P < 0.05$) (Fig. 4.2B). During hyperthermia, time to recovery was positively correlated with failure temperature in Control and heat shocked (HS) locusts, i.e. animals whose ventilatory motor pattern failed at a higher temperature had a longer time to recovery when temperature returned to normal levels and HS pre-conditioning shifted this relationship (Rodgers et al. 2007).

There was a similar response to NaN_3 application in that a longer time to arrest meant a

longer time to recovery (Fig. 4.2B, C). There was a strong and significant positive correlation between time to arrest of ventilatory motor pattern generation during NaN_3 application and time to subsequent recovery (Pearson Product Moment Correlation, $r=0.85$, $P<0.0001$) (Fig. 4.2C). This suggests that the triggered event is adaptive and represents a neural off-switch to conserve energy and to prevent hyperexcitation during stressful conditions. We also bath-applied two lower concentrations of NaN_3 , 10^{-4}M and 10^{-5}M NaN_3 , and neither of these doses induced vCPG arrest (Fig. 4.2D, E). There was no main effect of NaN_3 dose (10^{-4}M , 10^{-5}M) on normalized burst durations (two-way RM-ANOVA, $P=0.340$, $F_{(2,104)}=1.205$), however burst durations of Control, 10^{-5}M and 10^{-4}M NaN_3 -treated preparations responded differently over time (statistically significant interaction: two-way RM-ANOVA, $P<0.001$, $F_{(22,104)}=4.418$) (Fig. 4.2D). There was a main effect of NaN_3 dose (10^{-4}M , 10^{-5}M) on normalized burst periods (two-way RM-ANOVA, $P=0.021$, $F_{(2,104)}=5.824$), and burst periods of Control, 10^{-5}M and 10^{-4}M NaN_3 -treated preparations responded differently over time (statistically significant interaction: two-way RM-ANOVA, $P<0.001$, $F_{(22,104)}=6.099$) (Fig. 4.2E). A separate analysis was conducted to compare the initial response of the ventilatory motor pattern during 10^{-5}M , 10^{-4}M and $5 \times 10^{-4}\text{M}$ NaN_3 application, and we found that there was a concentration-dependent increase in ventilatory frequency during the first 5 minutes of treatment (Fig 4.2D, E).

Locusts ventilate continuously when stressed and discontinuously while at rest, and therefore discontinuous ventilation arguably represents a non-stressed state. Burst durations and periods following recovery from NaN_3 -induced arrest gradually increased

over time, and it was of interest to determine if this deviance from the Control rhythm represented a switch to discontinuous ventilation or permanent damage from NaN_3 reflected in an eventual inability to maintain a pattern (Fig. 4.3). To determine if the vCPG was capable of generating the pre-stress motor pattern following recovery from NaN_3 -induced arrest we increased the internal temperature of the preparation, a treatment that usually results in increased ventilatory frequency. Turning the heater on 10-15 minutes following recovery from NaN_3 -induced arrest and increasing internal temperature 5°C resulted in an increased ventilatory rate to the point where the motor pattern resembled Control values (Fig. 4.3). There was a main effect of NaN_3 treatment and NaN_3 treatment followed by heat on normalized burst durations (two-way RM-ANOVA, $P < 0.001$, $F_{(2,94)} = 26.091$) and normalized burst periods (two-way RM-ANOVA, $P = 0.013$, $F_{(2,95)} = 7.878$) compared to Control preparations (Fig. 4.3). Normalized burst durations (Fig. 4.3A) and periods (Fig. 4.3B) of NaN_3 -treated preparations were not significantly different than in Control preparations after a temperature increase of 5°C from room temperature applied post-recovery of motor pattern generation (*post hoc* Tukey tests, $P < 0.05$). When the heater was turned off, ventilatory burst durations and periods deviated from the Control motor pattern and there was a gradual decrease in ventilatory rate (Fig. 4.3A, B).

AMPK activation induces a switch in motor pattern behavior resembling that post-recovery from NaN_3 -induced vCPG arrest

AMPK is activated by cell stress, i.e. decreased energy status triggers an increase in AMPK. When AMPK is activated in cells, this signals metabolic stress and ATP-

utilizing processes shut down and ATP-generating processes turn on. It was our goal to determine if AMPK activation using the AMPK activator AICAR would mimic the motor pattern changes induced by a NaN_3 -induced shutdown. 10^{-3}M AICAR was bath-applied in the absence of NaN_3 , artificially signaling decreased energy status, and 10^{-4}M compound-C was also bath-applied in non-stressed (Control) preparations (Fig. 4.4). There were significant treatment effects on both normalized burst durations (two-way RM-ANOVA, $P=0.003$, $F_{(2,198)}=8.496$) and periods (two-way RM-ANOVA, $P=0.001$, $F_{(2,198)}=10.182$) (Fig. 4.4). Activation of AMPK using 10^{-3}M AICAR did not induce vCPG shutdown or an abrupt surge in $[\text{K}^+]_o$, but caused an immediate increase in ventilatory rate and shortened burst durations and periods by ~ 0.7 and ~ 0.5 seconds, respectively, within 5 minutes relative to pre-AICAR values (Fig. 4.4). Inhibition of AMPK using 10^{-4}M compound-C had no effect on ventilatory burst durations or periods when induced in non-stressed preparations, possibly because there was no stress signal and thus nothing to inhibit (Fig. 4.4). Normalized burst durations (Fig. 4.4A) and periods (Fig. 4.4B) in preparations treated with 10^{-3}M AICAR were significantly different than in Control preparations and those treated with 10^{-4}M compound-C after 5 minutes of application (*post hoc* Tukey tests, $P<0.05$).

The result that AMPK activation using 10^{-3}M AICAR caused the ventilatory rhythm to speed up is interesting, however we speculated whether a higher dose of AICAR would have effects on the motor pattern that resemble the marked change in burst durations and periods following recovery from NaN_3 -induced arrest. Ventilatory burst durations and periods shortened, i.e. ventilatory frequency increased, by 2 minutes of 10^{-2}M AICAR

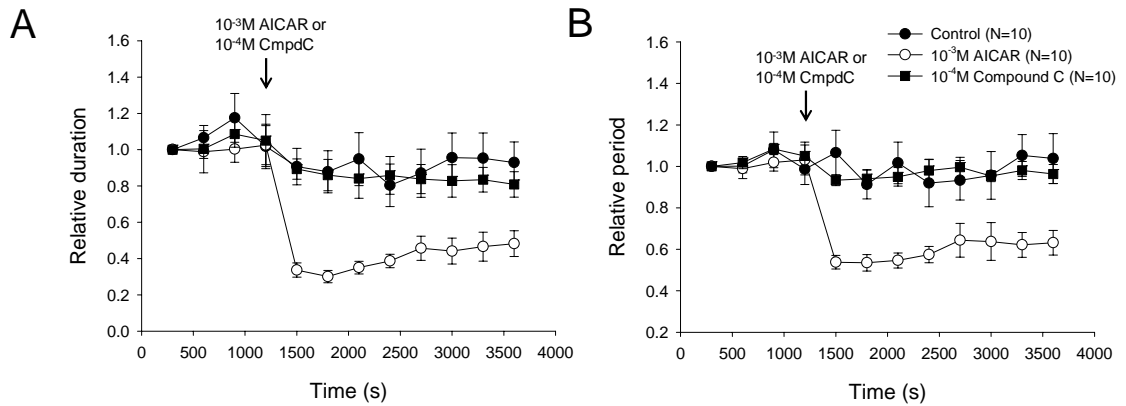


Figure 4.4. Activation of AMP-activated protein kinase (AMPK) increased ventilatory frequency and inhibition of AMPK had no effect when induced in non-stressed (Control) preparations. **A, B.** Relative to the start of the experiment, AMPK activation using 10^{-3} M AICAR significantly shortened burst durations and periods by proportions of ~ 0.7 and ~ 0.5 , respectively, within 5 minutes compared to Control and 10^{-4} M compound-C-treated preparations. Inhibition of AMPK using 10^{-4} M compound-C had no effect on normalized burst durations and periods compared to Control. Error bars represent SEM.

application (Fig. 4.5, Fig. 4.6C, D). Following the initial increase in ventilatory rate AMPK activation using AICAR had multiple effects on the rhythm that can be divided into four distinct categories: A) the pre-AICAR motor pattern was replaced with continuous tonic buzzing, B) the pre-AICAR motor pattern was replaced with unpatterned “gasps” or large amplitude bursts, C) another long duration/long period rhythm was interspersed with the pre-AICAR motor pattern, and D) the second long duration/long period rhythm replaced the pre-AICAR rhythm, which became completely phased out (Fig. 4.5).

AMPK inhibition reverses the AICAR- and NaN₃-induced switch in ventilatory motor pattern behaviour and glucose mimicked the effects of AMPK inhibition

Following 20 minutes of AICAR bath-application, 10⁻⁴M compound-C was bath-applied for 20 minutes (Fig. 4.5). Regardless of the effect of AICAR, 10⁻⁴M compound-C recovered the ventilatory motor pattern to near pre-AICAR duration and period values (Fig. 4.5, Fig. 4.6C, D). Bath-application of 10⁻⁴M compound-C in combination with 10⁻²M AICAR had similar effects as when applied alone in standard locust saline, and saline washout following 20 minutes of 10⁻²M AICAR reversed the effects of AICAR on the motor pattern (data not shown). There was a main effect of AMPK activation and inhibition on normalized burst durations (one-way ANOVA, $P=0.004$, $F_{(4,42)}=4.590$) and periods (one-way ANOVA, $P<0.001$, $F_{(4,44)}=16.521$) compared to pre-treatment (Control) values (Fig. 4.6C, D). 10⁻²M AICAR significantly shortened burst durations and periods within 5 minutes compared to pre-AICAR values and 10⁻⁴M compound-C subsequently significantly increased burst durations and periods to near Control values (*post hoc* Tukey

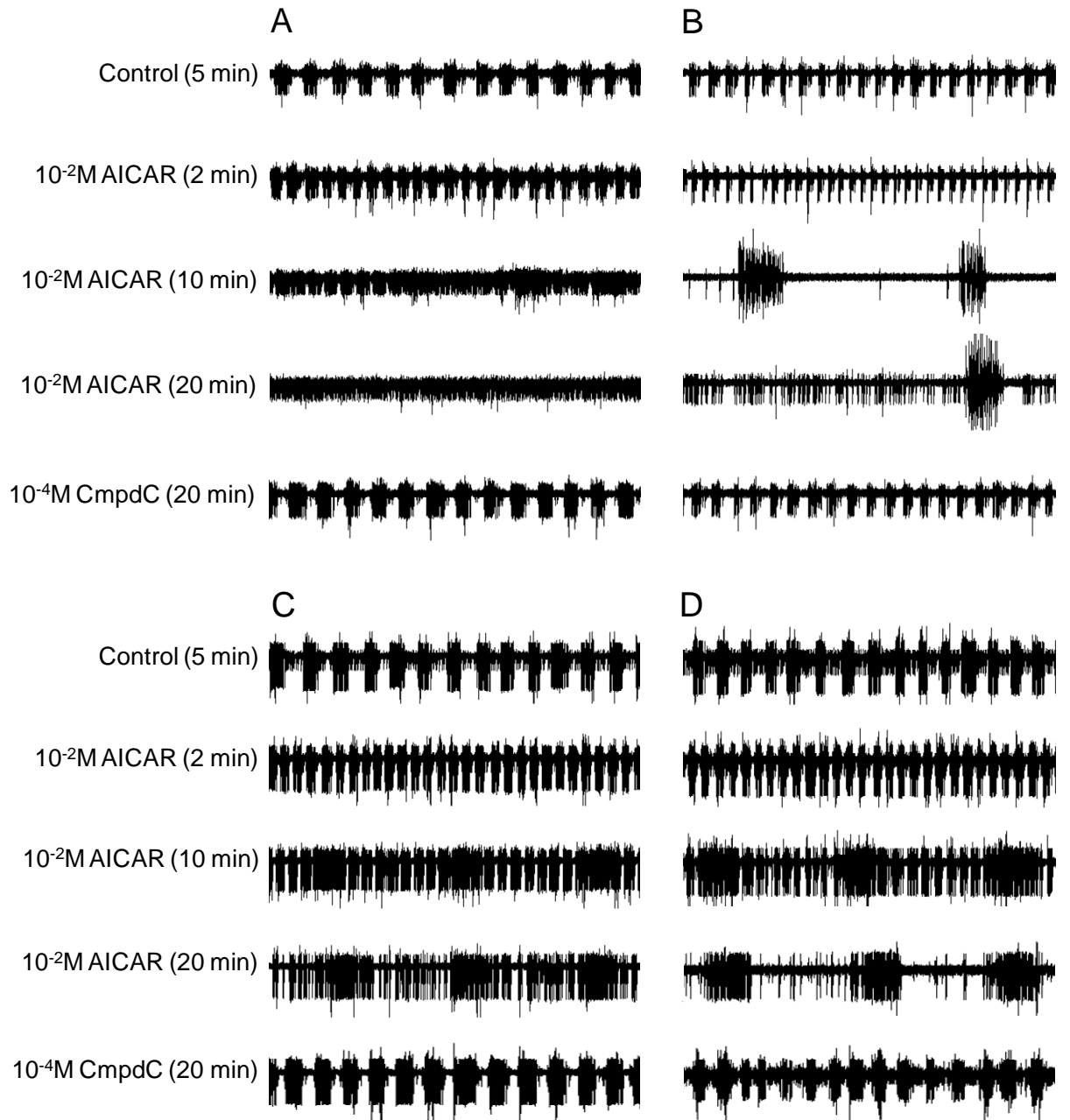


Figure 4.5

Figure 4.5. AMPK inhibition using compound-C reversed the effects of a high dose of AICAR on the ventilatory motor pattern. **A-D.** 10^{-2} M AICAR was bath-applied in preparations for 20 min, followed by bath-application of 10^{-4} M compound-C for 20 min. Control (5 min) = 5 minutes following standard locust saline application; AICAR (2 min), (10 min), and (20 min) = 2, 10, and 20 minutes following 10^{-2} M AICAR bath-application, respectively; CmpdC (20 min) = 20 minutes following 10^{-4} M compound-C bath-application. 10^{-2} M AICAR caused an immediate increase in ventilatory rate within 1-2 minutes post-entry into the preparation and this was followed by multiple effects on the ventilatory rhythm, some resembling the recovered motor pattern following NaN_3 -induced arrest: **A.** Continuous tonic buzzing, **B.** Loss of the pre-AICAR motor pattern and unpatterned, high amplitude “gaspings”, **C.** Another long duration/long period rhythm interspersed with the initial motor pattern, and **D.** The second long duration/long period rhythm replaced the initial rhythm, which became completely phased out. Regardless of the effect of AICAR, 10^{-4} M compound-C recovered the rhythm to pre-AICAR duration and period values.

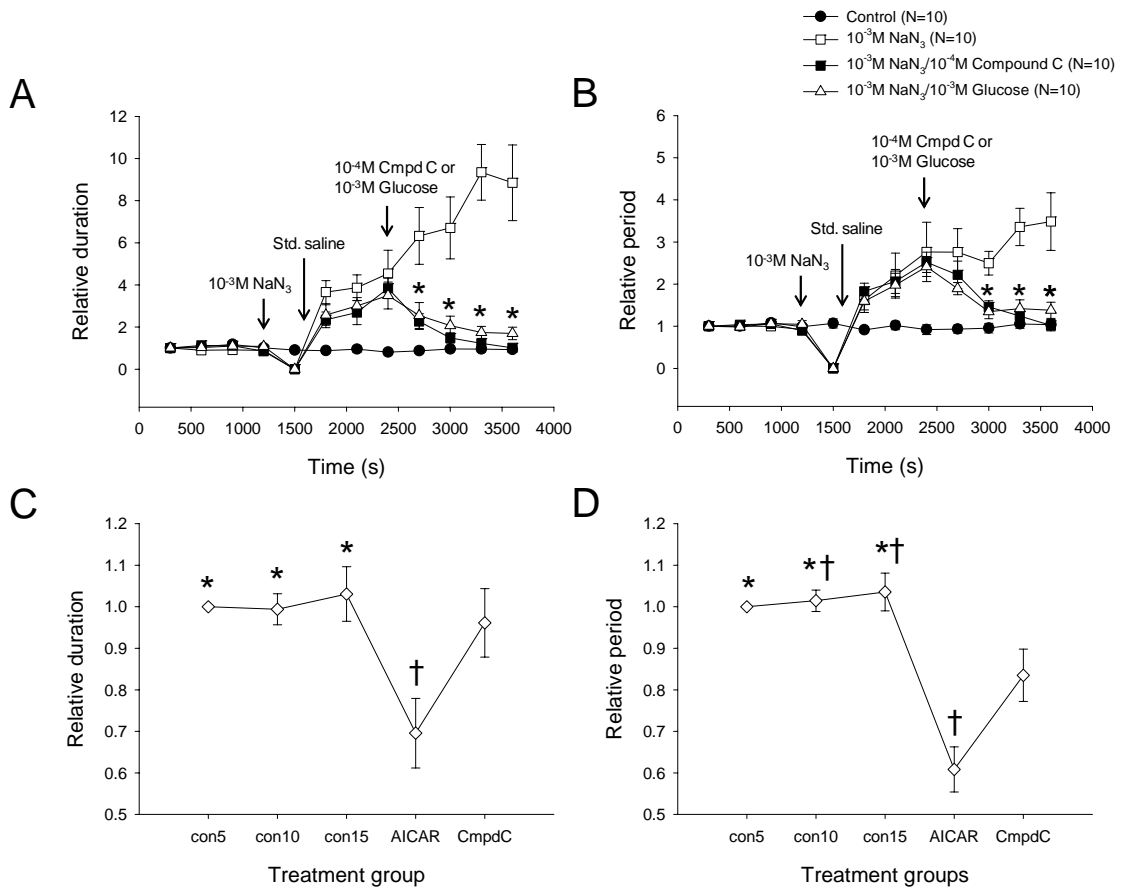


Figure 4.6

Figure 4.6. AMPK inhibition using compound-C “reversed” the effects of NaN₃ and AICAR on the ventilatory motor pattern by returning burst durations and periods to Control values, and glucose mimicked the effects of compound-C. **A, B.** 10⁻³M NaN₃ was bath-applied in preparations until 1 minute post-arrest of ventilatory motor pattern generation, at which point preparations were allowed to recover in standard locust saline. 10⁻⁴M compound-C or 10⁻³M glucose were bath-applied 10-15 minutes following recovery from NaN₃-induced vCPG arrest. There was a significant effect of both compound-C and glucose on normalized burst durations (**A**) and normalized burst periods (**B**) which resembled Control values by 20 minutes of application. Normalized durations and normalized periods in preparations treated with 10⁻⁴M compound-C or 10⁻³M glucose following recovery from NaN₃-induced vCPG arrest were not significantly different than in Control preparations at 50-60 minutes into the experiment. Asterisks indicate significantly different burst durations and periods compared to preparations that were allowed to recover from NaN₃-induced vCPG arrest in standard locust saline. **C, D.** AMPK inhibition using compound-C reversed the effects of AICAR on the ventilatory motor pattern. “con5”, “con10”, and “con15” represent 5, 10, and 15 minutes after standard locust saline application. 10⁻²M AICAR was bath-applied after 20 minutes of standard locust saline application and after 5 minutes of 10⁻²M AICAR application (“AICAR”) burst durations shortened by ~0.3 seconds on average and burst periods shortened by ~0.4 seconds on average relative to initial values. 10⁻⁴M compound-C was bath-applied in preparations following 20 minutes of AICAR application and after 20 minutes of compound C application burst durations and periods returned to near Control

values. Asterisks indicate a significant difference from AICAR and daggers indicate a significant difference from compound-C. Error bars represent SEM.

tests, $P < 0.05$) (Fig. 4.6C, D). Since compound-C reversed the effects of AICAR, it was of interest to determine if blocking AMPK activation would have a similar effect following NaN_3 -induced arrest. Following NaN_3 -induced arrest burst durations and periods gradually increased over time (Fig. 4.1B, C, D). We bath-applied 10^{-4}M compound-C as well as 10^{-3}M glucose 10-15 minutes following recovery from NaN_3 -induced arrest to determine of the effect of these treatments on the recovered motor pattern (Fig. 4.6A, B). There were significant treatment effects on both normalized burst durations (two-way RM-ANOVA, $P < 0.001$, $F_{(3,208)} = 20.096$) and periods (two-way RM-ANOVA, $P < 0.001$, $F_{(3,274)} = 8.812$) (Fig. 4.6A, B). Application of 10^{-4}M compound-C following recovery from NaN_3 -induced arrest returned the motor pattern to a faster continuous state resembling Control durations and periods by 20 minutes of application (Fig. 4.6A, B). Application of 10^{-3}M glucose mimicked the effect of compound-C on the motor pattern and returned ventilatory burst durations and periods to near Control values (Fig. 4.6A, B). In preparations treated with either 10^{-4}M compound-C or 10^{-3}M glucose following NaN_3 -induced vCPG arrest, normalized burst durations and periods were not significantly different than Control values after 10 minutes of application (*post hoc* Tukey tests, $P < 0.05$) (Fig. 4.6A, B).

AMPK inhibition suppresses ouabain-induced SD-like events

Continuous bath-application of 10^{-4}M ouabain induces repetitive vCPG arrest, with each period of electrical silence coinciding with an abrupt surge in $[\text{K}^+]_o$ (Rodgers et al. 2007, 2009) (Fig. 4.7). In this study, the time to onset of the initial ouabain-induced SD-like $[\text{K}^+]_o$ event was ~ 12 minutes and there were ~ 3 SD-like events on average within 35

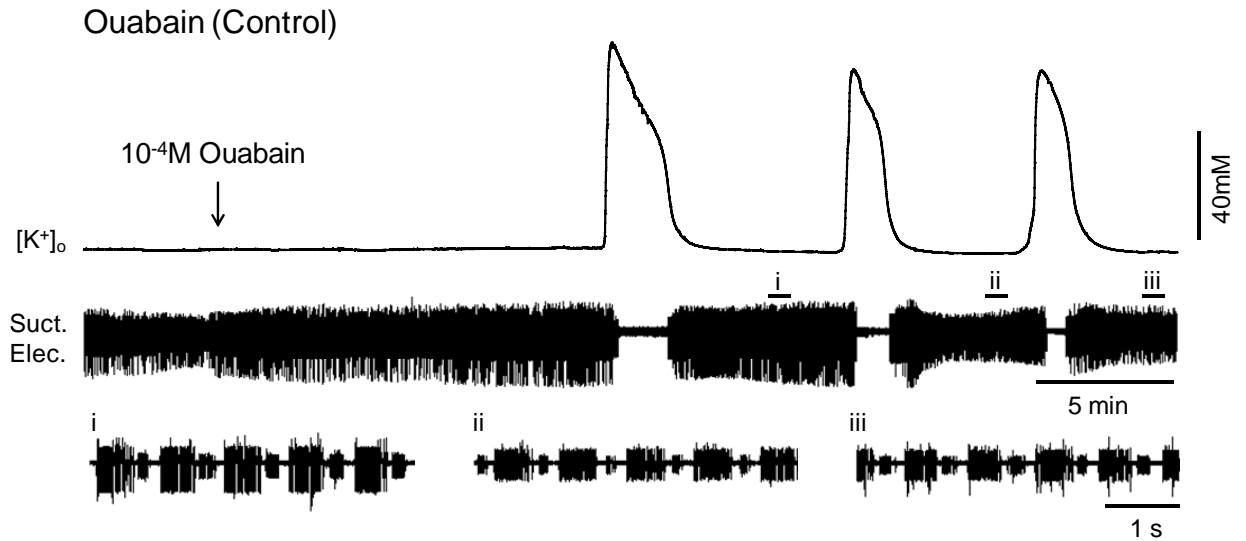


Figure 4.7. Ouabain-induced repetitive SD-like events in the locust MTG. Simultaneous recording of electrical activity from the median ventilatory nerve originating at the A3 neuromere of the MTG (“Suct. Elec.”) and the extracellular potassium concentration ($[K^+]_o$) surrounding the vCPG. Following 20 minutes of standard locust saline bath-application, $10^{-4}M$ ouabain was bath-applied for 35 minutes. $10^{-4}M$ ouabain induced repetitive abrupt surges in $[K^+]_o$ where the rise and fall of $[K^+]_o$ were associated with arrest and recovery, respectively, of ventilatory motor pattern generation (N=10). $10^{-4}M$ ouabain initiated repetitive SD-like events at ~12 minutes of application and induced ~3 SD-like events on average. 100% of preparations had at least one SD-like event within 35 minutes of application. The expansions (i, ii, iii) show the motor pattern trace following each SD-like event in Control preparations.

minutes of application (Fig. 4.7). Also, all preparations had at least one SD-like event over the course of ouabain treatment. There were striking similarities in this study between the ventilatory motor pattern during AMPK activation using AICAR and the ventilatory motor pattern post-recovery from NaN_3 -induced vCPG arrest and associated SD-like event. In addition, compound-C returned ventilatory burst durations and periods to Control values in both cases. Given these results we hypothesized that SD-like events in the locust induced by a milder stress such as impairment of ionic homeostasis using ouabain may be modulated by AMPK activation. For this investigation, we pre-treated preparations by bath-applying either 10^{-2}M AICAR or 10^{-4}M compound-C for 15 minutes, followed by bath-application of either 10^{-2}M AICAR or 10^{-4}M compound-C in combination with 10^{-4}M ouabain for 35 minutes. Preparations treated with 10^{-4}M ouabain alone represent “Control” preparations. Ouabain-induced repetitive SD-like events were exacerbated by 10^{-2}M AICAR and suppressed by 10^{-4}M compound-C (Fig. 4.8). Pre-treatment with 10^{-2}M AICAR caused a modest $\sim 5\text{mM}$ increase in $[\text{K}^+]_o$ and had effects on the ventilatory motor pattern as seen in Fig. 4.5 (Fig. 4.8A). An examination of the ventilatory motor pattern following multiple ouabain-induced SD-like events revealed a complete switch to a long duration and long period motor pattern when AICAR was bath-applied in combination with ouabain (Fig. 4.8A). 10^{-2}M AICAR significantly decreased the time to onset of SD-like events and significantly increased the number of SD-like events compared to Control preparations and those treated with 10^{-4}M compound-C (*post hoc* Tukey tests, $P < 0.05$) (Fig. 4.8A, D, E). In the majority of preparations, 10^{-4}M compound-C treatment completely abolished ouabain-induced SD-like events (Fig. 4.8B, C). Compared to Control preparations and those treated with 10^{-

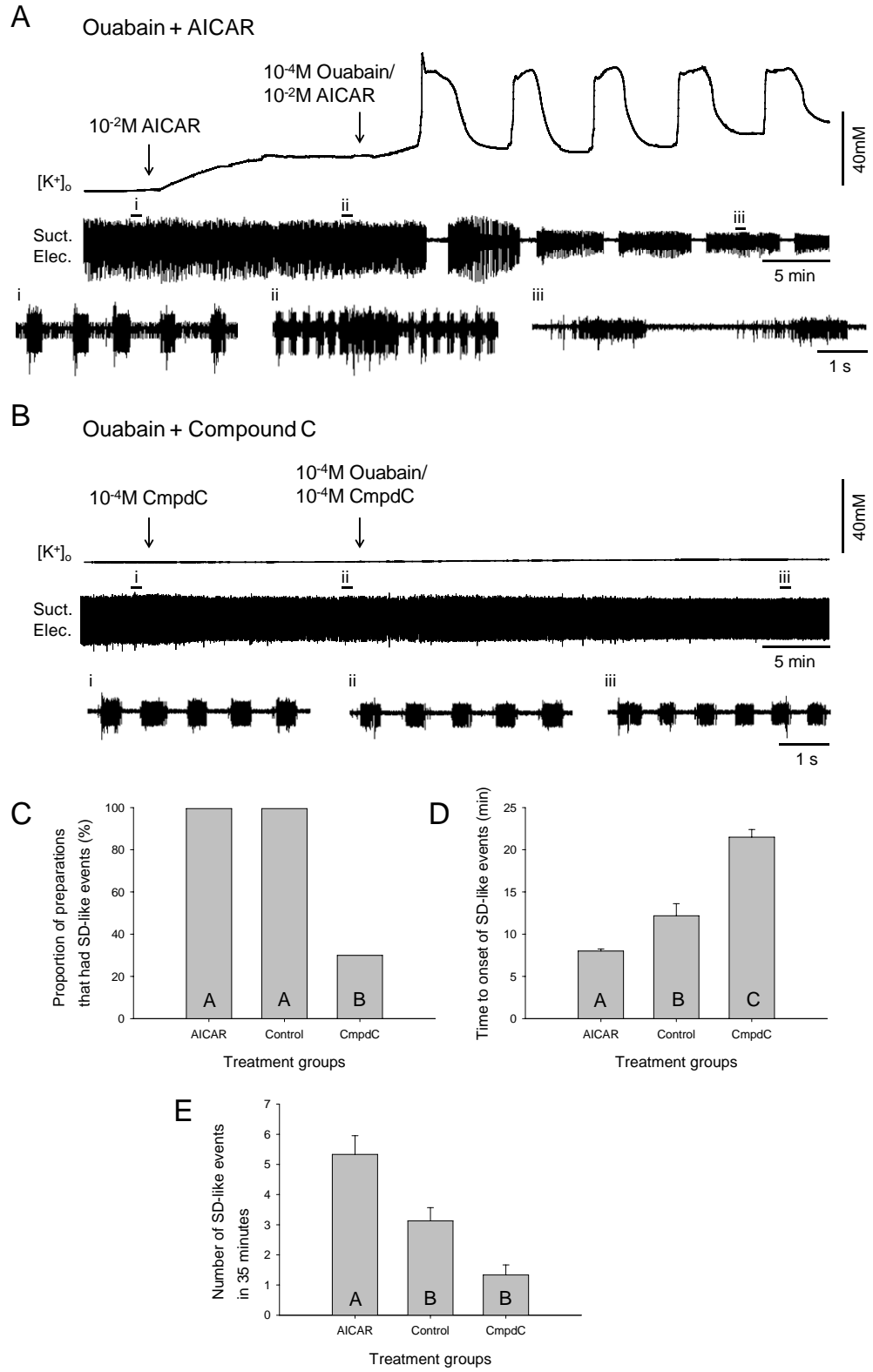


Figure 4.8

Figure 4.8. AMPK inhibition suppresses ouabain-induced spreading depression. **A, B.** Simultaneous recording of electrical activity from the median ventilatory nerve originating at the A3 neuromere of the MTG (“Suct. Elec.”) and the extracellular potassium concentration ($[K^+]_o$) surrounding the vCPG. Following 20 minutes of standard locust saline bath-application, preparations were pre-treated with either 10^{-2} M AICAR or 10^{-4} M compound-C for 15 minutes. 10^{-2} M AICAR or 10^{-4} M compound-C were then bath-applied in combination with 10^{-4} M ouabain for 35 minutes. Expansions show the motor pattern trace at different time points: i) prior to pre-treatment, ii) after 15 minutes of AICAR or compound-C pre-treatment and iii) after 25-35 minutes of bath-application of ouabain in combination with AICAR or compound-C. AMPK activation increased the propensity for ouabain-induced SD-like events (**A**) and AMPK inhibition suppressed ouabain-induced SD-like events (**B**). **C.** AMPK inhibition resulted in a 70% decrease in the number of preparations having at least one ouabain-induced SD-like event. **D.** Time to onset of ouabain-induced SD-like events was significantly decreased by AMPK activation and significantly increased by AMPK inhibition. Significant treatment effects were found (one-way ANOVA, $P < 0.001$, $F_{(2,19)} = 15.860$; Control and AICAR, $N = 10$; CmpdC, $N = 3$) where letters (A, B, C) denote significant differences using a *post hoc* test (Tukey, $P < 0.05$). **E.** AMPK activation also increased the number of SD-like events compared to Control preparations and those treated with 10^{-4} M compound-C and significant effects of treatment were found (one-way ANOVA, $P = 0.001$, $F_{(2,14)} = 10.785$; Control and AICAR, $N = 10$; CmpdC, $N = 3$). Control preparations and those treated with compound-C were not significantly different, likely due to the small sample size as a result of the low proportion of preparations treated with

compound-C that had at least one SD-like event. Letters in histogram bars represent statistical groupings whereby bars with different letters are significantly different using a *post hoc* Tukey test ($P < 0.05$). Error bars represent SEM.

10^{-2} M AICAR, AMPK inhibition using 10^{-4} M compound-C significantly reduced the proportion of preparations having at least one SD-like event (z -test, $z=3.027$, $P=0.002$) (Fig. 4.8C). In the 3 out of 10 preparations that had at least one SD-like event, 10^{-4} M compound-C significantly delayed the time to onset of ouabain-induced SD-like events (*post hoc* Tukey tests, $P<0.05$) (Fig. 4.8D; Fig. 4.9A). Preparations treated with 10^{-4} M compound-C also had significantly fewer SD-like events compared to preparations treated with 10^{-2} M AICAR, but not compared to Control preparations, likely due to the small sample size (*post hoc* Tukey tests, $P<0.05$) (Fig. 4.8E).

Following initiation of locust SD, AMPK inhibition aborts subsequent ouabain-induced SD-like events

Although AMPK inhibition resulted in complete suppression of ouabain-induced SD-like events in 70% of preparations, delayed SD-like events were elicited in the remaining 30% of preparations (Fig. 4.8B-E). There was an interesting effect of compound-C in these preparations in that the abrupt ouabain-induced increases in $[K^+]_o$ were not accompanied by electrical silence or vCPG arrest (Fig. 4.9A). Surprisingly, when compound-C was bath-applied in combination with ouabain, ventilatory motor pattern generation continued during ouabain-induced SD-like events, where $[K^+]_o$ increased to around the same amplitude as in Control preparations (compound-c, 55-65mM; Control, 60-70mM). Thus, compound-C not only delayed the onset and thus decreased the number of ouabain-induced SD-like events in these preparations, but also prevented shutdown of neuronal activity, an important characteristic of SD-like events in both locust and mammalian cortex (Fig. 4.9A). In a separate set of experiments, we induced SD-like events using 10^{-2}

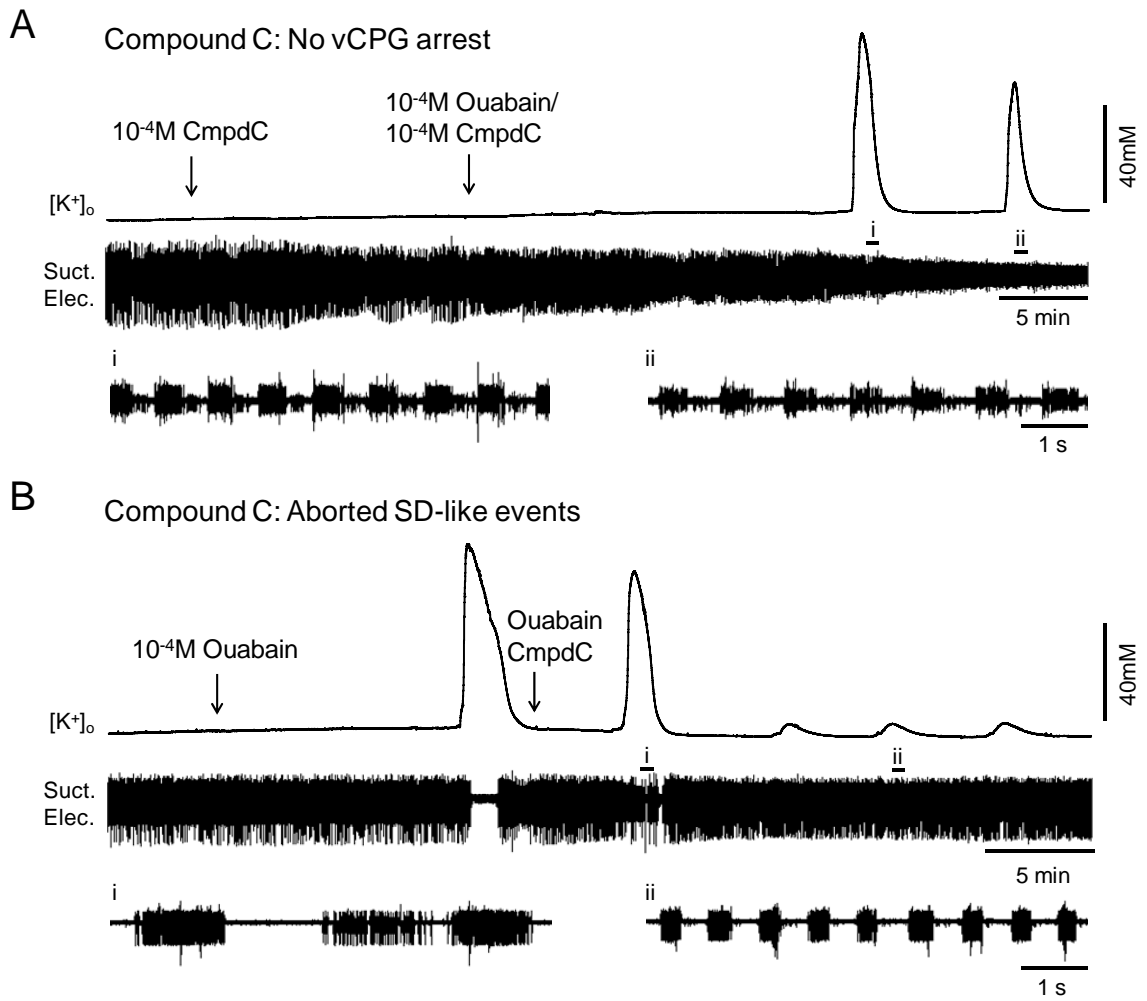


Figure 4.9

Figure 4.9. Additional effects of AMPK inhibition on ouabain-induced repetitive SD-like events in the locust MTG. **A, B.** Simultaneous recording of electrical activity from the median ventilatory nerve originating at the A3 neuromere of the MTG (“Suct. Elec.”) and the extracellular potassium concentration ($[K^+]_o$) surrounding the vCPG. **A.** AMPK inhibition resulted in a significant decrease in the number of preparations having at least one ouabain-induced SD-like event. In the few preparations (30%) in which ouabain-induced SD-like events were generated, vCPG shutdown did not occur during abrupt increases in $[K^+]_o$. **B.** 10^{-4} M ouabain was bath-applied following 20 minutes of standard locust saline application, and 10^{-4} M compound-C was bath-applied in combination with 10^{-4} M ouabain following the initial ouabain-induced SD-like event. Subsequent $[K^+]_o$ surges were aborted and motor pattern generation continued during these events. Expansions (i, ii) show the motor pattern trace coinciding with various SD-like events.

10^{-4} M ouabain in exactly the same fashion as in Control preparations, but we then bath-applied 10^{-4} M compound-C in combination with 10^{-4} M ouabain directly following the initial ouabain-induced SD-like event (Fig. 4.9B). As a result of compound-C introduction into preparations following SD onset, subsequent $[K^+]_o$ increases were substantially decreased in amplitude and duration compared to in Control preparations, and these muted $[K^+]_o$ surges did not coincide with electrical silence or vCPG arrest (Fig. 4.9B).

4.5 Discussion

This study demonstrates that AMPK activation mimics the effect of an acute energy stress on ventilatory motor pattern properties and increases the propensity for and severity of ouabain-induced SD-like events in the locust. Upon initial application of NaN_3 , ventilatory rate increased in a concentration-dependent manner. 10^{-3}M and $5 \times 10^{-4}\text{M}$ NaN_3 induced vCPG arrest and an associated SD-like event, and the time from NaN_3 application to vCPG arrest was concentration-dependent. There was an interesting trade-off such that early vCPG arrest induced by 10^{-3}M and $5 \times 10^{-4}\text{M}$ NaN_3 doses was associated with shorter times to recovery. This supports the hypothesis that the triggered event is adaptive and represents a neural off-switch to conserve energy. Following SD-like events induced by 10^{-3}M NaN_3 , the motor pattern recovered and deviated from the pre- NaN_3 motor pattern, and this occurred to a lesser degree following vCPG arrest induced by $5 \times 10^{-4}\text{M}$ NaN_3 . Ventilatory rate gradually slowed and ventilatory burst durations and periods increased over time. AMPK activation using AICAR did not induce vCPG arrest and an abrupt rise in $[\text{K}^+]_o$ but caused the ventilatory rhythm to initially speed up, then had multidimensional effects at a high dose (10^{-2}M), some mimicking the effect of NaN_3 in reducing motor pattern frequency. In some cases there appeared to be a complete switch in vCPG output to a slower motor pattern. This indicates that AMPK activation reduces energy use at the expense of neuronal performance following an initial increase in O_2 uptake. Application of heat following recovery from NaN_3 -induced vCPG arrest returned burst durations and periods to pre- NaN_3 values. This demonstrates that complete energy deprivation by chemical anoxia is not permanently damaging to the locust vCPG but could alter output in preparation for

future stresses. It is not clear why neural activity recovers in the locust but in cortical tissue cells die as a result of low O₂ and energy deprivation. Ganglion architecture and tracheal supply of oxygen in the locust have a different type of complexity than a vascular supply of blood carrying oxygen and glucose in cortical tissue. Vascular O₂ supply is very important for recovery from SD and the associated depolarization in cortical tissue even in normoxic conditions (Takano et al. 2007). In locusts NaN₃-induced vCPG arrest does not coincide with complete neuronal depolarization (Armstrong et al. 2009). This may allow for energy-conserving mechanisms, such as AMPK, to be activated during SD-like events. We propose that SD-like events in the locust trigger the activation of AMPK to conserve energy.

AMPK activation triggers changes in breathing rhythms in response to metabolic insults (Kr neisz et al. 2009). Carotid body glomus cells sense O₂ availability to regulate breathing and AMPK activation by NaN₃ or hypoxia inhibits background K⁺ channels TREK-1 and TREK-2 in these cells (Kr neisz et al. 2009). Thus metabolic activity has been directly linked to cell excitability by AMPK (Kr neisz et al. 2009). We have provided evidence for a link between AMPK activation and ventilatory central pattern generation in an insect model. The AICAR-induced switch to a long duration and period motor pattern was similar to the reduced frequency motor pattern following NaN₃-induced arrest and it is reasonable to suggest that these changes involved AMPK activation. AMPK inhibition using compound-C did not alter the ventilatory rhythm when applied in non-stressed preparations but reversed the effects of AICAR and NaN₃ by returning ventilation to the pre-stress condition.

AMPK activation caused a modest increase in $[K^+]_o$ levels (5mM) during pre-treatment with AICAR, then exacerbated ouabain-induced SD-like events. Compared to Control preparations, AICAR decreased the time to onset and increased the number of ouabain-induced SD-like events. The initial AICAR-induced increase in $[K^+]_o$ may be due to inhibition of Na^+/K^+ -ATPase complexes within the MTG. The Na^+/K^+ -ATPase is both energy-requiring and essential for maintenance of the K^+ equilibrium, and we have already shown that disruption of the Na^+/K^+ -ATPase using ouabain results in the generation of SD-like events in a concentration-dependent manner (Rodgers et al. 2009). An AMPK-induced shutdown of Na^+/K^+ -ATPase activity when pumps are already subjected to ouabain would explain exacerbated SD-like events.

AMPK is expressed in cortical and hippocampal tissue and is involved in neuroprotection following stroke (McCullough et al. 2005) and neuronal plasticity involved in epileptogenesis (Potter et al. 2010). Aside from a major mechanistic role in learning and memory, long term potentiation (LTP) is also thought to play a role in epileptogenesis. Glycolytic inhibition using 2-deoxy-D-glucose (2DG) suppressed epileptogenesis (Garriga-Canut et al. 2006) and AMPK activation using 2DG, metformin, and AICAR prevented LTP maintenance by suppressing the mammalian Target of Rapamycin (mTOR) pathway in the mouse hippocampus (Potter et al. 2010). It is likely that AMPK activation inhibited the mTOR signaling pathway and induction of LTP because these processes are energy intensive. AMPK inhibition or lack of activation results in heightened mTOR activity and inappropriate LTP induction that underlie diseases or

conditions such as epilepsy that involve SD. We presume that AMPK activation exacerbated SD-like events in the locust by suppressing energy-requiring processes thereby affecting the electrochemical gradient leading to the generation of SD.

Inhibition of AMPK using compound-C suppressed SD in 70% of preparations. In the few preparations where $[K^+]_o$ events did occur during bath-application of compound-C, there was no interruption of vCPG operation despite $\sim 60\text{mM}$ $[K^+]_o$ increases measured in the area of the vCPG. When compound-C was applied following the initiation of repetitive ouabain-induced SD, subsequent $[K^+]_o$ waves had a shorter duration and smaller amplitude. These small $[K^+]_o$ increases did not share the same characteristics as the abrupt all-or-none type increases that usually occur coinciding with vCPG arrest in response to ouabain. One possibility is that inhibition of AMPK affected $[K^+]_o$ propagation throughout the MTG. Tapered $[K^+]_o$ diffusion across tissue would explain continued electrical activity and muted $[K^+]_o$ surges within the MTG upon application of compound-C. Recently it has been suggested that ouabain-induced repetitive SD-like events in the locust resemble the spontaneous peri-infarct depolarizations (PIDs) that expand the penumbra during stroke in vertebrate cortical tissue (Rodgers et al. 2010). PIDs prevent the restoration of energy balance during ischemia that is critical to cell survival following stroke and therefore increase the size of the infarct and the volume of neuronal damage (Fabricius et al. 2005; Dohmen et al. 2008; Dreier et al. 2009). A similarity between PIDs in cortex and ouabain-induced $[K^+]_o$ surges in the locust is that vCPG recovery is less likely following each $[K^+]_o$ event and there is a concentration-dependence to this effect (Rodgers et al. 2009). Neuronal AMPK is elevated and

activated after induction of cerebral ischemia in mice (McCullough et al. 2005). The volume of stroke damage is reduced by pharmacological inhibition of AMPK by either C75 (increases ATP levels) or compound-C and exacerbated by AICAR activation of AMPK (McCullough et al. 2005). Thus, AMPK activation following cerebral ischemia is detrimental to neuronal survival whereas inactivation of AMPK may be neuroprotective (McCullough et al. 2005). A novel finding in the current study was that AMPK inhibition suppresses SD-like events once locust SD has been initiated.

Nitric-oxide synthase (NOS) may play a role in neuronal survival after ischemic stress, as mice deficient in neuronal NOS (nNOS) demonstrated a decrease in both stroke damage and AMPK activation compared with wild type (McCullough et al. 2005). During OGD, stimulation of NOS by increasing Ca^{2+} levels causes accumulations of NO, superoxide, peroxynitrite (ONOO), and free radicals, contributing to cell damage (Snider et al. 1999; Love, 2003). AMPK can be activated independently of changes in AMP, for example by the NO/ONOO pathway (Almeida et al. 2004). An increase in NO production results in formation of ONOO, a potent oxidant by-product and key player in induction of ischemic damage. Production of NO has previously been shown to increase in the locust CNS in response to heat and anoxia (Armstrong et al. 2009) and has been shown to affect locust CPGs and rhythmic movements (Newland and Yates, 2007). Activation of the NO/cGMP/PKG pathway exacerbates ouabain-induced SD and inhibition of this pathway suppresses SD-like events in the locust (Armstrong et al. 2009). In the absence of AMPK inducers or inhibitors, the generation of SD-like events in response to stress in the locust could be attributed to increased NO in the nervous system and activation of AMPK.

Drops in cellular ATP could also activate AMPK and lead to continued activation following recovery from SD-like events, altering the ventilatory motor pattern. As part of the response to ischemia, AMPK activates numerous transcription factors and proteins, including endothelial NOS. Another possibility is that AMPK activation in response to stress activates NOS, leading to NO production, increased PKG, and SD in the locust MTG. The ATP-depleting effects of NO/cGMP/PKG activation by AMPK may contribute to exacerbated SD-like events. Thus, AMPK could be mechanistically related to NO, ONOO, and nNOS in the locust.

We have shown the locust vCPG responds to acute energy stress by switching motor pattern behavior and manipulation of an energy sensing pathway ‘tunes’ the propensity of neuronal tissue in the locust to display SD-like events. The switch in rhythm frequency in response to a NaN_3 -induced shutdown could be mimicked by AMPK activation and reversed by AMPK inhibition. In addition to altering ventilatory motor pattern properties AMPK activation exacerbated ouabain-induced SD. Our results suggest that a shutdown of neural function and SD-like events in response to ATP deprivation in the locust do not result in neural tissue damage. Thus we provide evidence that AMPK has a role in stress-induced comas and SD-like events in the locust and may trigger a switch in motor pattern behavior at the expense of neuronal performance.

4.6 References

Almeida A, Moncada S, Bolaños JP (2004) Nitric oxide switches on glycolysis through the AMP protein kinase and 6-phosphofructo-2-kinase pathway. *Nat Cell Biol* 6:45-51.

Armstrong GAB, Rodgers CI, Money TGA, Robertson RM (2009) Suppression of spreading depression-like events in locusts by inhibition of the NO/cGMP/PKG pathway. *J Neurosci* 29:8225-8235.

Dohmen C, Sakowitz OW, Fabricius M, Bosche B, Reithmeier T, Ernestus RI, Brinker G, Dreier JP, Woitzik J, Strong AJ, Graf R (2008) Spreading depolarizations occur in human ischemic stroke with high incidence. *Ann Neurol* 63:720-728.

Dreier JP, Major S, Manning A, Woitzik J, Drenckhahn C, Steinbrink J, Tolias C, Oliveira-Ferreira AI, Fabricius M, Hartings JA, Vajkoczy P, Lauritzen M, Dirnagl U, Bohner G, Strong AJ (2009) Cortical spreading ischaemia is a novel process involved in ischaemic damage in patients with aneurysmal subarachnoid haemorrhage. *Brain* 132:1866-1881.

Evans AM (2006) AMP-activated protein kinase and the regulation of Ca²⁺ signalling in O₂-sensing cells. *J Physiol* 574.1:113-123.

Fabricius M, Fuhr S, Bhatia R, Boutelle M, Hashemi P, Strong AJ, Lauritzen M (2005) Cortical spreading depression and peri-infarct depolarization in acutely injured human cerebral cortex. *Brain* 129:778-790.

Garriga-Canut M, Schoenike B, Qazi R, Bergendahl K, Daley TJ, Pfender RM, Morrison JF, Ockuly J, Stafstrom C, Sutula T, Roopra A (2006) 2-Deoxy-D-glucose reduces epilepsy progression by NRSF-CtBP-dependent metabolic regulation of chromatin structure. *Nat Neurosci* 9:1382–1387.

Hardie DG, Hawley SA, Scott JW (2006) AMP-activated protein kinase – development of the energy sensor concept. *J Physiol* 574.1:7-15.

Hardie DG, Scott JW, Pan DA, Hudson ER (2003) Management of cellular energy by the AMP-activated protein kinase system. *FEBS Letters* 546:113-120.

Kréneisz O, Benoit JP, Bayliss DA, Mulkey DK (2009) AMP-activated protein kinase inhibits TREK channels. *J Physiol* 587.24:5819-5830.

Love S (2003) Apoptosis and brain ischaemia. *Prog Neuropsychopharmacol Biol Psychiatry* 27:267-282.

- McCullough LD, Zeng Z, Li H, Landree LE, McFadden J, Ronnett GV (2005) Pharmacological inhibition of AMP-activated protein kinase provides neuroprotection in stroke. *J Biol Chem* 280:20493-20502.
- Newland PL, Yates P (2007) Nitroergic modulation of an oviposition digging rhythm in locusts. *J Exp Biol* 210:4448-4456.
- Potter WB, O’Riordan KJ, Barnett D, Osting SMK, Wagoner M, Burger C, Roopra A (2010) Metabolic regulation of neuronal plasticity by the energy sensor AMPK. *PLoS ONE* 5:e8996.
- Rodgers CI, Armstrong GAB, Shoemaker KL, LaBrie JD, Moyes CD, Robertson RM (2007) Stress preconditioning of spreading depression in the locust CNS. *PLoS ONE* 2:e1366.
- Rodgers CI, LaBrie JD, Robertson RM (2009) K⁺ homeostasis and central pattern generation in the metathoracic ganglion of the locust. *J Insect Physiol* 55:599-607.
- Rodgers CI*, Armstrong GAB*, Robertson RM (2010) Coma in response to environmental stress in the locust: A model for cortical spreading depression. *J Insect Physiol* (Epub ahead of print, doi:10.1016/j.jinsphys.2010.03.030).

Snider BJ, Gottron FJ, Choi DW (1999) Apoptosis and necrosis in cerebrovascular disease. *Ann N Y Acad Sci* 893:243-253.

Takano T, Tian G-F, Peng W, Lou N, Lovatt D, Hansen AJ, Kasischke KA, Nedergaard M (2007) Cortical spreading depression causes and coincides with tissue hypoxia. *Nat Neurosci* 10:754-762.

Chapter 5

5.1 General Discussion

Environmental stressors such as high temperature and low oxygen can have profound effects on the neuronal function and behavior of animals and thus are detrimental to survival. Locusts are poikilothermic animals that inhabit hot and arid environments where extremely high temperatures pose a challenge to the ability to reproduce and survive. Low oxygen conditions are also a natural hazard for locusts as high rainfall is intricately associated with development of individuals (Rainey, 1951; Pedgley, 1979; Stige et al. 2007). The ability of the locust to generate crucial motor patterns in a stressful environment depends on the mechanisms that compensate for external disturbances. In my thesis I examined the effects of various stresses on the central pattern generator responsible for controlling rhythmic ventilatory movements, the ventilatory central pattern generator (vCPG). The vCPG is crucial to protect as it is responsible for circulation of respiratory gases and delivery of oxygen directly to tissues and cells through the tracheal system of the locust. Failure and recovery of vCPG operation are unequivocal, which makes it an ideal system to measure and compare tolerance to various stresses. The overall objective of my thesis was to investigate the nature of stress-induced vCPG arrest in the context of K^+ ion changes surrounding the vCPG.

In the second chapter of my thesis I investigated whether or not spreading depression (SD)-like increases in extracellular potassium concentration ($[K^+]_o$) occurred exclusively

at the moment of vCPG arrest induced by high temperature stress (Robertson, 2004b). The abrupt all-or-none type rise in $[K^+]_o$ was not exclusive to hyperthermia-induced vCPG arrest in the locust, but could also be generated in response to anoxia (N_2 gas), ATP depletion (sodium azide, NaN_3), Na^+/K^+ -ATPase impairment (ouabain), and neuropile nano-injections of K^+ (Rodgers et al. 2007). SD-like $[K^+]_o$ increases occurred in the metathoracic ganglion (MTG) in response to two types of anoxia treatment: the semi-intact preparation was contained within a N_2 -filled chamber, or NaN_3 (mitochondrial blocker) was bath-applied in the same fashion as standard locust saline. The $[K^+]_o$ peaks induced by NaN_3 and anoxia were significantly higher than the peak $[K^+]_o$ induced by hyperthermia (NaN_3 peak: 85 ± 2 mM, Anoxia peak: 79 ± 3 mM, compared to 52 ± 2 mM during hyperthermia). Subsequent recovery of ventilatory motor patterning from the anoxic coma occurred if NaN_3 was flushed out with standard locust saline or if N_2 gas was cut off and air allowed to enter the chamber, and this was associated with restoration of $[K^+]_o$ to normal baseline levels. Maintenance of the K^+ equilibrium is largely attributed to Na^+/K^+ -ATPase activity and we tested the effect of Na^+/K^+ -ATPase inhibition using ouabain. Continuous bath application of 10^{-4} M ouabain demonstrated recurring $[K^+]_o$ events where the rise and fall of $[K^+]_o$ was associated with failure and recovery of the ventilatory motor pattern, respectively. Finally, we could also induce coma and associated SD-like increase in $[K^+]_o$ by delivering nano-injections of saline containing high KCl content directly into the ventilatory neuropile, which induced an abrupt $[K^+]_o$ surge once a threshold was reached. In this manner we were able to directly disturb E_k just enough to bring $[K^+]_o$ to threshold for an abrupt surge. The stress-induced comas described here and the associated abrupt all-or-none increases in $[K^+]_o$ in the

locust MTG share many of the major characteristics of SD in mammalian cortical tissue, at least with respect to $[K^+]_o$. The major aim of my second chapter was to describe the occurrence of these events in the locust and their resemblance to SD-like events that occur in mammalian cortical tissue, termed cortical SD (CSD).

SD is a widely studied phenomenon due to its role in mammalian pathologies such as migraine, ischemic injury or stroke, and seizures. $[K^+]_o$ changes in the locust MTG are strikingly similar to those that occur during SD in mammalian cortical tissue, both in terms of the speed of $[K^+]_o$ increase and the amplitude of $[K^+]_o$ increase. There was not a gradual increase in $[K^+]_o$ in response to cellular stressors in the locust, but an abrupt, all-or-none type increase characteristic of mammalian SD-like events. SD-like events in the locust could be induced by the same stressors that induce SD in cortical gray matter. The hyperthermic SD-like event in the locust is very similar to SD-like events in the rat hippocampus during hyperthermia (Wu and Fisher, 2000). Notably, hyperthermic SDs in rat hippocampal slices were associated with an abrupt, reversible rise in $[K^+]_o$ to a mean peak of 43 ± 10.9 mM (from a mean baseline of 6.4 ± 0.2 mM) (Wu and Fisher, 2000). In the locust, $[K^+]_o$ increased from a baseline level of 10 mM to ~50 mM at the moment of heat-induced vCPG arrest. $[K^+]_o$ recovered to baseline levels when the heater was turned off and the temperature was allowed to return to room levels and this was associated with vCPG recovery. SD in the mammalian nervous system can also be evoked by mitochondrial blockers, KCl application, and inhibition of Na^+/K^+ -ATPase activity (Leão, 1944; Leão and Morrison, 1945; Balestrino et al. 1999; Müller and Ballanyi, 2003). The Na^+/K^+ -ATPase is essential for proper neuronal activity due to its

role in maintaining ionic concentration gradients and targeting of the Na^+/K^+ -ATPase using ouabain has been widely used to induce SD in cortical tissue (Haglund and Schwartzkroin, 1990; Balestrino et al. 1999; Menna et al. 2000; Xiong and Stringer, 2000; Leis et al. 2005). In the second chapter of my thesis I showed that continuous bath application of ouabain interestingly elicited repetitive SD-like events in the locust MTG. Prodromal spikes are also a characteristic feature during mammalian SD-like events consisting of a short burst of action potentials or intense synaptic noise at the leading edge of SD. This excitation is likely due to neuron membrane depolarization from increased $[\text{K}^+]_o$. Unpatterned bursts of spikes frequently occurred at the leading edge of SD-like events induced by all of the above cellular stressors in the locust (Rodgers et al. 2007).

One of the key features of CSD is that neurons completely depolarize, and the depolarization and associated synaptic activity cessation propagate across cortical gray matter. The extent of neuronal depolarization during SD-like events in the locust has also been investigated using sharp intracellular microelectrodes to record neuronal activity within the MTG concurrently with recordings of $[\text{K}^+]_o$ (Armstrong et al. 2009). During SD-like events evoked by NaN_3 , locust ventilatory neurons depolarized modestly by about 13 mV on average coinciding with a surge in $[\text{K}^+]_o$ (Armstrong et al. 2009). This modest depolarization is in contrast to that of neurons in the mammalian CNS that depolarize completely resulting in a membrane potential of 0 mV (Collewyn and Van Harreveld, 1966). There was also a significant decrease in input resistance in neurons during SD-like events induced by NaN_3 in the locust (Armstrong et al. 2009). The

decrease in input resistance is likely caused by opening of voltage-dependent and other membrane channels during SD-like events. In the second chapter of my thesis we were also able to show that similar to SD-like events in mammalian cortical tissue, waves of $[K^+]_o$ propagate within the locust nervous system (Rodgers et al. 2007). In the locust there was a mean SD-like propagation speed of 2.4 mm/min within the MTG. In mammalian brain tissue grey matter contains neural cell bodies, whereas white matter mostly contains myelinated axon tracts. In the locust, waves of $[K^+]_o$ propagated locally within the MTG (grey matter) and were unable to propagate through the connectives (white matter) to the mesothoracic ganglion and vice versa, an observation that is consistent with SD phenomena occurring in mammals (Van Harreveld et al. 1956). The mechanism of SD wave propagation is poorly understood. The initiation of CSD waves can be prevented using NMDA receptor antagonists and gap junction inhibitors, but once a propagating wave of CSD is evoked it is insensitive to a number of NMDA receptor antagonists and channel inhibitors (Takano et al. 2007). It is likely that the generation of SD-like events in response to these stressors in both mammals and locusts is caused by the inability to provide enough energy required to maintain ionic gradients. The forward movement of CSD could be driven by K^+ and hypoxia rather than opening of specific channels or activation of transmitter systems. One theory is that the increased $[K^+]_o$ in combination with low energy allows $[K^+]_o$ to diffuse forward along its concentration gradient and propagate across cortex (due to the inability to clear $[K^+]_o$) (Takano et al. 2007). Studies of SD in vertebrate cortical tissue have revealed the possible involvement of intercellular gap junctions as a mechanism of propagation (Nedergaard et al. 1995; Largo et al. 1997; Thompson et al. 2006). Glial cells are involved in ion homeostasis,

function, and development of the insect brain (Kretzschmar and Pflugfelder, 2002) and thus similar mechanisms of SD propagation may exist in the locust MTG. The mechanism of $[K^+]_o$ propagation and the role of glia during locust SD are currently being investigated.

We were able to manipulate SD-like events in the locust using drugs that act on ion channels and cellular signaling pathways. Tetrodotoxin (TTX), a Na^+ channel blocker, and tetraethylammonium chloride (TEA), a K^+ channel blocker, have been used in studies of mammalian CSD and we have seen similar effects during locust SD-like events. SD-like events in the locust are delayed by Na^+ channel block using TTX and diminished by K^+ channel block using TEA (Rodgers et al. 2007). In the third chapter of my thesis I also showed that K^+ channel inhibition using TEA suppressed the onset and decreased the amplitude of ouabain-induced repetitive $[K^+]_o$ waves (Rodgers et al. 2009). These results further demonstrate the similarity between SD-like events that occur in locust neural tissue and mammalian cortical tissue. The effect of activating and inhibiting the NO/cGMP/PKG pathway on the propensity to generate and the severity of SD-like events occurring in the locust CNS has been investigated (Armstrong et al. 2009). Pre-treatment with KT5823, a PKG antagonist, decreased the length of SD-like events evoked by nanoinjections of KCl, whereas pre-treatment with 8-Br-cGMP, a PKG agonist, lengthened the duration of the SD-like event (Armstrong et al. 2009). In addition, PKG inhibition using KT5823 shortened the length of time taken for the vCPG to recover, whereas PKG activation resulted in a longer time to recovery of vCPG activity following

a KCl-induced SD-like event (Armstrong et al. 2009). These data show that the duration of the SD-like event can be altered by differing levels of PKG activity.

The vCPG displays a robust response to HS preconditioning and I was also interested in the effect of HS on $[K^+]_o$ dynamics during stress. A HS pre-treatment of 3 hours at 45°C resulted in an improved ability of the vCPG to withstand and recover from sustained high temperatures (Newman et al. 2003). These established results provided a foundation for an investigation of the effect of HS pre-treatment on the onset and severity of $[K^+]_o$ changes associated with vCPG arrest. In the second chapter of my thesis I found that SD-like events in the locust MTG could be preconditioned by prior HS treatment.

Downregulation of K^+ currents has been shown to mimic the thermoprotective effects of a prior HS treatment and is protective by prolonging the duration of action potentials and reducing $[K^+]_o$ accumulation (Ramirez et al. 1999; Wu et al. 2001). I hypothesized that HS-induced protection is due to stabilizing $[K^+]_o$ during stress, possibly via Na^+/K^+ -ATPase activation. HS treatment did not abolish or reduce the degree of SD-like increases in $[K^+]_o$ in the locust but delayed the onset of the heat-induced SD-like event. The delayed onset of the SD-like event allowed for continued vCPG operation at elevated temperature in HS-treated animals. The rate of $[K^+]_o$ clearance following hyperthermic arrest was examined to determine if preconditioning improved $[K^+]_o$ stabilization, and the role of the Na^+/K^+ -ATPase in this preconditioning was also tested. HS-treated locusts showed an increase in $[K^+]_o$ clearance rates, which was correlated with a faster vCPG recovery. There were no changes in steady-state Na^+/K^+ -ATPase activity within the MTG, i.e. the ouabain-sensitive fraction of total Na^+/K^+ -ATPase activity, following HS

pre-treatment. This suggests that the increased rate of $[K^+]_o$ clearance was not linked to changes in total Na^+/K^+ -ATPase activity within the MTG, however a protective effect of HS on the Na^+/K^+ -ATPase has not been ruled out. Measurements of Na^+/K^+ -ATPase activity in the locust MTG did not take into account the possibility of trafficking of pumps in neuronal and glial membranes. The heat shock protein HSP70 has a thermoprotective effect on mammalian muscle sarco/endoplasmic reticulum Ca^{2+} -ATPase (Tupling et al. 2004) and thus HS-induced upregulation of this protein may have a protective effect on Na^+/K^+ -ATPase pump activity. HSP70 is believed to play a critical role in recovery and survival after HS (Mayer and Bukau, 1998) and a two-fold increase in expression of HSP70 occurs in locust fat body after being exposed to HS (Qin et al. 2003). HSP70 is synthesized in all cells following ischemia and heat shock, and has been shown to protect the brain against injury produced by ischemia and seizures (Yenari et al. 1998). As a result of ischemia, denatured proteins initiate the process of HSP70 synthesis. Directly outside of the ischemic core, HSP70 promotes the survival of glia and neurons in the area of mild to moderately ischemic tissue where peri-infarct depolarizations (PIDs) occur (Sharp et al. 1999). Thus, HSP70 reduces neuronal damage in the wake of CSD and may have similar protective effects when induced by HS in the locust. Currently the nature of the preconditioning mechanism in the locust is unresolved.

In cortical tissue compromised by stroke or injury, PIDs are 'spontaneous' spreading depression waves that propagate through the penumbra region of cortical infarcts into normally healthy tissue thereby increasing the final infarct volume (Fabricius et al. 2005).

These repeated spreading depolarizations have been shown to occur during ischemic stroke in the human brain (Fabricius et al. 2005; Dohmen et al. 2008; Dreier et al. 2009). PIDs increase the metabolic requirements for recovery from CSD and lead to an increase in final infarct size that is directly related to the number of PIDs (Dohmen et al. 2008). We suggest that the ouabain-induced repetitive or ‘spontaneous’ SD-like events in the locust MTG represent a good model for investigating PIDs that occur in mammalian cortical tissue. In the second and third chapters of my thesis I showed that during a continuous bath application of 10^{-4} M ouabain, $[K^+]_o$ returns to baseline and there is recovery of motor pattern generation following each $[K^+]_o$ event (Rodgers et al. 2007, 2009). This suggests that 10^{-4} M ouabain does not cause complete inhibition of Na^+/K^+ -ATPase and bath-application of higher doses demonstrates a concentration-dependence to the effect of ouabain. In the third chapter I further investigated the spontaneous and repetitive nature of ouabain-induced SD-like events in the locust. In comparison to 10^{-4} M ouabain, 10^{-5} M ouabain had no significant effect, while 10^{-3} M ouabain magnified its effects. 10^{-3} M ouabain shortened the time to onset of the initial $[K^+]_o$ surge, gradually increased baseline $[K^+]_o$ following each $[K^+]_o$ surge, prolonged surge duration, diminished $[K^+]_o$ surge amplitude, and motor pattern recovery was significantly less likely following a surge in preparations treated with 10^{-3} M ouabain compared to 10^{-4} M ouabain (Rodgers et al. 2009). Use of ouabain doses greater than 10^{-4} M (10^{-3} M, 10^{-2} M) result in a gradual increase in the baseline level of $[K^+]_o$ such that a “ceiling” level of $[K^+]_o$ is reached where eventually $[K^+]_o$ does not return to baseline following surges and the motor pattern does not recover. This may be equivalent to the effect of repeated PIDs

expanding the penumbral region of affected cortical tissue, further contributing to energy compromise and permanent tissue damage.

Interventional strategies such as NMDA receptor antagonists and hypothermia have been shown to decrease the incidence of CSD and PIDs in cortical tissue (Chen et al. 1993). In a study of temperature modulation of cerebral depolarization during focal cerebral ischemia in rats, animals subjected to hypothermia exhibited no infarct volume in comparison to normothermic and hyperthermic animals that had 10.2 +/- 12.3% and 36.5 +/- 3.4% infarct volumes, respectively (Chen et al. 1993). Another interesting result worth mentioning but that is not included in my thesis is that sharp SD-like rises in $[K^+]_o$ also occurred in response to hypothermic stress in the locust (Rodgers et al. 2010). In an initial set of experiments the temperature of the superfusing saline was decreased to 5°C, which induced cessation of motor pattern generation but was not sufficient to induce an abrupt $[K^+]_o$ surge in the majority of cases (N=10). This is an interesting result as it demonstrates that in this case vCPG arrest is independent of the SD-like event and is not the result of the wave in $[K^+]_o$. In contrast to vCPG arrest in response to hyperthermia and the metabolic stressors described above, the lack of operation of the vCPG during hypothermia may be the result of lower O₂ demand rather than a shutdown of neural function. The mean change in $[K^+]_o$ ($\Delta[K^+]_o$) from the beginning of the cold ramp to arrest of motor pattern generation (the point at which continuous bursting could no longer be detected) was 3mM. This is in comparison to a mean $\Delta[K^+]_o$ of 16mM from the beginning of a heat ramp to hyperthermia-induced vCPG arrest and a mean $\Delta[K^+]_o$ of 44mM from the beginning of a heat ramp to the plateau of the $[K^+]_o$ increase. The small

increase in $[K^+]_o$ with decreased internal temperature may be due to dysregulation of the Na^+/K^+ -ATPase, but not to the point of complete loss of the K^+ gradient. Due to the inability to bring the internal temperature of preparations below $5^\circ C$, a SD-like surge in $[K^+]_o$ was associated with vCPG cessation during hypothermia in only two out of twelve preparations. In these cooling experiments, the average temperature at vCPG arrest was $9.4^\circ C$ and the average temperature at subsequent recovery was $14.7^\circ C$. In a separate experiment, the locust thoracic ganglia were removed from the preparation and placed on a cooling plate during $[K^+]_o$ measurement within the MTG, enabling a temperature decrease to $<5^\circ C$ which was sufficient to bring $[K^+]_o$ to threshold for induction of an abrupt surge (Armstrong, unpublished).

An interesting hypothesis is that SD-like events in the locust can be considered an adaptive strategy to conserve energy and prevent neuronal hyperexcitation (Walter and Nelson, 1975; Rodgers et al. 2007, 2009). I suggested this in the second and third chapters of my thesis, but did not provide hard evidence supporting this hypothesis. Unlike mammalian neurons during CSD, locust ventilatory neurons only partially depolarized during SD-like events (Armstrong et al. 2009) and neuronal operation always recovered following removal of the applied stress, even after ATP depletion using NaN_3 (Rodgers et al. 2007). The frequency and duration of the recovered ventilatory motor pattern became more variable following each $[K^+]_o$ event during ouabain-induced repetitive SD (Rodgers et al. 2007). Although the recovered motor pattern following anoxia was robust, it was not identical to the pre-stress motor pattern, and as in CSD the

likelihood and quality of recovery may depend on the severity of the O₂ and energy deprivation, however this has not been investigated in the locust. vCPG operation post-recovery from arrest induced by severe cellular stressors such as anoxia and NaN₃ that result in energy deprivation has not been quantified. CSD in mammals is associated with local tissue hypoxia and neuronal swelling due to energy consumption that is not met with adequate oxygen supply and SD is linked with drops in ATP availability even in the absence of O₂ depletion, resulting in cell death (Thompson et al. 2006; Takano et al. 2007). There is much evidence that vCPG arrest and the abrupt SD-like increases in [K⁺]_o in the locust MTG occur before irreversible cellular collapse (Rodgers et al. 2007). A continued increase in temperature beyond hyperthermic vCPG arrest and the associated SD-like event resulted in a second, higher [K⁺]_o plateau of 100mM on average. When the heat stress was removed, [K⁺]_o remained elevated and motor pattern generation failed to recover (Rodgers et al. 2007). Interestingly, there was no correlation between ganglionic ATP levels and the occurrence of stress-induced motor pattern arrest and subsequent recovery in the locust (Rodgers et al. 2007). These results suggest that the trigger for SD-like events in the locust is not a fall in ATP (i.e. energetic stress), but the ATP measure by itself does not provide a completely accurate account of cellular metabolic status and changes in adenylates such as AMP have not been tested. The energy status of a cell can change and trigger signaling pathways without measurable effects on ATP (Lindsley and Rutter, 2004; Hardie et al. 2006). Thus, the ATP measure by itself may not provide an accurate account of cellular metabolic status. Further evidence for an adaptive role stems from the fact that SD-like events in the locust are plastic and can be manipulated in many different ways. As discussed above, SD-like events in the locust were delayed by Na⁺

channel block using TTX, diminished by K⁺ channel block using TEA (Rodgers et al. 2007), suppressed by inhibition of the NO/cGMP/PKG pathway and exacerbated by its activation (Armstrong et al. 2009), and HS preconditioning resulted in an increased rate of [K⁺]_o clearance associated with recovery of motor pattern generation (Rodgers et al. 2007). As suggested above, SD-like events in response to stress in the locust could be interpreted as a strategy to conserve energy by entering a state of coma during which energy-utilizing mechanisms to restore ion gradients are suspended (Rodgers et al. 2007). Regulatory mechanisms that monitor cellular metabolic state such as the AMP-activated protein kinase (AMPK) cascade could be triggered well before ATP levels are depleted, signaling metabolic stress before complete energy deprivation.

The AMPK is a universal signaling molecule of all eukaryotic cells that reflects cellular energy status (Hardie et al. 2003). AMPK is activated by any stress that negatively affects ATP levels such as heat shock, metabolic inhibitors (arsenite or oligomycin), hypoxia or ischemia, and glucose deprivation (Hardie et al. 2003). AMPK is also allosterically activated by increased cellular AMP and is involved in a sophisticated regulatory system that improves cellular energy levels by stimulating ATP production (Hardie et al. 2003). There was no correlation between ganglionic ATP levels and the occurrence of stress-induced motor pattern arrest and subsequent recovery in the locust (Rodgers et al. 2007), however metabolic stresses can trigger the activation of signaling pathways before changes in ATP can be detected (Evans, 2006; Hardie et al. 2006). AMPK activation prior to complete energy depletion would explain the lack of

correlation between SD-like events and ATP levels within the locust MTG, and would also explain the ability of the vCPG to recover operation following NaN_3 -induced shutdown. In the fourth chapter of my thesis I tested the hypothesis that stress-induced vCPG arrest and subsequent recovery results in changes to the nature of the ventilatory motor pattern, and that these changes represent a strategy to conserve energy in a trade-off with performance. I examined the potential role of AMPK in this switch using the AMPK activator 5-aminoimidazole-4-carboxamide-1-riboside (AICA-riboside, or AICAR) and inhibitor compound-C. AICAR is rapidly transported into cells and phosphorylated to form the AMP mimetic AICA-ribotide (ZMP) which allosterically activates AMPK. AICAR has been used in combination with the anti-diabetic drug metformin, which does not deplete ATP and activates AMPK by an AMP-independent mechanism (Hardie et al. 2003; Lindsley and Rutter, 2004). Treatment of cells with the AMPK activator AICAR causes many of the same phenotypes as exercise, glucose deprivation and hypoxia. I hypothesized that AMPK activation using AICAR would mimic the effect of NaN_3 on the ventilatory motor pattern.

I found that NaN_3 caused an initial increase in ventilatory rate in a concentration-dependent manner, and there was an interesting correlation such that early vCPG arrest induced by higher NaN_3 doses (10^{-3} M, 5×10^{-4} M) was associated with shorter times to recovery (Rodgers et al. unpublished). This supports the hypothesis that the triggered event is adaptive and represents a neural off-switch to conserve energy. Ventilatory rate gradually decreased over time following recovery from chemical anoxia using NaN_3 and the associated SD-like event. Both 10^{-3} M and 10^{-2} M AICAR doses caused an immediate

increase in ventilatory rate, however 10^{-2} M AICAR had subsequent multiple effects on the ventilatory rhythm, some resembling the switch to a reduced ventilatory frequency following recovery from NaN_3 -induced arrest. Application of 10^{-4} M compound-C did not alter the ventilatory pattern when applied in the absence of stress. Interestingly, compound-C applied during recovery from NaN_3 -induced arrest and during AICAR-induced disruption of the motor pattern gradually returned burst durations and periods to Control values, and glucose mimicked the effects of compound-C (Rodgers et al. unpublished). Thus, it is likely that AICAR induced AMPK activation in this study and compound-C reversed the effects of AICAR by inhibiting AMPK activation.

If AMPK is activated within the locust MTG during cellular stress it is equally likely that this activation would be protective or damaging. In cases of neuronal energy compromise, over-activation of cellular pathways that sense drops in ATP may lead to further energy crisis and cell death (McCullough et al. 2005). Also, treatment with NaN_3 may have many secondary consequences unrelated to AMPK activation, and compound-C may be blocking these effects rather than directly inhibiting AMPK. It is also important to note that AICAR and compound-C do not specifically target AMPK. AICAR is converted to ZMP which allosterically activates AMPK, and ZMP is an effector of other enzymes that are regulated by AMP such as phosphorylase and fructose-1,6-bisphosphatase (Hardie et al. 2003). AICAR has numerous other effects in cells, including induction of adenosine (Gadalla et al. 2004). AMPK activation with AICAR has protective effects in cultured hippocampal neurons (Culmsee et al. 2001) and ischemic cardiomyocytes (Kingma et al. 1994) as well as detrimental effects in numerous

cell lines, including hepatocytes (Meisse et al. 2002), neuroblastoma cells (Garcia-Gil et al. 2003; Jung et al. 2004), and mouse pancreatic β -cells (Kefas et al. 2003), suggesting that the effects of AICAR are dependent on both the cell type and model system used (McCullough et al. 2005). Use of AICAR to activate AMPK coincides with a drop in mean arterial pressure after ischemic insults in mice, which may explain effects on stroke damage independent of the effects of AMPK (McCullough et al. 2005). In our study compound-C reversed the effects of AICAR and thus it is likely that AICAR induced AMPK activation.

The AMPK is a heterotrimeric complex with a catalytic α subunit and regulatory β and γ subunits (Hardie and Hawley, 2001). The α subunit contains a serine/threonine kinase domain (T172) and a carboxy-terminal regulatory domain. Activation of AMPK requires phosphorylation of T172 that is catalysed by phosphorylation by an upstream kinase LKB1, as well as allosteric binding of AMP. The γ subunit contains four cystathionine- β -synthase (CBS) domains that play a role in allosterically binding AMP and ATP. The β subunit acts as a scaffold for binding the other two subunits and contains a glycogen-binding domain. AMPK activation is repressed by high cellular glycogen in muscle, suggesting that AMPK is a glycogen sensor in addition to sensing AMP and ATP (Hardie et al. 2003). The glycogen-binding domain in the β subunits of AMPKs is conserved across all eukaryotes and has been implicated in the regulation of AMPK by glycogen (Hardie et al. 2003). In chapter four I showed that glucose mimicked the effects of compound-C post-recovery from NaN_3 -induced arrest by returning ventilatory burst durations and periods to Control values (Rodgers et al. unpublished). The activation of

AMPK by reduced energy levels as a result of NaN_3 treatment could have been suppressed by glucose, and the ultimate effect of increased glucose on AMPK may involve the glycogen-binding domain.

Ouabain-induced SD-like events in the locust CNS were suppressed by inhibition of AMPK and exacerbated by its activation (Rodgers et al. unpublished). There was a modest (5 mM) increase in $[\text{K}^+]_o$ during pre-treatment with 10^{-2} M AICAR. Given that AMPK switches off energy-using pathways, it is conceivable that the Na^+/K^+ -ATPase is a target of AMPK. Inhibition of the Na^+/K^+ -ATPase by AMPK would also explain the decreased time to onset of ouabain-induced SD-like events when ouabain was applied in combination with AICAR. Nitric oxide synthase (NOS) is also a target protein for AMPK (Almeida et al. 2004). Neuronal NOS (nNOS) is phosphorylated by AMPK and activated (Chen et al. 1999) and there is evidence that NOS activity is required for the effects of AMPK on glucose uptake in muscle (Fryer et al. 2000). Our lab has shown that activation of the NO/cGMP/PKG pathway exacerbates ouabain-induced SD and inhibition of this pathway suppresses SD-like events in the locust (Armstrong et al. 2009). An interesting avenue for future research would be to determine if and how the AMPK pathway interacts with the NO/cGMP/PKG pathway. One possibility is that stress-induced NO production in the locust nervous system leads to activation of both PKG and AMPK and the generation of SD-like events. In the fourth chapter of my thesis I also showed that application of compound-C following an initial ouabain-induced SD-like event suppressed subsequent $[\text{K}^+]_o$ waves which appeared to be aborted, suggesting that AMPK inhibition may be involved in $[\text{K}^+]_o$ propagation throughout the ganglion.

Since the initial intriguing discovery that ouabain induces repetitive SD-like events in the locust, ouabain-induced SD has become a popular control group for many investigations of the mechanisms involved in locust SD. It seems clear that SD-like events in mammals are triggered by positive feedback processes involving an initial ionic disturbance reaching a threshold and caused by neuronal overexcitation or by treatments or conditions that impair ionic homeostasis (Grafstein, 1956; van Harreveld, 1978; Balestrino et al. 1999; Somjen, 2001; Rodgers et al. 2007). A model describing a possible mechanism for the abrupt increase and decrease in $[K^+]_o$ in response to cellular stressors in the locust MTG was proposed in the third chapter of my thesis and a subsequent paper from our lab (Rodgers et al. 2009; Armstrong et al. 2009). The rationale behind this model is that the repetitive nature of $[K^+]_o$ surges induced by ouabain depends on the balance of $[K^+]_o$ accumulation and clearance in the restricted space of the locust MTG. Extracellular K^+ concentration depends on processes of accumulation (K^+ conductances) and counteracting processes of clearance (transport processes including the Na/K pump and glial buffering/siphoning). At rest these balance to maintain a constant extracellular concentration. When Na/K pumps are inhibited by ouabain, the ability of neurons and glia to remove accumulating $[K^+]_o$ from the extracellular space is impaired and $[K^+]_o$ accumulation results during neuronal activity. Eventually, the increase in $[K^+]_o$ is sufficient to decrease the equilibrium potential for potassium (E_k), resulting in membrane depolarization (V_m). Depolarization results in the opening of voltage-gated K^+ and Na^+ channels, further increasing activity and $[K^+]_o$ resulting in further depolarization. This positive feedback cycle could give rise to the explosive rise in $[K^+]_o$ at the leading

edge of the surge without invoking special channels. The surge occurs when the build-up in $[K^+]_o$ is already sufficient to shift the equilibrium potential and depolarize membranes. Other factors such as HS pre-treatment, PKG activation or inhibition, and AMPK activation or inhibition shift the balance towards $[K^+]_o$ accumulation or $[K^+]_o$ clearance. Arrest of neuronal activity and electrical activity silence once $[K^+]_o$ reaches its peak may allow uninhibited Na^+/K^+ -ATPases to clear excess K^+ from the extracellular space thereby restoring E_k and allowing recovery of neuronal function.

The discovery that SD-like events occur in the locust MTG was fortuitous as it has allowed an investigation of mechanisms involved in SD-like events while neural circuits are intact and functioning. Given the convenience of the locust preparation and the accessibility of an intact, functioning nervous system, experiments can be conducted with ease and studies on the role of glia, ion channels, and energy-sensing pathways such as the AMP-activated protein kinase (AMPK) pathway in SD-like events are currently underway. It is our hope that our findings will be useful for those investigating the treatment of mammalian disorders such as seizures and migraine. At the very least, much knowledge has been gained over the past few years about the mechanisms involved in neural circuit arrest in response to stress. In addition to the many benefits of the locust model for studying SD there are limitations to the extent to which we can draw comparisons to CSD. For example, stroke and ischemia in vertebrate brain tissue are induced via oxygen/glucose deprivation by occluding blood vessels and arteries thereby cutting off blood flow. The locust nervous system lacks vasculature and thus the effects

of oxygen and energy stress have a different type of complexity than in mammalian brain tissue. This could be the reason why locust neurons recover from anoxia-induced SD whereas mammalian neurons do not recover from anoxic or terminal depolarization. Important questions remain. First, why is the level of depolarization in locust ventilatory interneurons modest compared to that of mammalian cortical neurons during SD and does this account for the ability of locusts to survive long periods of anoxic coma? Second, which physiological properties are crucial for preventing tissue damage from hypoxia/low sugar in the locust? Clearly the locust is an appropriate and interesting experimental animal for addressing this question. Third, do locust SD-like events represent an adaptive strategy to tolerate severe stresses? Fourth, given that locusts are dangerous pests how can SD be induced more easily to immobilize these animals? Lastly, to what extent are the pathways and mechanisms for HS-induced protection in the locust shared among other eukaryotes?

5.2 Summary

- 1) Locusts enter comas in response to stress during which neural and muscular systems shut down until the stress is removed.
- 2) Stress-induced arrest of vCPG operation is associated with SD-like events in the locust MTG that closely resemble CSD.
- 3) Locust SD-like events can be induced by ATP depletion, anoxia, Na⁺/K⁺-ATPase impairment and neuropile injections of high [K⁺] saline at normal temperature as well as hyperthermia.
- 4) SD-like events in the locust are characterized by large increases in [K⁺]_o from a baseline of ~10 mM to peaks of 52±2 mM (hyperthermia), 85±2 mM (sodium azide, NaN₃), and 79±3 mM (anoxia) that propagate within the MTG.
- 5) Following the hyperthermic SD-like event, [K⁺]_o increases to a second higher plateau of about 100 mM when temperature is increased to ~60°C and vCPG recovery is precluded.
- 6) The hyperthermic [K⁺]_o event was delayed by Na⁺ channel block using TTX and diminished by K⁺ channel block using TEA.
- 7) Stress-induced arrest of the vCPG and subsequent recovery were not linked to changes in MTG ATP levels and HS preconditioning did not increase ATP levels.
- 8) HS pre-treatment and ouabain treatment affected baseline [K⁺]_o in the MTG in the absence of additional stress.
- 9) There was an interesting trade-off in our measures of thermotolerance of ventilatory pattern generation such that early failure (i.e. low failure temperature) was associated with shorter times to recovery.
- 10) A prior HS treatment resulted in a delayed hyperthermic [K⁺]_o event and an increased rate of [K⁺]_o clearance associated with vCPG recovery.
- 11) The HS-induced increased rate of [K⁺]_o clearance was not linked to changes in ATP levels or total Na⁺/K⁺-ATPase activity within the MTG.
- 12) Na⁺/K⁺-ATPase inhibition using ouabain elicits repetitive [K⁺]_o events in a concentration-dependent manner.
- 13) 10⁻³ M ouabain progressively increased non-surge [K⁺]_o, decreased peak [K⁺]_o, diminished [K⁺]_o surge amplitude, and decreased the probability of motor pattern recovery following a [K⁺]_o surge compared to 10⁻⁴ M ouabain.

- 14) TEA decreased the proportion of preparations that produced had at least one $[K^+]_o$ event, delayed the onset of $[K^+]_o$ events, and decreased the amplitude of $[K^+]_o$ events induced by ouabain.
- 15) I suggest that the repetitive nature of $[K^+]_o$ surges induced by ouabain depends on the balance of $[K^+]_o$ accumulation and clearance in the restricted space of the locust MTG.
- 16) Ventilatory rate gradually decreased following recovery from chemical anoxia using sodium azide (NaN_3) and the associated SD-like event.
- 17) Application of heat following recovery from NaN_3 -induced arrest returned the ventilatory motor pattern to Control values, indicating that chemical anoxia does not cause permanent damage to the vCPG.
- 18) Activation of AMPK in non-stressed preparations using 10^{-3} M AICAR caused an immediate increase in ventilatory rate.
- 19) Treatment with 10^{-2} M AICAR had multiple effects on the ventilatory rhythm, some resembling the recovered motor pattern following NaN_3 -induced arrest.
- 20) AMPK inhibition using 10^{-4} M compound-C during recovery from NaN_3 -induced arrest and during AICAR-induced disruption of the motor pattern gradually returned burst durations and periods to Control values.
- 21) Glucose application mimicked the effects of compound-C.
- 22) Ouabain-induced SD-like events in the locust CNS were suppressed by inhibition of AMPK and exacerbated by its activation.
- 23) Application of compound-C following initiation of ouabain-induced SD-like events aborted subsequent $[K^+]_o$ surges, suggesting that AMPK inhibition may be involved in $[K^+]_o$ propagation.
- 24) We provide evidence that AMPK activation is involved in recovery from SD-like events, and we suggest that this may be a mechanism to conserve energy and prevent permanent neuronal damage in response to severe stressors.

5.3 References

Almeida A, Moncada S, Bolaños JP (2004) Nitric oxide switches on glycolysis through the AMP protein kinase and 6-phosphofructo-2-kinase pathway. *Nat Cell Biol* 6:45-51.

Armstrong GAB, Rodgers CI, Money TGA, Robertson RM (2009) Suppression of spreading depression-like events in locusts by inhibition of the NO/cGMP/PKG pathway. *J Neurosci* 29:8225-8235.

Balestrino M, Young J, Aitken PG (1999) Block of (Na⁺,K⁺)ATPase with ouabain induced spreading depression-like depolarization in hippocampal slices. *Brain Res* 838:37-44.

Chen Q, Chopp M, Bodzin G, Chen H (1993) Temperature modulation of cerebral depolarization during focal cerebral ischemia in rats: correlation with ischemic injury. *J Cereb Blood Flow Metab* 13:389-394.

Chen ZP, Mitchelhill KI, Michell BJ, Stapleton D, Rodriguez-Crespo I, Witters LA, Power DA, Ortiz de Montellano PR, Kemp BE (1999) AMP-activated protein kinase phosphorylation of endothelial NO synthase. *FEBS Lett* 443:285-9.

Collewijn H, Van Harreveld A (1966) Membrane potential of cerebral cortical cells during spreading depression and asphyxia. *Exp Neurol* 15:425-436.

Culmsee C, Monnig J, Kemp BE, Mattson MP (2001) AMP-activated protein kinase is highly expressed in neurons in the developing rat brain and promotes neuronal survival following glucose deprivation. *J Mol Neurosci* 17:45-58.

Dohmen C, Sakowitz OW, Fabricius M, Bosche B, Reithmeier T, Ernestus R-I, Brinker G, Dreier JP, Woitzik J, Strong AJ, Graf R (2008) Spreading depolarizations occur in human ischemic stroke with high incidence. *Ann Neurol* 63:720-728.

Dreier JP, Major S, Manning A, Woitzik J, Drenckhahn C, Steinbrink J, Tolias C, Oliveira-Ferreira AI, Fabricius M, Hartings JA, Vajkoczy P, Lauritzen M, Dirnagl U, Bohner G, Strong AJ (2009) Cortical spreading ischaemia is a novel process involved in ischaemic damage in patients with aneurysmal subarachnoid haemorrhage. *Brain* 132:1866-1881.

Evans AM (2006) AMP-activated protein kinase and the regulation of Ca²⁺ signalling in O₂-sensing cells. *J Physiol* 574.1:113-123.

Fabricius M, Fuhr S, Bhatia R, Boutelle M, Hashemi P, Strong AJ, Lauritzen M (2005) Cortical spreading depression and peri-infarct depolarization in acutely injured human cerebral cortex. *Brain* 129:778-790.

Fryer LGD, Hajdich E, Rencurel F, Salt IP, Hundal HS, Hardie DG, Carling D (2000) Activation of glucose transport by AMP-activated protein kinase via stimulation of nitric oxide synthase. *Diabetes* 49:1978-1985.

Gadalla AE, Pearson T, Currie AJ, Dale N, Hawley SA, Sheehan M, Hirst W, Michel AD, Randall A, Hardie DG, Frenguelli BG (2004) AICA riboside both activates AMP-activated protein kinase and competes with adenosine for the nucleoside transporter in the CA1 region of the rat hippocampus. *J Neurochem* 88:1272-1282.

Garcia-Gil M, Pesi R, Perna S, Allegrini S, Giannecchini M, Camici M, Tozzi MG (2003) 5-Aminoimidazole-4-carboxamide riboside induces apoptosis in human neuroblastoma cells. *Neuroscience* 117:811-820.

Grafstein B (1956) Mechanism of spreading cortical depression. *J Neurophysiol* 19:154-171.

Haglund MM, Schwartzkroin PA (1990) Role of Na-K pump potassium regulation and IPSPs in seizures and spreading depression in immature rabbit hippocampal slices. *J Neurophysiol* 63:225-239.

Hardie DG, Hawley SA (2001) AMP-activated protein kinase: the energy charge hypothesis revisited. *BioEssays* 23, 1112-1119.

Hardie DG, Hawley SA, Scott JW (2006) AMP-activated protein kinase – development of the energy sensor concept. *J Physiol* 574.1:7-15.

Hardie DG, Scott JW, Pan DA, Hudson ER (2003) Management of cellular energy by the AMP-activated protein kinase system. *FEBS Letters* 546:113-120.

Jung JE, Lee J, Ha J, Kim SS, Cho YH, Baik HH, Kang I (2004) 5-Aminoimidazole-4-carboxamide-ribonucleoside enhances oxidative stress-induced apoptosis through activation of nuclear factor-kappaB in mouse Neuro 2a neuroblastoma cells. *Neurosci Lett* 354:197-200.

Kefas BA, Cai Y, Ling Z, Heimberg H, Hue L, Pipeleers D, Van de Castele M (2003) AMP-activated protein kinase can induce apoptosis of insulin-producing MIN6 cells through stimulation of c-Jun-N-terminal kinase. *J Mol Endocrinol* 30:151-161.

Kingma JG Jr, Simard D, Rouleau JR (1994) Timely administration of AICA riboside reduces reperfusion injury in rabbits. *Cardiovasc Res* 28:1003-1007.

Kretschmar D, Pflugfelder GO (2002) Glia in development, function, and neurodegeneration of the adult insect brain. *Brain Res Bull* 57:121-131.

Largo C, Tombaugh GC, Aitken PG, Herreras O, Somjen GG (1997) Heptanol but not fluoroacetate prevents the propagation of spreading depression in rat hippocampal slices. *J Neurophysiol* 77:9-16.

Leão AAP (1944) Spreading depression of activity in the cerebral cortex. *J Neurophysiol* 7:359-390.

Leão AAP, Morrison RS (1945) Propagation of spreading cortical depression. *J Neurophysiol* 8:33-45.

Leis JA, Bekar LK, Walz W (2005) Potassium homeostasis in the ischemic brain. *Glia* 50:407-416.

Lindsley JE, Rutter J (2004) Nutrient sensing and metabolic decisions. *Comp Biochem Physiol B Biochem Mol Biol* 139:543-559.

Mayer MP, Bukau B (1998) Hsp70 chaperone systems: diversity of cellular functions and mechanisms of action. *J Biol Chem* 273:261-268.

McCullough LD, Zeng Z, Li H, Landree LE, McFadden J, Ronnett GV (2005) Pharmacological inhibition of AMP-activated protein kinase provides neuroprotection in stroke. *J Biol Chem* 280:20493-20502.

Meisse D, Van de Castele M, Beauloye C, Hainault I, Kefas BA, Rider MH, Foufelle F, Hue L (2002) Sustained activation of AMP-activated protein kinase induces c-Jun N-terminal kinase activation and apoptosis in liver cells. FEBS Lett 526:38-42.

Menna G, Tong CK, Chesler M (2000) Extracellular pH changes and accompanying cation shifts during ouabain-induced spreading depression. J Neurophysiol 83:1338-1345.

Müller M, Ballanyi K (2003) Dynamic recording of cell death in the in vitro dorsal vagal nucleus of rats in response to metabolic arrest. J Neurophysiol 89:551-561.

Nedergaard M, Cooper AJL, Goldman SA (1995) Gap junctions are required for the propagation of spreading depression. J Neurobiol 28:433-444.

Newman AEM, Foerster M, Shoemaker KL, Robertson RM (2003) Stress-induced thermotolerance of ventilatory motor pattern generation in the locust, *Locusta migratoria*. J Insect Physiol 49:1039-1047.

Pedgley DE (1979) Weather during desert locust plague upsurges. Phil Trans R Soc Lond B 287:387.

Qin W, Tyshenko MG, Wu BS, Walker VK, Robertson RM (2003) Cloning and characterization of a member of hsp70 gene family from *Locusta migratoria*, a highly thermotolerant insect. Cell Stress Chaperones 8:144-152.

Rainey RC (1951) Weather and the movements of locust swarms: a new hypothesis.

Nature 168:1057.

Ramirez JM, Elsen FP, Robertson RM (1999) Long-term effects of prior heat shock on neuronal potassium currents recorded in a novel insect ganglion slice preparation. J

Neurophysiol 81:795-802.

Robertson RM (2004b) Thermal stress and neural function: adaptive mechanisms in insect model systems. J Therm Biol 29: 351-358.

Rodgers CI*, Armstrong GAB*, Robertson RM (2010) Coma in response to environmental stress in the locust: A model for cortical spreading depression. J Insect Physiol 56:980-990.

Rodgers CI, Armstrong GAB, Shoemaker KL, LaBrie JD, Moyes CD, Robertson RM (2007) Stress preconditioning of spreading depression in the locust CNS. PLoS ONE 2:e1366.

Rodgers CI, LaBrie JD, Robertson RM (2009) K⁺ homeostasis and central pattern generation in the metathoracic ganglion of the locust. J Insect Physiol 55:599-607.

Sharp FR, Massa SM, Swanson RA (1999) Heat-shock protein protection. Trends Neurosci 22:97–99.

Somjen GG (2001) Mechanisms of spreading depression and hypoxic spreading depression-like depolarization. Physiol Rev 81:1065-1096.

Stige LC, Chan K-S, Zhang Z, Frank D, Stenseth NC (2007) Thousand-year-long Chinese time series reveals climatic forcing of decadal locust dynamics. Proc Natl Acad Sci USA 104:16188.

Takano T, Tian G-F, Peng W, Lou N, Lovatt D, Hansen AJ, Kasischke KA, Nedergaard M (2007) Cortical spreading depression causes and coincides with tissue hypoxia. Nat Neurosci 10:754-762.

Thompson RJ, Zhou N, MacVicar BA (2006) Ischemia opens neuronal gap junction hemichannels. Science 312:924-927.

Tupling AR, Gramolini AO, Duhamel TA, Kondo H, Asahi M, et al. (2004) HSP70 binds to the fast-twitch skeletal muscle sarco(endo)plasmic reticulum Ca^{2+} -ATPase (SERCA1a) and prevents thermal inactivation. J Biol Chem 279: 52382-52389.

van Harreveld, A (1978) Two mechanisms for spreading depression in the chicken retina. J Neurobiol 9:419-431.

Van Harreveld A, Stamm JS, Christensen E (1956) Spreading depression in rabbit, cat and monkey. *Am J Physiol* 184:312-320.

Walter DC, Nelson SR (1975) Energy metabolism and nerve function in cockroaches (*Periplaneta americana*). *Brain Res* 94:485-490.

Wu BS, Walker VK, Robertson RM (2001) Heat shock-induced thermoprotection of action potentials in the locust flight system. *J Neurobiology* 49:188-199.

Wu J, Fisher RS (2000) Hyperthermic spreading depressions in the immature rat hippocampal slice. *J Neurophysiol* 84:1355-1360.

Xiong ZQ, Stringer JL (2000) Sodium pump activity, not glial spatial buffering, clears potassium after epileptiform activity induced in the dentate gyrus. *J Neurophysiol* 83:1443-1451.

Yenari MA, Fink SL, Sun GH, Chang LK, Patel MK, Kunis DM, Onley D, Ho DY, Sapolsky RM, Steinbrg GK (1998) Gene therapy with HSP72 is neuroprotective in rat models of stroke and epilepsy. *Ann Neurol* 44:584-591.